University of Canterbury

School of Physical and Chemical Sciences

Inhibiting MenD

An Essential Enzyme in Menaquinone Biosynthesis in *Mycobacterium tuberculosis*

Connor O'Rourke

Supervisors: Dr. Jodie Johnston and Dr. Timothy Allison

Abstract

Menaquinone (MQ) is an important electron carrier for electron transport across the membrane, which as a result is essential for energy generation for many bacteria in anaerobic and aerobic respiration. MenD (2-succinyl-5-enolpyruvyl-6-hydroxy-3-cyclohexene-1-carboxylate [SEPHCHC] synthase) is the enzyme responsible for the first committed step in the classical MQ biosynthesis pathway and as such is a central element for investigation into the inhibition of the classical MQ pathway.

The aim of this thesis was to purify a newly developed construct of *Smeg*-MenD that could have the His-tag cleaved, and to use this and MenD enzymes from *E. coli* (purified in this thesis) and *S. aureus* (obtained purified) to expand upon previous work from the Johnston laboratory characterising the MenD from *M. tuberculosis*. This thesis details the results from two different bioanalytical techniques (intrinsic protein fluorescence and differential scanning fluorimetry) to probe the MenD interaction with a variety of well-known natural ligands (both allosteric- and active-site binders) and a small set of potential inhibitors of the MenD enzyme.

Differential scanning fluorimetry proved to be the most useful technique for investigation of the MenD enzymes, with the small volumes required, ability of replicates, and the broad conditions of ligands that were tested proving invaluable from this technique. DHNA, the ligand that binds to the allosteric site in *Mtb*-MenD was found to have an effect on MenD from all three species investigated in this work, suggesting the potential for an allosteric site to be present in all MenD species. Three of the potential inhibitors screened also displayed potential as inhibitors and warrant further investigation into the effectiveness of these ligands.

Acknowledgements

Firstly, I would like to thank my supervisors Dr. Jodie Johnston and Dr. Tim Allison for the sheer amount of support and feedback they have provided me throughout this work. Their patience in explaining and guiding me through this work has been greatly appreciated and have been a main factor in finishing this thesis.

I would also like to thank both Dr. Thu Ho and Dr. Tamsyn Stanborough for their endless help and guidance in the labs without which I would have been lost. Both their technical know-how and their positive attitude in the labs created a fantastic environment to be working in and I always knew I could check in with them whenever I was unsure on how to use a piece of equipment or the best way to set up an experiment.

I would like to thank my family for their constant encouragement and support throughout this whole process, they gave me the confidence to keep going and stick to it. I finally want to thank Rosemary, whose patience in listening to all my explanations in processes she knows nothing about and providing support throughout the writing process has been the greatest help of all.

Contents

List of Figures

List of Tables

Abbreviation

ADP	Adenosine diphosphate
AIDS	Acquired immune deficiency syndrome
Ala	Alanine
AMP	Ampicillin
Arg	Arginine
Asp	Aspartate
ATP	Adenosine triphosphate
CHD	2,4-cyclohexadiene
DHNA	1,4-dihydroxy-2-napthoate
DMSO	Dimethyl sulfoxide
DNA	Deoxyribonucleic acid
DSF	Differential scanning fluorimetry
DTT	1,4-dithiothreitol
Ec-MenD	*Escherichia coli* MenD
E. coli	*Escherichia coli*
Gln	Glutamine
Glu	Glutamate
HEPES	(4-(2-hydroxyethyl)-1-piperazineethanesulfonic acid)
His	Histidine
HIV	Human immunodeficiency virus
HYG^R	Hygromycin
IFQ	Intrinsic fluorescence quenching
IMAC	Immobilised metal affinity chromatography
Ile	Isoleucine
IPTG	Isopropyl β-D-1-thiogalactopyranoside
KAN	Kanamycin
LB	Luria broth
Leu	Leucine
LTBI	Latent tuberculosis infection
Lys	Lysine
MK	Menaquinone
MQ	Menaquinone
M. smegmatis	*Mycobacterium smegmatis*
M. tb	*Mycobacterium tuberculosis*
Mtb-MenD	*Mycobacterium tuberculosis* MenD
M. tuberculosis	*Mycobacterium tuberculosis*
PCR	Polymerase chain reaction
Phe	Phenylalanine
PPG	Polypropylene glycol
RNA	Ribonucleic acid
Sau-MenD	*Staphylococcus aureus* MenD
S. aureus	*Staphylococcus aureus*
SDS-PAGE	Sodium dodecyl sulfate polyacrylamide gel electrophoresis
SEC	Size exclusion chromatography
SEPHCHC	2-Succinyl-5-enolpyruval-6-hydroxy-3-cyclohexene-1-carboxylate
Ser	Serine
SHCHC	2-succinyl-6-hydroxy-2,4-cyclohexadiene-1-carboxylic acid
Smeg-MenD	*Mycobacterium smegmatis* MenD
SOB	Super optimal broth
SOC	Super optimal broth with catabolite repression

TB	Tuberculosis
TB medium	Terrific broth medium
TCEP	tris(2-carboxyethyl) phosphine
TEMED	Tetramethyl ethylenediamine
TEV	Tobacco etch virus protease
ThDP	Thiamine pyrophosphate
Thr	Threonine
Trp	Tryptophan
Tyr	Tyrosine

Chapter 1. Introduction

1.1 MenD and Menaquinone Biosynthesis

Menaquinone (MQ), also known as Vitamin K_2, is a small molecule involved in electron transfer and consequentially bacterial energy generation. For some bacteria such as *Mycobacterium tuberculosis* (*M. tb*), MQ is essential as it is the sole electron carrier. Notably, humans do not have MQ biosynthesis pathways and instead receive MQ from diet. As such, MQ has been of particular interest for drug design to many research groups in terms of the biosynthesis of MQ and the proteins responsible for the MQ biosynthesis pathway [1, 2].

1.1.1 Menaquinone Biosynthesis

Menaquinone is a lipid-soluble molecule that resides in the bacterial membrane. The structure of MQ is comprised of a naphthoquinone head group and an isoprenyl tail, which varies in length and saturation dependent on bacterial species [3]. For Gram positive bacteria, MQ with 7 to 11 isoprenoid residues (MK-7 – MK-11) are considered critical lipid-soluble electron carriers. MQ is the sole quinone for Gram positive bacteria and mycobacteria and as such is essential for survival [2]. As shown in Figure 1, MQ (MK in Figure 1) transfers two electrons from the electron donor to the electron acceptor. The flow of electrons across the membrane causes proton build-up that cross the lipid bilayer via ATP synthase travel. This movement causes ATP synthase to produce ATP from ADP and phosphate due to a proton motive force production [2]. Humans neither make MQ or use MQ in electron transport chains. MQ instead is used in human blood coagulation using MQ-4 (Vitamin K_2) as a cofactor for vitamin K-dependent proteins like γ-glutamyl carboxylase, which is responsible for catalysing the carboxylation of glutamic acids in numerous blood coagulation related proteins [2]. Humans receive the MQ-4 they use primarily from conversions of MQ-7-15 found in their diet. This mainly is from phylloquinone-containing plants but can also be from meat, eggs, and dairy products. Additionally, gut bacteria are also a potential source [4]. The tail group of the MQ are converted while the headgroup is not made. Based on this knowledge, the menaquinone biosynthesis pathway is highlighted as an ideal drug target due to its absence in humans and the reduced likelihood of detrimental effects upon humans in that regard.

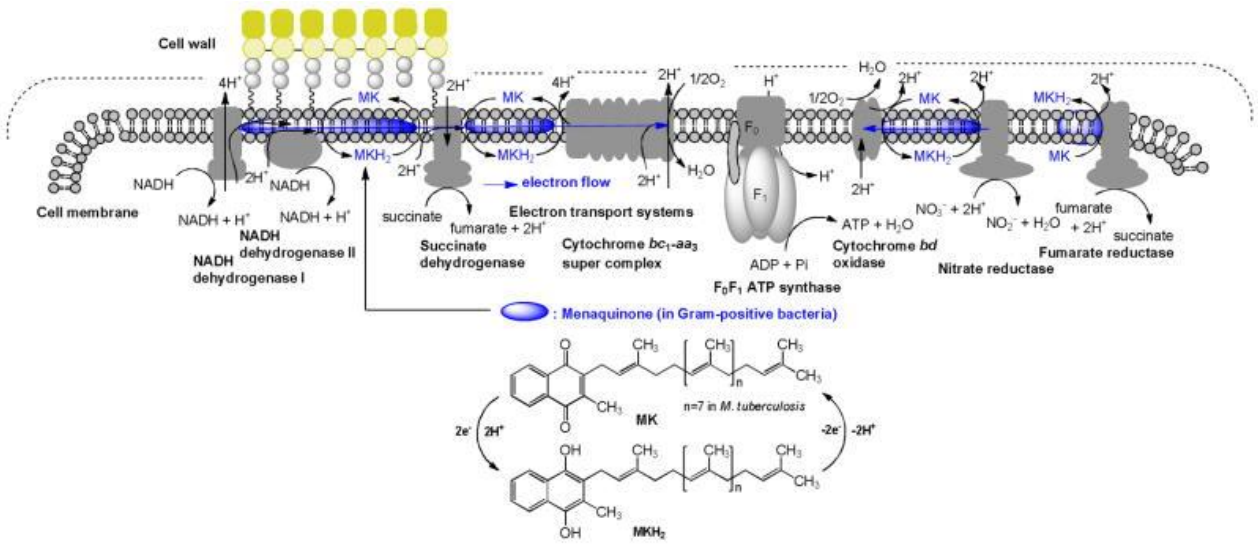

Figure 1: Top: The electron flow system of *M. tb*. The menaquinone mediated pathway is highlighted in blue. Electrons are carried between the membrane proteins via MK. Protons are pumped out of the cell and back through the ATP synthase to allow ATP generation. **Bottom:** The structures of reduced and non-reduced menaquinone. The menaquinone in *M. tb* is most commonly composed of nine isoprenoid residues in its 'tail'. (Image taken from ([5]).

MQ has two potential pathways of synthesis, the futalosine pathway and the classical (Men) pathway. It is uncommon for bacteria to have both pathways [6]. The distribution of these pathways in human gut microbiome show half of the quinone biosynthesis is through the Men pathway. Ubiquinone and futalosine pathways only account for 9% and 5%, respectively [6]. *M. tb* utilises the Men pathway for MQ biosynthesis. The Men pathway was initially thought to be the only pathway for MQ synthesis. The Men pathway generally involves 8-10 genes, of which six are identified as essential [7]. These resulting enzymes are named as MenA to MenJ, though as shown in Figure 2, the order of these enzymes in the pathway is not alphabetical. These enzymes are required to produce menaquinone from chorismate [2, 8, 9]. The full Men pathway can be seen in Figure 2. The focus for work on the Men biosynthesis pathway has been primarily upon the Gram-negative bacteria *E. coli* as a model. Unlike Gram-positive bacteria, *E. coli* and other Gram-negative species make both MQ and ubiquinone, as they are not sole quinone users. There have been nine *men* genes identified in the *E. coli* model, of which six are also found in *M. tb*. These six genes encode the proteins MenA, MenB, MenC, MenD, MenE, MenG/UbiE. For this work, the protein of the most interest is that which performs the first committed step in the pathway, MenD [6, 10].

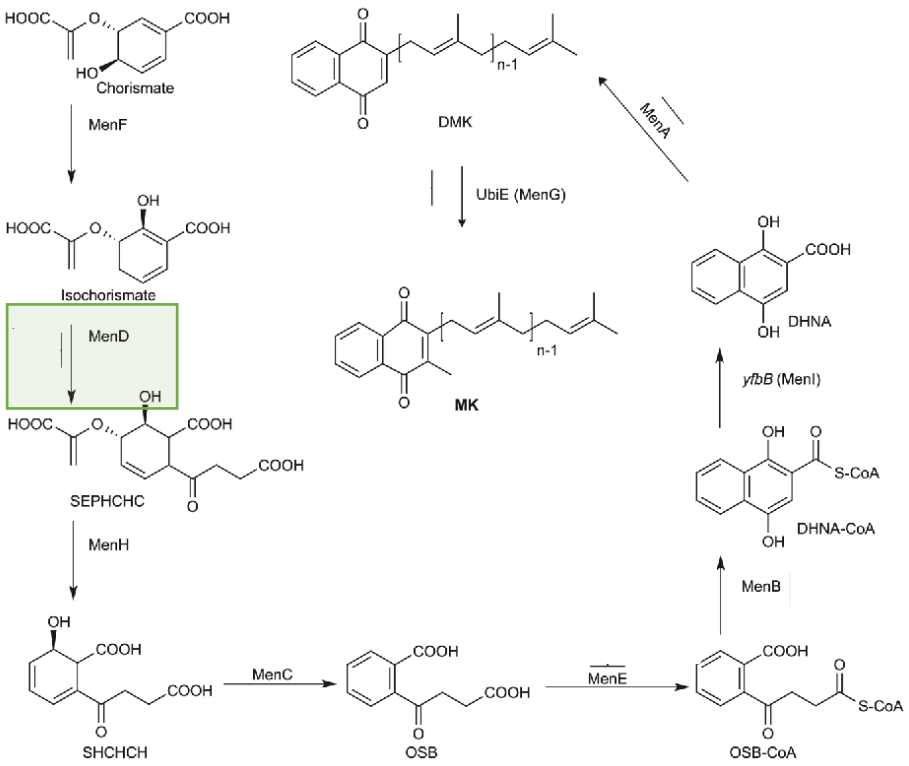

Figure 2: The classical biosynthesis pathway of menaquinone. The classical pathway begins with chorismate as the substrate and through the enzymes MenF, MenD, MenH, MenC, MenE, MenB, MenI, MenA and MenG synthesise menaquinone as the final product. Highlighted in green is the first committed step, catalysed by MenD, the conversion of isochorismate to SEPHCHC. (Diagram adapted from [10]).

1.1.2 MenD

2-Succinyl-5-enolpyruval-6-hydroxy-3-cyclohexene-1-carboxylate (SEPHCHC) synthase (MenD) is the enzyme responsible for catalysing the first committed step in the classical MQ biosynthesis pathway. Originally thought to be responsible for forming 2-succinyl-6-hydroxy-2,4-cyclohexadiene-1-carboxylic acid (SHCHC) from isochorismate and 2-ketoglutarate, MenD instead was found to be a highly efficient enzyme for SEPHCHC synthesis and determined as essential for MQ synthesis [11]. As MenD is known to catalyse the first committed step, the interest in this enzyme as a potential drug target is significant and several groups are currently working with MenD as such [11, 12].

MenD is a member of a family of thiamine diphosphate (ThDP)-dependent decarboxylase enzymes [12]. All members of the ThDP-dependent decarboxylase enzyme family bind ThDP in a divalent metal ion-dependent manner, share a common protein fold, and catalyse the decarboxylation of a 2-oxo acid. The second step of the reaction for this enzyme family deviates between enzymes, and ranges from ligation to a second substrate, protonation, oxidative/reductive processes, carbon-carbon bond formation, and more [12]. All reactions undertaken by this family of enzymes are mediated by the ThDP cofactor, which forms several intermediates along the reaction cycle as shown in Figure 3. ThDP mediation of these enzymes occurs through conformational changes of ThDP upon binding to the enzyme. With this shift in the conformation, ThDP is ‘activated’ and capable of reacting in the first decarboxylation step. As can be seen in Figure 3, both steps from intermediate I and intermediate II require involvement of the cofactor ThDP. ThDP is thought to have resonance capabilities in the aminopyrimidine ring, which is observed throughout the reaction cycle [13].

MenD, like all ThDP-dependent enzymes, catalyses the decarboxylation reaction of a 2-oxo acid, which for MenD is α-ketoglutarate. In this thesis it will instead be referred to by its alternative name 2-oxoglutarate [12]. The second step of the MenD catalysed reaction is of interest due to the unique formation of a new carbon-carbon bond with the substrate isochorismate. This carbon-carbon bond is formed between the decarboxylated 2-oxoglutarate and isochorismate through a Stetter-like 1,4 addition [14]. The MenD reaction cycle is shown in Figure 3. The first step of this cycle involves activated-ThDP and 2-oxoglutarate. ThDP reacts with 2-oxoglutarate to form a ThDP adduct, which then decarboxylates forming the first covalent intermediate (Intermediate I). It is thought that this intermediate is in resonance between the enamine and carbanion forms [11, 12, 14]. The second step, a Stetter-like 1,4 addition, involves a 1,4 addition of isochorismate to Intermediate I. This occurs via nucleophilic attack from the anionic carbon found on intermediate I and forms a carbon-carbon bond and thus the second intermediate (Intermediate II). Finally, cleavage of the product SEPHCHC from Intermediate II occurs in the second part of the reaction. While SEPHCHC is cleaved, ThDP is retained in the enzyme for the next cycle [11].

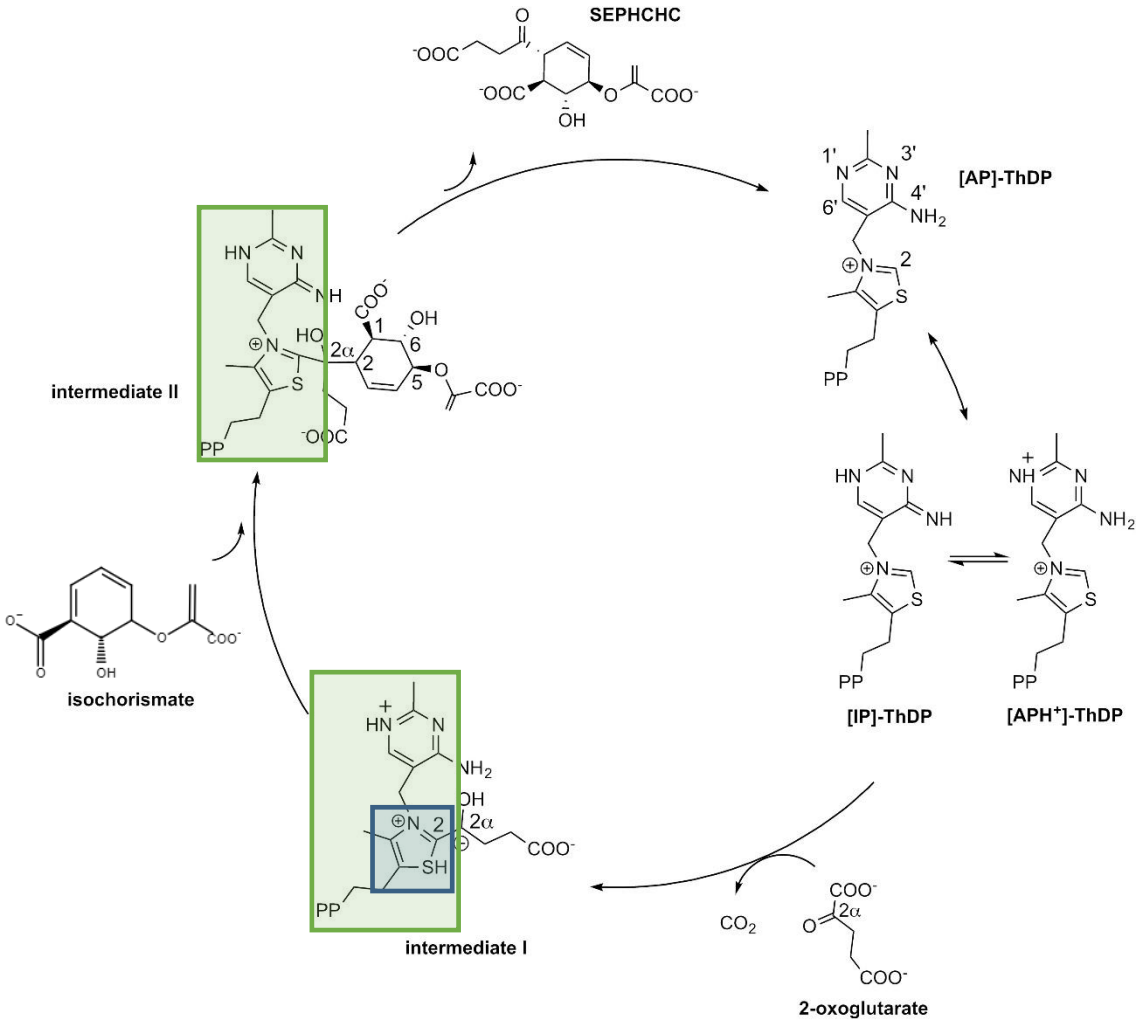

Figure 3: MenD reaction cycle for SEPHCHC formation. MenD binds and activates ThDP for attack and binding of 2-oxoglutarate (bottom right) for decarboxylation. The first covalent intermediate is then formed and undergoes the second reaction step with binding of isochorismate for a Stetter-like 1,4 addition at the thiazolium moiety (blue box) of Intermediate I to form Intermediate II. Cleavage results in release of SEPHCHC from Intermediate II while ThDP is recycled. In the green boxes are the retained ThDP structure throughout the cycle. Adapted from Jirgis *et al.* [15].

1.2 *Mtb*-MenD

1.2.1 Tuberculosis

Mycobacterium tuberculosis is the bacterium responsible for the human disease tuberculosis (TB). As of 2017, TB was the leading cause of death from an infectious disease. This statistic is greater than for HIV, which coincidentally can amplify the fatality rate from TB infections (Figure 4) [16].

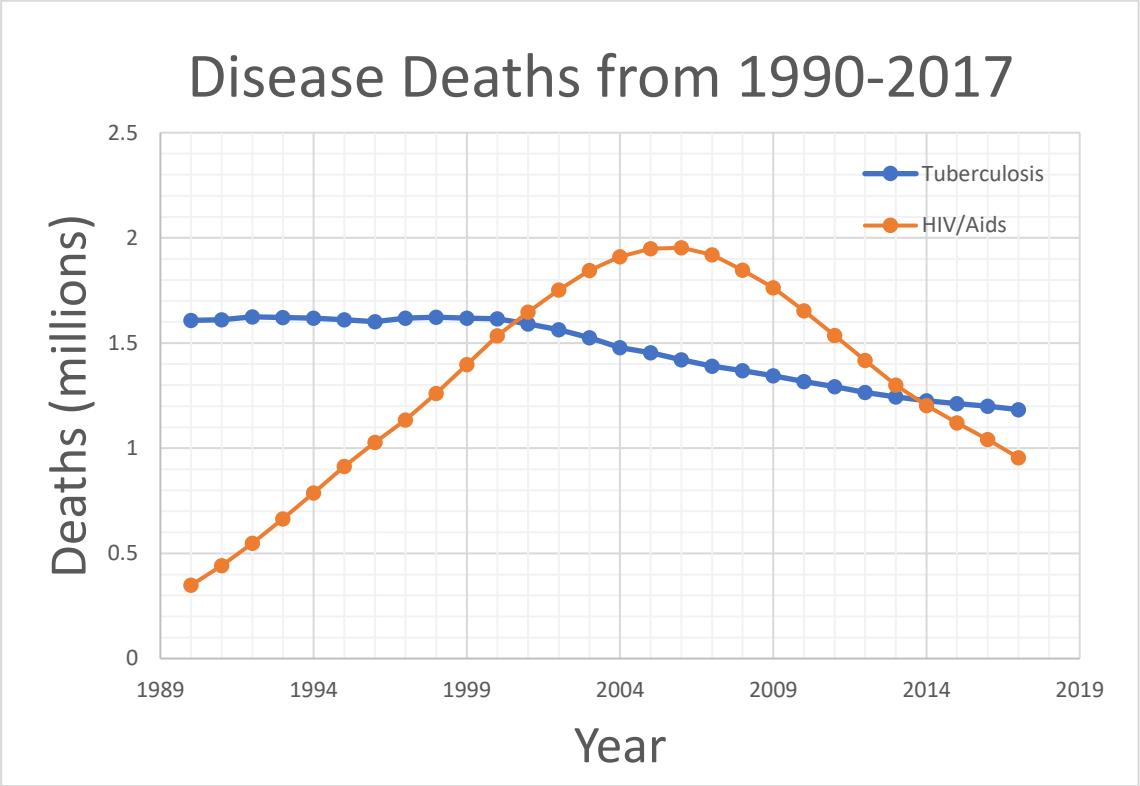

Figure 4: Graph from Global Health Data Exchange of TB and HIV/AIDS deaths over the past 27 years.

Tuberculosis is a highly contagious disease transmitted via inhalation of the bacterium expelled by someone with the active disease, resulting in either an active or latent *M. tb* infection [17, 18]. For infection the inhaled tubercle bacilli must first reach the alveoli (air sacs of the lungs) of the host, survive being phagocytised by the immune system and then start replicating in the host macrophages [19]. This is especially important to the infection as this allows the bacilli to diffuse to nearby cells, which drastically increases the population of the bacteria [20]. The bacilli can also spread from the lung to other organs of the body for further replication before auto immune responses finally gain some control on replication [21].

Table 1: World Health Organisation Classification of anti-TB

Group	Drugs
Group 1 – first line agents (oral)	Isoniazid, rifampicin, ethambutol, pyrazinamide
Group 2 – injectable agents	Streptomycin, amikacin, kanamycin, capreomycin
Group 3 – Fluoroquinolone group	Moxifloxacin, ofloxacin, levofloxacin, gatifloxacin
Group 4 – Other, second line agents (bacteriostatic)	Ethionamide, protionamide, cyloserine, PAS (para-aminosalicylic acid)
Group 5 – Agents of uncertain efficacy (not routinely recommended)	Clofazamine, amoxicillin-clavulanate, clarithromycin, linezolid

Source: Guidelines for the programmatic management of drug resistant tuberculosis: emergency update[22]

The current understanding of TB infection proposes that the main difference between latent and active forms of TB are based on the presence of a dynamic equilibrium between bacilli and host immune responses. If these are in equilibrium the disease remains in the latent form as the replicating bacilli, known as 'scouts', are constantly killed by the immune system [23]. If for any reason the immune system fails to control these scouts, the replication will lead to the active disease [24]. The active form of TB is responsible for the high mortality of this disease (~2 million deaths/year), with the results of untreated TB being lesions forming in the airways and tissue breakdown, among other complications [25]. However, the ability to form the dormant state inside the body classified as Latent Tuberculosis Infection (LTBI), effectively 'hiding' until the situation becomes more favourable, is what makes TB extremely difficult to fully destroy [26]. The World Health Organisation has estimated that one third of the world's population is infected by the latent form of the disease, and while the latent form is not infectious it forms a reservoir of infection and ~10% of those latently infected will develop active TB during their lifetime [24, 27]. One of the challenges for new therapeutic developments and research into TB treatment is to focus not only on active TB, which already has many treatments, but on the latent form; to fully destroy the disease in the population so there can be no risks of the disease reappearing in former patients. Active tuberculosis is generally treated by using a variety of drugs consisting of isoniazid (H), rifampicin (R), ethambutol (E) and pyrazinamide (Z) for six months (Table 1, 2). This treatment regimen is useable for both pulmonary and non-pulmonary TB with the only exceptions being to the central nervous system, bone and miliary (throughout the body) TB [28]. The latent form is not susceptible to these drugs that kill actively growing TB bacteria, and this makes it a challenge to successfully treat. In New Zealand, the most common method to attempt to treat LTBI is through an ongoing dosage of isoniazid for 6 to 9 months [29]. Even in active disease cases, a subpopulation is likely in the LTBI state, which results in longer treatment times overall. These longer treatment times include further adverse side effects and more chance for treatment non-

compliance and the development of drug resistance [30, 31]. Another challenge to tuberculosis eradication is drug resistant and multi-drug resistance infections as different infections can become resistant to one or several of the initial drugs provided for treatment. Drug resistant TB results in a modified version of treatment for TB consisting of different drug dosages and durations of treatment but can generally be worked around.

Multi-drug resistant TB is a form which is resistant to the two most important TB drugs, rifampicin and isoniazid, and requires at least 18 months of treatment with at least four drugs that a patient has not already been exposed to and to which the TB is susceptible. While still treatable, it is much more difficult to do so and is overall a much more uncertain time for the patient based upon the types of drugs they will be treated with.

Table 2: Suggested regimens for mono- and poly-drug resistance

Pattern of Drug Resistance	**Suggested Regimen**	**Minimum Duration of Treatment (Months)**
H (± S)	R, Z and E	6-9
H and Z	R, E and fluoroquinolones	9-12
H and E	R, Z and fluoroquinolones	9-12
R	H, E, fluoroquinolones plus at least 2 months of Z	12-18
R and E (± S)	H, Z, fluoroquinolones plus and injectable agent for at least the first 2-3 months	18
R and Z (± S)	H, E, fluoroquinolones plus an injectable agent for at least the first 2-3 months	18
H, E, Z (± S)	R, fluoroquinolones plus an oral second-line agent, plus an injectable agent for the first 2-3 months	18

Source: Guidelines for the programmatic management of drug resistant tuberculosis: emergency update[22]

In all cases, the side effects from these treatments are less than ideal, with gastrointestinal side effects being a major factor in standard treatment as well as potential nerve damage (Table 3). In the multi drug resistant cases, depending on the severity of resistance the side effects will vary in severity.

Table 3: Adverse effects of tuberculosis drugs

Drug	Adverse side-effects
Aminoglycosides (amikacin, capreomycin, kanamycin, streptomycin)	Ototoxicity (lowest incidence with streptomycin); renal damage, skin rashes, fevers, circum-oral paraesthesiae, neuromuscular blockade
Para-amino-salicylic acid	Gastrointestinal effects, hepatitis, fever, rash and hypothyroidism
Cycloserine	Dose-related central nervous system effects (drowsiness, vertigo, disorientation, confusion, coma and psychosis)
Ethambutol	Optic neuropathy (dose-related); peripheral neuropathy, arthralgia or rash are rare
Ethionamide	Gastrointestinal effects, liver toxicity; rarely hypothyroidism, hypotension, hypoglycaemia, alopecia, convulsions and neuropathy
Fluoroquinolones	Gastrointestinal disturbances, dizziness, anxiety, depression, confusion and convulsions; rarely, achilles tendon rupture, arthropathy and photosensitivity. For use in children, consult a paediatric tuberculosis expert.
Isoniazid	Isoniazid hepatotoxicity: Hypersensitivity reactions are unusual. Peripheral neuropathy, optic neuritis, fever, hepatitis, ataxia, euphoria, convulsions, tinnitus, insomnia, hyperglycaemia, gynaecomastia, dry mouth, epigastric discomfort, urinary retention, anaemia, arthralgias. Contraindicated in manic states and porphyria. Idiosyncratic reactions may include a (usually reversible) lupus-like syndrome (fever, arthritis, pleuritis, pericarditis, positive rheumatoid factors, etc), and, very rarely, a rheumatoid arthritis-like syndrome, and agranulocytosis. Very rare hypersensitivity reactions include eosinophilia, angiitis, toxic psychosis, and meningo-encephalitis. Toxic doses decrease the synthesis of the inhibitory neurotransmitter gamma aminobutyric acid. Central nervous system depression or stimulation may result.

Pyrazinamide	Gastrointestinal side effects, hyperuricaemia, hepatotoxicity, fever, anorexia, nausea and vomiting; precipitation of gout, arthralgias, urticaria, sideroblastic anaemia. Of the TB drugs, pyrazinamide is the most common cause of a rash.
Rifabutin	Rash, gastrointestinal disturbance, neutropaenia; uveitis, particularly in combination with macrolide antibiotics
Rifampicin	Gastrointestinal disturbance, cholestatic hepatic dysfunction, transient elevation of hepatic enzymes. Danger with intermittent therapy: flu-like syndrome, shock, acute renal failure, death. Acute haemolytic anaemia. Rare reports of rifampicin-induced light chain proteinuria and renal failure, attributed to dehydration associated with fluid restriction for syndrome of inappropriate antidiuretic hormone.
Thiocetazone	Nausea, vomiting, diarrhoea, bone marrow depression, vertigo, ataxia, tinnitus, occasional liver toxicity, cutaneous hypersensitivity.

Source: Winter et al. (1984)[32]

New Zealand is part of the World Health Organisation "End TB strategy", which aims to end the TB epidemic globally by 2035 and achieve full elimination by 2050 [33]. While New Zealand has a low overall rate of TB infection, certain groups are disproportionately affected such as Maori and Pasifika, people with diabetes, and those in lower socioeconomic groups [34, 35]. In addition, treatment of TB cases has been shown to be a significant cost to the New Zealand health system, due to the cost and duration of the treatment plus the added time and cost for treatment of multidrug-resistant strains, and the challenges of effectively treating the latent form of disease [36, 37]. In 2006, one student from Palmerston North Boys' High was discovered to have the active form of TB, which then led to the infection of 206 others with 18 being other active cases of TB [38]. A single case of TB can affect over 200 people, a strong incentive to be rid of this disease entirely.

1.2.2 *Mycobacterium tuberculosis* MenD and Prior Work

Mtb-MenD has been purified and a variety of X-ray crystallography structures with different ligands bound have been solved. Similar to other ThDP-dependent enzymes, *Mtb*-MenD is comprised of three domains each with β-sheets sandwiched between α-helices (Figure 5, a). The first and third domain have very similar topology, with both consisting of six-stranded parallel β-sheets sandwiched between several α-helices. The main difference between these two domains is found in a loop linking equivalent β-sheets. In domain III a different orientation is observed, as are additional secondary structure elements and a longer length when compared to domain I. Domain II, the central domain only has five-stranded parallel β-sheets with six α-helices. In terms of binding responsibility, domain I binds the aminopyrimidine ring while domain III binds the diphosphate group of ThDP. Both domains are highly conserved in ThDP-dependent enzymes. Domain II in some enzymes binds a nucleotide for either structural or allosteric regulatory purposes depending on the enzyme [39]. Domain II does not participate in either cofactor or substrate binding nor is it heavily conserved [15]. *Mtb*-MenD has a tetrameric structure in solution, which is formed from a dimer of dimers (formed from chains A and D and B and C) [15, 40]. Domain II of *Mtb*-MenD has been recently reported to have an allosteric regulatory site and be subject to allosteric regulation, which has not been reported for any other MenD enzymes to date [41]. This allosteric site is located approximately 15-20 Å from the nearest active site formed by domain III of the same monomer. It is also found approximately 30-40 Å away from domain I as well. This allosteric site has been identified to tightly bind the product of MenI; 1,4-dihydroxy-2-napthoate (DHNA). DHNA appears to provide negative feedback to the MQ biosynthesis cycle.

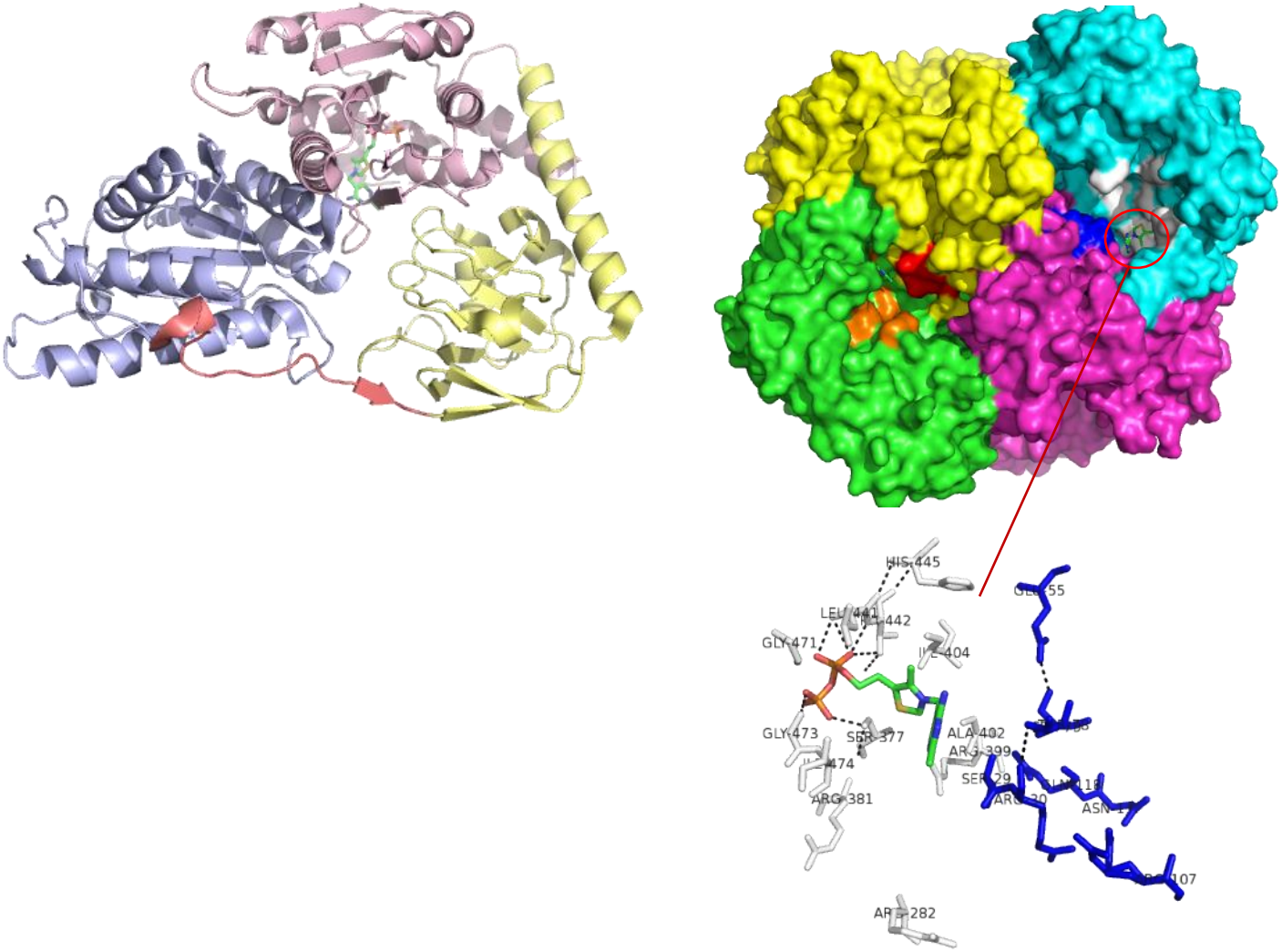

Figure 5: Structural views of *Mtb*-MenD. **Left (a):** The *Mtb*-MenD monomer with domains I, II and III shown in purple, yellow, and pink, respectively. The long link between domains I and II is shown in red. ThDP is shown bound in green. **Right (b):** Surface representation of the MenD tetramer. The residues from the four different monomers responsible for forming the active sites are coloured in orange, red, blue and white. The inset shows a closer look at one of the active sites in the tetramer with ThDP bound. The hydrogen bonds between the residues and the co-factor ThDP are shown.

Most of the prior work done by the Johnston group has focused on *Mtb*-MenD. As such the information concerning *Mtb*-MenD has primarily been provided by this group, including the allosteric site discovery [15, 41]. It is known that how the active site of MenD functions as ThDP anchors into the active site by domain III in the C-terminal through the divalent metal ions and the diphosphate part of ThDP. Glu55 along with Ile404, Ala402 and His445 all play key roles at the active site to hold ThDP in position as well. Glu55 is the key residue in the activity of MenD as when in the active state, the interaction with His445 and the pyrimidine group of ThDP are essential for the ThDP activation [15]. Once 2-oxoglutarate has bound and been decarboxylated, intermediate I can be formed by hydrogen bond formation between the carboxylate group of intermediate I and Arg381 and Arg399. Highly conserved residues found in domains I and III of the opposing monomer (Gln 118, Thr78, Arg107, Arg282, and peptide groups of Ser29 and Arg30) allow the binding of isochorismate to the enzyme, and consequentially the formation of intermediate II. This structural information provided invaluable progress towards inhibitor substrate design and production. In addition, the production of crystals which capture the reaction at various stages were also successfully created. Visualising these crystals via crystallography techniques provides inhibitor binding information, which can help for determining the effectiveness of potential inhibitor compounds to MenD. As mentioned previously, *Mtb*-MenD was discovered during this work to have an allosteric binding site in domain II. As this allosteric site binds to the product (DHNA) from an enzyme further along the MQ biosynthesis pathway, a negative feedback loop to MenD activity is provided via this interaction. The distribution of this allosteric site is currently unclear, conservation of key residues is only seen in mycobacteria and closely related bacteria however a number of key residues are conserved across a broader distribution of species [41]. The presence of this allosteric site has become of interest for drug discovery, with prior work investigating potential inhibitors capable of manipulating this allosteric site. Prior work revealed several compounds which bound similarly to either the substrates/intermediates for MenD or the allosteric regulator of *Mtb*-MenD. This was proven through X-ray crystallography work and these compounds showed potential for further inhibitor design. Because of the ease of access to these commercially available compounds, these were purchased and used in this work. This project aims to do two things. Firstly it aims to check the presence of absence of DHNA (the allosteric regulator) binding in MenD of different species (*E. coli, S. aureus and M. smegmatis)* all of which have varying levels of conservation of the allosteric site (very little in *E. coli* to some conservation in *S. aureus* to very similar in *M. smegmatis*). Secondly it will continue with the inhibitor work previously achieved, through the testing of these potential inhibitor compounds to these three MenD enzymes from different species. Seven compounds similar to the natural allosteric binder of *Mtb*-MenD will be tested. The three enzymes

under investigation in this work will be called *Sau*-MenD (*S. aureus)*, *Smeg*-MenD (*M. smegmatis*) and *Ec*-MenD (*E. coli*).

1.3 Characteristics of MenD Species

1.3.1 DHNA Binding Capabilities

1.3.2 *Escherichia coli*

E. coli is the most prolific and well-known pathogen in the world. Many *E. coli* species are commensal and live on humans and many other animals without any effect on the host. Most commonly found in the intestines of vertebrates, *E. coli* is an incredibly versatile pathogen with an extremely large population size of 10^{26} [42]. An incredibly accessible pathogen, *E. coli* is one of the best characterised model organisms, with many strains of *E. coli* being responsible for advancements in almost all fields of biology (genetics, molecular biology, physiology and biochemistry). This is in no small part due to the diversity found in the *E. coli* population [43].

As such, *E. coli* has also had major contributions to the understanding of the MQ biosynthesis pathway despite having very minor reliance upon this pathway. *E. coli* is the only Gram-negative bacterium investigated in this work, and as with all Gram-negative bacterium's preferentially utilises ubiquinone in aerobic conditions, only utilising MQ in anaerobic conditions [44]. MQ is still synthesised in Gram-negative bacteria, and as such can still be incredibly useful for investigating conserved residues and domains as well as inhibitor investigation for enzymes in the classical pathway. The structure of *Ec*-MenD and many of the other Men enzymes have been solved already, with no allosteric site activity tested for or considered previously in *Ec*-MenD [40]. This work has chosen to include *Ec*-MenD as a research enzyme due to its ease of access and how well studied it has been.

Extensive research has been conducted upon the *E. coli* menaquinone pathway and as such, *Ec*-MenD. This research includes identification of essential conserved residues in the MenD enzyme active site, determination of successful techniques for characterising and assessing the activity of the MenD enzyme, particularly with interactions between ThDP and MenD and reclassification of the function of the MenD enzyme in the Menaquinone synthesis pathway [45-49]. Previous research has successfully solved structures of *Ec*-MenD in both apo and cofactor bound states [40]. As with all ThDP-dependent enzymes, *Ec*-MenD forms dimeric and tetrameric structures due to the active site and cofactor binding sites being found from contributions by at least two subunits. As mentioned by Dawson *et al.*, *Ec*-MenD's predominant structure appeared to be a dimer, with smaller tetramer quantity present while in solution, however a mixture of monomer, dimer trimer

and tetramer was observed in solution, yet the structures remain consistently tetrameric [40]. It also appears that the presence of cofactor (ThDP and/or Mn^{2+}) induce significant conformational changes in the protein. The *Ec*-MenD subunit is shown to display the typical three-domain architecture expected of ThDP-dependent enzymes [40, 50] (Figure 6, a). Again, domain I is responsible for binding the aminopyrimidine ring of ThDP and helping form the active site, while domain III binds to the diphosphate group of ThDP and is also responsible for forming the active site. In the case of *Ec*-MenD, dependency on domain II is non-existent due to stabilization effects being observed elsewhere [40]. Domains I and III are responsible for the formation of the *Ec*-MenD dimer, whereas domain II plays a more significant role in the formation of the tetramer. The active site of *Ec*-MenD is formed from contributions from two subunits. The active site contains five arginine residues (Arg33, Arg107, Arg395 from chain A, Arg293 and Arg413 from chain B) as well as a lysine residue (Lys292) from chain B. Lys292 and Arg293 are both uniquely found further from the catalytic site than the other residues, located in domain II. Arg293 is not well conserved between MenD enzymes and is unlikely to bind any substrates directly, however it is thought to contribute to the active site in *Ec*-MenD. The active site also contains a hydrophobic patch created by the side chains of Ile474, Phe475 and Leu478 from chain B, all of which are strictly conserved in MenD enzymes. Of the most importance in the active is the glutamine residue (Glu55). This residue is strictly conserved and it has been observed that mutagenesis of this residues results in no activity of the *Ec*-MenD enzyme at all [51].

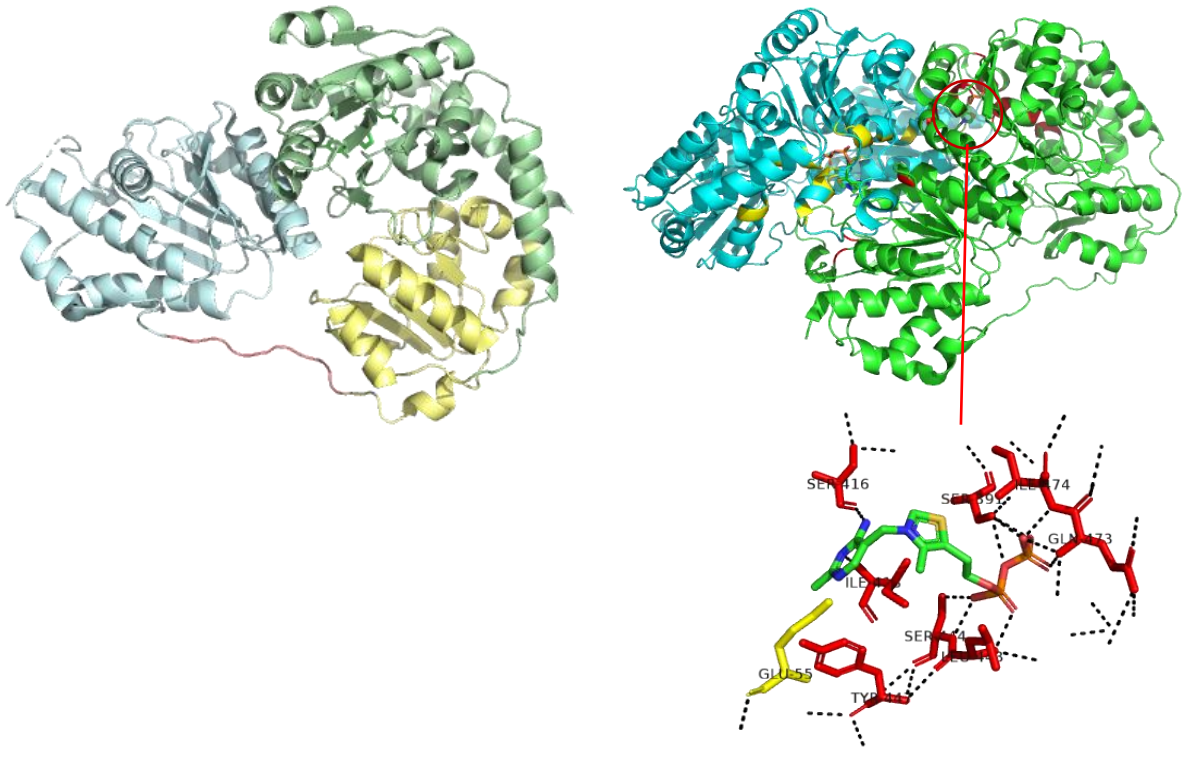

Figure 6: Structural views of *Ec*-MenD. **Left (a):** Diagram of the *Ec*-MenD subunit highlighting the three domains involved. Domain I is in blue, Domain II in yellow and Domain III in green. The long linker between Domains I and II is shown in red. **Right (b):** The *Ec*-MenD Dimer with ThDP bound at each active site. The residues responsible for forming the active sites from monomer A are coloured in red while the same residues in monomer B are in yellow. A closer look at one of the active sites is shown below with the residues responsible for binding to ThDP labelled and the hydrogen bonds shown.

1.3.3 *Mycobacterium smegmatis*

Another Gram-positive bacterium, *M. smegmatis* is generally used as a model for *M. tuberculosis* due to the high similarity between these bacteria [52]. *M. tuberculosis* enzymes are also frequently transformed into *M. smegmatis* cells to ensure similar activity to wild-type *M. tuberculosis*. *M. smegmatis* is described as non-pathogenic as it does not enter epithelial cells, does not persist in professional phagocytes and has none of the described pathogenic properties found in *M. tuberculosis* [53]. *M. smegmatis* and *M. tuberculosis* are both members of the *Mycobacterium* family and are very similar in sequence comparisons, with an 80% identical protein sequence between these proteins, including all the key allosteric site residues conserved between the two enzymes. The structure of *Smeg*-MenD has yet to be solved. Due to the relevance in disease treatment of *Mtb*-MenD, understanding the allosteric regulation of *Smeg*-MenD is, similarly to *Sau*-MenD, a focus for the Johnston research group.

1.3.4 *Staphylococcus aureus*

S. aureus is a Gram-positive bacterium known for its long history with humans in the form of a variety of diseases including pneumonia and toxic shock syndrome [54-56]. It is incredibly capable at being infectious, boasting an arsenal of toxins and virulence determinants allowing it to infect almost every organ in humans. This consequentially results in high morbidity and mortality rates of *S. aureus* infections. In addition to this, antibiotic resistant strains of *S. aureus* are becoming more widespread, demanding more need for new therapeutic target identification [54, 56].

S. aureus as a Gram-positive bacterium like *M. tuberculosis* meaning that the sole quinone used for electron transport and subsequentially respiration is MQ [8]. As such, the pathway of MQ biosynthesis for *S. aureus* is of particular importance to this work as various similarities could be present between *Sau*-MenD and *Mtb*-MenD that cannot be observed in the Gram-negative model created from *Ec*-MenD. *S. aureus* does in fact utilise the classical Men pathway for MQ biosynthesis, utilising at least eight of the same enzymes found in *M. tuberculosis*. Previous research from other groups has already proven that disruption of the MQ biosynthesis pathway can lead to successful resolutions of other diseases/conditions, such as haem toxicity, suggesting the

potential of this pathway as an effective treatment site [57]. Previously, MQ has been identified as the sole quinone used for respiration in *S. aureus*, it is the only quinone responsible for donating electrons to the haem molecules in the cytochromes, which *S. aureus* is known to possess two classes of similar to the model organism *Bacillus subtillus* [58, 59]. The structure of *Sau*-MenD has not yet been solved but is currently under investigation by other members in the Johnston group. As such, investigating if the allosteric site found in *Mtb*-MenD is conserved in this species is a high priority.

1.4 Objectives of The Study

The purpose of this work was to further characterise the interactions of MenD enzymes *Sau*-MenD, *Ec*-MenD, *Smeg*-MenD with a range of potential ligands using two main methods, intrinsic fluorescence quenching (IFQ), and differential scanning fluorimetry (DSF). Previous work with *Mtb*-MenD has utilised both an intrinsic fluorescence binding technique and DSF. Previous DSF experiments however focused upon a different set of potential ligands and only investigated the binding in relation to *Mtb*-MenD. This work will investigate binding of the natural ligands of *Mtb*-MenD upon the different MenD enzymes as well as the binding of seven different potential inhibitors (six of these known *Mtb*-MenD allosteric binders and one from the active site). The intrinsic fluorescence binding assay conducted in previous work used a different experimental technique than in this study. A 96-well microplate was used to investigate the quenching of each compound. Both these methods can be used to characterise ligand and protein interactions and can give different levels of information (with different advantages and disadvantages) and the goal was to use them with each protein and find any similarities between different MenD enzymes in terms of active and allosteric sites interactions with co-factor ThDP, substrates, DHNA and a small subset of the known inhibitor candidates.

The specific objectives of this research are:

Objective 1: Purify *Ec*-MenD and a new TEV cleavable construct of *Smeg*-MenD in large enough quantities and of sufficient purity for further work.

Objective 2: Use these two enzymes in conjunction with *Sau*-MenD (purified by Dr Tamsyn Stanborough) in IFQ experiments to analyse the interactions with known ligands (ThDP, 2-oxoglutarate and DHNA) in various combinations to compare and contrast binding properties across species.

Objective 3: Use these two enzymes in conjunction with *Sau*-MenD (purified by Dr Tamsyn Stanborough) in DSF experiments to analyse the interactions with known ligands (ThDP, 2-oxoglutarate and DHNA) in various combinations as well as with a small set of known *Mtb*-MenD inhibitor candidates to compare and contrast binding properties across species.

Chapter 2. Methods and Materials

2.1 MenD Constructs Used in this Study

2.1.1 pET19 *Ec*-MenD

The pET19 *Ec*-MenD plasmid was obtained from Prof. Michael Mueller's group in Germany. The pET19 vector (Figure 7) contains an ampicillin resistance region (AMP), which allows for selection of cells that have successfully incorporated the plasmid, both an AmpR and lac1 promoter region for the expression of the target protein, several restriction sites to incorporate the gene into the plasmid, and a His-tag on the N-terminal side.

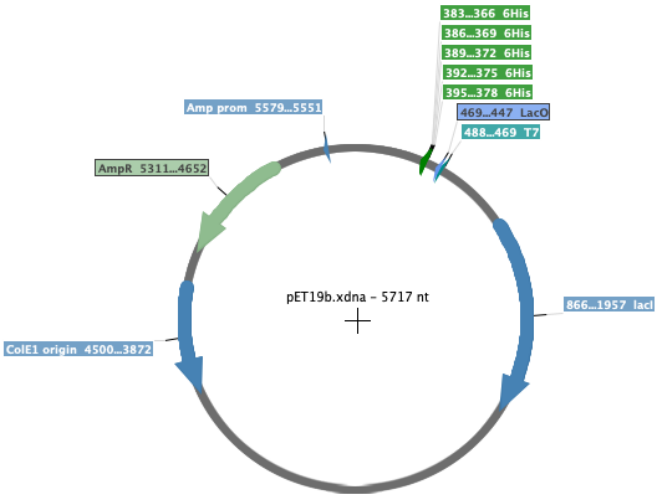

Figure 7: pET19 vector map highlighting features of interest (His-tag, AmpR, Lac1 region). Vector map created in SerialCloner.

2.1.2 pET30a *Sau*-MenD

The pET30a *Sau*-MenD plasmid was made previously by Dr Tamsyn Stanborough in our laboratory. The pET30a vector (Figure 8) contains a kanamycin resistance region (KAN) which again allows selection of cells that have incorporated the plasmid, a T7 promoter region for target protein expression, and a His-tag on both the N-terminus and C-terminus. The N-terminus also contains a thrombin cleavage site.

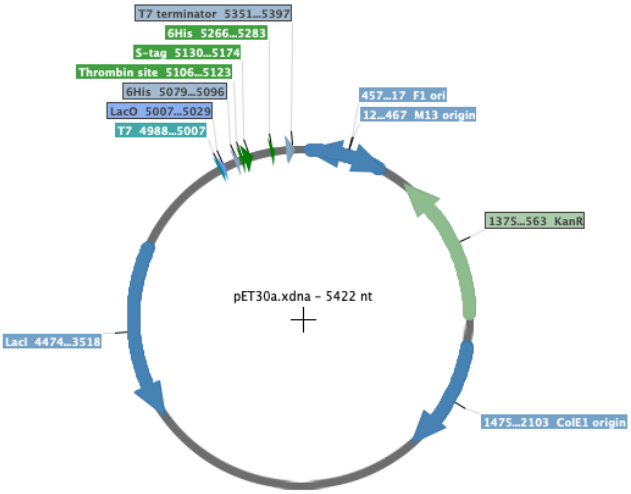

Figure 8: pET30a vector map highlighting features of interest (KAN resistance region, T7 promoter region, His-tags, Thrombin cleavage site). Vector map created in SerialCloner.

2.1.3 pYUB28b-TEV-*smeg*MenD

pYUB28b-TEV-*smeg*MenD was made previously by Dr Tamsyn Stanborough in our laboratory. pYUB28b-TEV vector is based upon the pYUB28b vector so is structurally identical with one exception. The pYUB28b vector was made by Dr Ghader Bashiri and Mr Ehab Jirgis from the pET28b vector [60]. The vector contains a hygromycin resistance region (HYG^R) for cell selectivity, a T7 promoter region for target protein expression, and a His-tag on both N-terminus and C-terminus (Figure 9). The difference in this construct is the replacement of the thrombin site with a TEV site. This was achieved through mutagenesis using In-Fusion HD Cloning Plus. In-Fusion HD Cloning Plus is a product developed by Takara capable of cloning of any PCR fragment into any linearised vector in one 15-minute reaction. Techniques such as mutagenesis are also possible with the kit. The In-Fusion HD Cloning Plus kit provides a PCR premix and an enzyme premix which are used for this mutagenesis. Primers were designed with a 15 base pair overlap at the 5' end, making the mutation of interest incorporated into the vector [61].

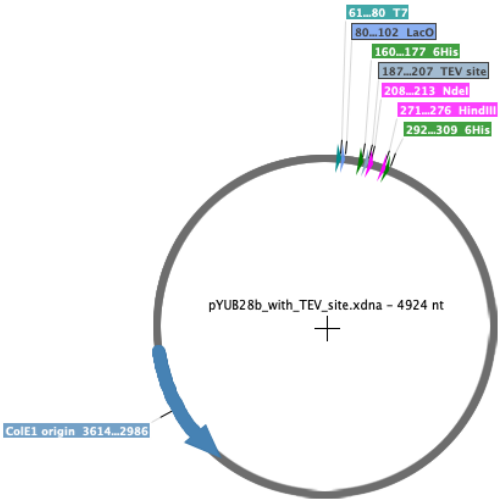

Figure 9: pYUB28b-TEV vector map highlighting features of interest (HYG^R resistance region, His-tags, T7 promoter region, TEV cleavage site) Vector map created in SerialCloner.

2.2 Cell Lines Used in this Study

2.2.1 *Escherichia coli* BL21 Expression Strain

The *E. coli* BL21 DE3 strain was used to express *Ec*-MenD and *Staphylococcus aureus* MenD. This strain was generated from a previously prepared sample from the Dobson group by Dr Thu Ho. By using the *E. coli* cells for *Ec*-MenD, proper folding and the production of active protein has a higher chance of occurring. However, for *Sau*-MenD, *S. aureus* cells were not used for expression, increasing the risk for incorrect folding.

2.2.2 *Escherichia coli* C41 Expression Strain

The *E. coli* C41 strain was used to express *Mycobacterium smegmatis* MenD. This strain was generated from an imported agar plate by Dr Thu Ho. The *E. coli* cells being used for *Smeg*-MenD may not provide the proper folding for the protein nor the proper function of active protein which could become an issue in the results provided.

2.2.3 *Mycobacterium smegmatis* mc^{2}4517 Expression Strain

The *M. smegmatis* mc^{2}4517 was used to express *Mycobacterium tuberculosis* MenD. This strain was generated from *M. smegmatis* mc^{2}155 by integrating a copy of T7 RNA polymerase which will induce the expression of recombinant protein by acetamide, lactose, or IPTG [62]. Much like using the *E. coli* cells for *Ec*-MenD, using closely related mycobacterial cells for production of mycobacterial proteins will provide the optimal opportunities for proper folding and functional protein production.

2.3 Preparation of Expression Cells

The chemically competent *E. coli* cells were prepared previously by Dr Jodie Johnston and Dr Thu Ho. These cells were grown using a SOB and TB medium system. The components of these are shown in Table 4.

The electrocompetent *M. smegmatis* cells were also previously prepared by Dr Thu Ho and Dr Tamsyn Stanborough. These cells were grown using a 7H9/ADC/Tween-80 comprised medium as shown in Table 4.

Table 4: Components of various mediums

SOB 250 ml	TB	7H9/ADC/Tween-80
20 g/L Tryptone	10 mM PIPES	4.7 g/L Middlebrook 7H9 broth base
5 g/L Yeast Extract	15 mM $CaCl_2$	0.05% v/v Glycerol
10 mM NaCl	250 mM KCl	10% v/v ADC
98% Water and autoclave before next addition	pH 6.7 using KOH	0.05% v/v Tween-80
10 mM $MgCl_2$	55 mM $MnCl_2$	
10 mM $MgSO_4$		

2.4 Transformation of Plasmids into Expression Cell Lines

2.4.1 Antibiotics for Transformant Selection

The antibiotic used for the *E. coli* BL21 expression system consists of ampicillin (50 µg/mL) or kanamycin (50 µg/mL). pET19 *Ec*-MenD has ampicillin resistance while BL21 has no antibiotic resistance, whereas the pET30a *Sau*-MenD has kanamycin resistance. These antibiotics will allow for selective growth so that all cells grown will have been transformed successfully.

For the *E. coli* C41 expression system, the antibiotics used consist of hygromycin (50 µg/mL). pYUB28b-TEV-*smeg*MenD has hygromycin resistance whereas the C41 strain has no antibiotic resistance. Again, this will ensure selective growth of transformed cells.

2.4.2 Transformation into *Escherichia coli* BL21 and C41 cells

The pET19 *Ec*-MenD or pET30a *Sau*-MenD constructs were transformed into the *E. coli* BL21 cells for the expression of MenD. 1 µL of pET19 *Ec*-MenD or pET30a *Sau*-MenD construct were mixed with 50 µL of electrocompetent *E. coli* BL21 cells and incubated on ice for 15 minutes. The mixture was then heat shocked at 42 °C for 45 seconds, 500 µL of SOC medium was added and the mixture was incubated on ice again for 2 minutes. The mixture was then incubated at 37 °C for 1 hour and plated on LB agar containing 1 µL/mL ampicillin.

Similar to the pET19 or pET30a transformations, 1 µL of the pYUB28b-TEV-*smeg*MenD construct was added to 50 µL of electrocompetent *E. coli* C41 cells and incubated on ice for 15 minutes. This was then followed by heat shock for 45 seconds at 42 °C, addition of 500 µL of SOC medium and further incubation on ice for 2 minutes and then 37 °C incubation for 1 hour. This was then plated on LB agar containing 1 µL/mL hygromycin. These agar plates were then dried and sealed with parafilm and incubated at 37 °C for 1 day.

2.5 Protein Expression

2.5.1 Media for Auto-Induction Expression

Auto-induction expression is a protein expression method which utilises the ability of lactose to induce production of a target protein without the need to monitor the growth or add inducer at a set time to ensure protein production. The technique identifies that lactose has the potential to cause automatic growth of BL21 cells if the compounds which prevent it from doing so are removed. There are three major factors that need to be considered when using an autoinduction system. These are; ensuring a source of carbon and energy being available, the importance of aeration for the level of target protein growth, and an inclusion of glucose into the auto-induction media at a reasonable concentration. This is done to ensure that cell growth to high density can be supported from the glucose presence, but also to ensure that lactose induction is not prevented from the glucose presence as lactose is the preferred metabolite for cells [63]. The media that was used in the auto-induction system for this work therefore had to cover all factors to ensure the most efficient growth.

Tartoff-Hobbs (Terrific) Broth Medium is a nutritionally rich medium for bacteria growth that is recommended for the cultivation of *E. coli* recombinant strains. While in this medium, these strains have extended growth phases. The medium supports both high cellular density and mass as well as maintaining logarithmic growth for a long time, providing much higher yields of proteins and plasmid DNA. The media and purification process used utilises procedures established by previous work in this lab. The full list of ingredients used in this modified TB media are shown in Table 5 [64]. This work utilises an auto-induction system which includes both Luria Broth and the TB media.

Colonies from the expression cells were taken and inoculated into ‘LB cultures’ of Luria Broth (LB) and the appropriate antibiotic for the plasmid. These LB cultures contained 30-50 mL of LB in Falcon Tubes. Depending on the cells growing, the LB cultures were then incubated at 37 °C for 1 day for *E. coli* and 3 days for *M. smegmatis*. Once expressed, these overnight cultures would then be used to inoculate the TB media for the next stage of the auto-induction system.

All components of the Terrific Broth Media (TB Media) were sterilised by autoclaving at 121 °C for 15 minutes and filtered through a 0.2 µm filter. Any small filtration was done using sterilised plastic syringes using a 0.2 µm Minisart syringe filter while any larger volumes were instead filtered using a vacuum pump with the appropriate filtration apparatus and a Corning® 0.2 µm filter. All components of the TB media are shown in Table 5. The media used for the cultivation of *E. coli* were supplemented with polypropylene glycol 2000 (PPG) and the appropriate antibiotic for the plasmid present (ampicillin, kanamycin or hygromycin). PPG is used to prevent the build-up of foam in the media during incubation without a negative effect on cell growth. For the *M. smegmatis* cells Tween-80 is supplemented instead of PPG. Large flasks were used to ensure proper aeration for growth, such as growing 500 mL culture in 1.5 L flasks and growing 1 L in 3 L flasks. The amount of overnight culture used for each TB media was 10 mL/L. 3 L of culture were grown to ensure enough cell pellet will be present for purification as well as to ensure redundancy in case one was to fail to grow. The *E. coli* culture was incubated at 37 °C for 3-4 hours before being left overnight in 18 °C with shaking, while the *M. smegmatis* culture is left at 37 °C for 3 days while shaking.

Table 5: Contents of TB Media and the components involved

TB Media	Phosphate Mix (10x)	Autoinduction Sugars
12 g/L Tryptone	0.540 M K_2HPO_4	0.021 M Glucose
24 g/L Yeast Extract	0.162 M KH_2PO_4	0.365 M Lactose
0.8% Glycerol		
10% Phosphate Mix		
MQ Water		
1% Autoinduction Sugars		
1.5% Aspartic Acid (25%)		
0.2% $MgSO_4$		
1 Drop PPG		
Antibiotics		

2.5.2 Cell Harvest and Storage

Cells were harvested from the flasks through centrifugation at 5000 *g* for 10 minutes at 4 °C. These were resuspended in a minimal amount of supernatant/MQ and aliquoted into 50 mL Falcon tubes for a further centrifugation step at 5000 *g* for 10 minutes at 4 °C. The supernatant was discarded, and the cell pellets were stored at -20 °C for future use.

2.6 Protein Purification

2.6.1 Protein Purification Buffers

All buffers and solutions were filtered using a vacuum pump and a 0.2 µm filter and prepared with Milli-Q water. For the different cells, different buffers were used in some cases, these are shown in Tables 6-8.

Table 6: Purification buffer contents for *Sau*-MenD

2x Lysis Buffer	1x Lysis Buffer	Size Exclusion Buffer	Elution Buffer
40 mM HEPES pH 8.0	20 mM HEPES pH 8.0	20 mM HEPES pH 8.0	20 mM HEPES pH 8.0
300 mM NaCl	150 mM NaCl	150 mM NaCl	150 mM NaCl
10 mM $MgCl_2$	5 mM $MgCl_2$	5 mM $MgCl_2$	5 mM $MgCl_2$
10% Glycerol	5% Glycerol	5% Glycerol	5% Glycerol
2 mM TCEP	1 mM TCEP	1 mM TCEP	1 mM TCEP
100 mM Imidazole	50 mM Imidazole		500 mM Imidazole

Table 7: Purification buffer contents for *Ec*-MenD

2x Lysis Buffer	1x Lysis Buffer	Size Exclusion Buffer	Elution Buffer
40 mM HEPES pH 8.0	20 mM HEPES pH 8.0	20 mM HEPES pH 8.0	20 mM HEPES pH 8.0
150 mM NaCl	75 mM NaCl	75 mM NaCl	75 mM NaCl
10% Glycerol	5% Glycerol	5% Glycerol	5% Glycerol
2 mM TCEP	1 mM TCEP	1 mM TCEP	1 mM TCEP
100 mM Imidazole	50 mM Imidazole		500 mM Imidazole

Table 8: Purification buffer contents for *Smeg*-MenD

2x Lysis Buffer	1x Lysis Buffer	Size Exclusion Buffer	Elution Buffer
40 mM HEPES pH 8.0	20 mM HEPES pH 8.0	20 mM HEPES pH 8.0	20 mM HEPES pH 8.0
300 mM NaCl	150 mM NaCl	150 mM NaCl	150 mM NaCl
10% Glycerol	5% Glycerol	5% Glycerol	5% Glycerol
2 mM TCEP	1 mM TCEP	1 mM TCEP	1 mM TCEP
100 mM Imidazole	50 mM Imidazole		500 mM Imidazole

2.6.2 Protein Gel Electrophoresis

Sodium Dodecyl Sulfate Polyacrylamide Gel Electrophoresis (SDS-PAGE) is used to analyse the protein's purity during the purification process. With the assistance of a protein molecular weight marker, the size of the protein sample can be estimated through observation of the band of a loaded sample. The SDS-PAGE gels were prepared in two different parts. Firstly, the resolving gel solution was prepared, which also included the use of isopropanol to remove any air bubbles found in the cast. This is left for an hour to set and is followed by the removal of the isopropanol and the addition of the stacking gel solution with a comb to form the wells for loading. The gel solutions components are shown in Table 9. The solution used for loading the wells with protein consisted of 4× loading buffer mixed with protein solution and incubated for 5 minutes at 98 °C to denature the protein. These samples are then loaded into the wells and the SDS-PAGE is mounted into a gel box filled with running buffer and run at 200 V and 30 mA for approximately 1 hour but until the dye has reached the bottom of the gel. The protein gel is then stained with Coomassie Blue stain solution overnight and destained with MQ. In each of the gel runs, protein molecular weight markers were loaded into the first well to measure protein size.

Table 9: SDS-PAGE solution contents

Resolving Gel Solution	Stacking Gel Solution	SDS Gel Loading Buffer
12% Acrylamide	2.68% Acrylamide	62.5 mM Tris-HCl pH 6.8 (Stacking Buffer)
1% SDS	0.375% SDS	10% v/v Glycerol
1% APS	1.6% APS	2% w/v SDS
0.1% TEMED	1 drop 1% Bromophenol Blue	100 mM DTT
Resolving Buffer	0.13% TEMED	0.05% w/v
MQ	Stacking Buffer	
	MQ	

2.6.3 Cell Lysis

Cell pellets were resuspended in 2× lysis buffer equal to the volume of cell pellet and were then lysed via cell disruption using the microfluidizer (M-110p) and 1× lysis buffer. Both the *E. coli* BL21 and C41 cells were passed through the microfluidizer to ensure complete lysis. To remove the proteins from cell debris centrifugation at 13000 rpm for 30 minutes at 4 °C. The supernatant is collected and chilled on ice for purification step.

2.6.4 Immobilised Metal Affinity Chromatography (IMAC)

IMAC is a purification technique that uses packed resins inside a column with immobilised metal ions present to bind specifically to residues with high affinity to metal ions. These ions are generally Ni^{2+} or Co^{2+} and are consistently found binding to His tags. In the case of all three purification in this work, a column with Ni^{2+} was used. The supernatant which contained the protein was filtered first with a sterile 0.8 µm syringe filter followed by a 0.5 µm syringe filter then loaded onto the column using an AKTA system pump which had a 0.8 µm and 0.5 µm connected to the column in the AKTA path. The loading of the protein was then washed using 1× lysis buffer.

Once loaded, the AKTA then ran a gradient wash through the column which used the elution buffer containing high imidazole content. The gradient progressed from 50 mM to 500 mM imidazole while fractions of 5 mL were collected. The fractions were analysed using SDS-PAGE to identify fractions containing protein. These fractions were pooled together according to the observations from the gel and prepared for the next step in the purification process. For the pYUB28b-TEV-*smeg*-MenD protein, an additional step was taken to remove the histidine tag.

2.6.5 rTEV digestion

The pYUB-TEV-*smeg*MenD protein as mentioned previously contains a histidine tag incorporated which ultimately must be removed to observe intended interactions of the proteins during experimental testing. Using recombinant Tobacco etch virus protease (rTEV protease), this histidine tag can be cleaved from the purified protein. The protease was created during previous work and provided for this study. A buffer identical to the size exclusion buffer used for pYUB28b-TEV-*smeg*MenD was used to soak the dialysis membrane tubing which had a molecular weight cut off of 10 kDa used in this digestion.

500 µL of 1.3 mg/mL rTEV protease was mixed with 50 mL of the protein fractions and dialysed at 25 °C overnight. Cleavage was checked with SDS-PAGE which did not display clear cleavage. Another IMAC purification step was then used on the protein and the rTEV cleavage was reattempted. 1 mL of rTEV protease was mixed with 30 mL of the protein fractions and dialysed at 37 °C for 5 hours and at 4 °C for a further 2 days. Determination of cleavage from this was achieved using SDS-PAGE.

2.6.6 Size Exclusion Chromatography (SEC)

Size exclusion chromatography is a purification technique that allows proteins to be purified based upon size. Beads with various sized pores are found in the column allowing proteins to pass through. These beads separate proteins based on their size and this size also determines how long elution takes. Large proteins will elute quickly as they do not pass through any of the pores in the column, while the smallest proteins will pass through every pore, resulting in a much longer time before elution. All proteins present will range between these two situations and therefore knowing the size of the protein will help determine how long it will take to elute.

Before loading onto the SEC column, the protein fractions were first concentrated using a centrifugal filter (cut off molecular weight 10 kDa) by centrifuging at 5000 rpm at 4 °C. Once the protein was concentrated to an acceptable volume it was again filtered using a 0.2 µm syringe filter.

The SEC purification step used a Superdex 200 (10/300 GL) column on an AKTA system at room temperature. Before purification, the column was washed through with two column volumes of MQ followed by equilibration using the prepared SEC buffer. The concentrated protein was loaded into the system using a 0.2 µm syringe filter and then injected into the system. The eluted protein fractions were then collected in 1 mL volumes. The fractions showing any potential protein were analysed using SDS-PAGE.

2.7 Protein Concentration and Storage

The fractions which displayed a single band from the SDS-PAGE were pooled together and further concentrated to around 10 mg/mL. The actual concentration of the protein was recorded, and the protein was then snap frozen in liquid nitrogen in 100 µL units and stored at -80 °C.

The protein was concentrated using centrifugal filter concentrators of either 15 mL or 2 mL max volume with a molecular cut off of 10 kDa. These were centrifuged at 4000 rpm at 4 °C. To quantify the protein was successfully concentrating/at an acceptable concentration a NanoDrop 1000 Spectrophotometer was utilised. By receiving the absorbance of the sample at 280 nm and having knowledge of the proteins molecular weight and extinction coefficient the concentration of the protein could be determined using Beer's Law,

$$c = A/\varepsilon l$$

where c is protein concentration, A is absorbance at 280 nm, ε is the molar extinction coefficient and l is the path length of sample.

2.8 Compounds Used During Experiments

In this work several different compounds were used which were all purchased from available sources (Sigma-Aldrich). These compounds have been identified as positive hits for potential inhibitors using screening via soaking of *Mtb*-MenD crystals and analysis of the resulting structures.

2.9 Differential Scanning Fluorimetry (DSF)

Differential Scanning Fluorimetry (DSF) is an assay technique that is used to assess the stability of a protein in the presence of various potential binding ligands at various temperatures. The DSF experiments were set up with 25 µL reaction volumes of each condition in PCR 96-wells plates. The contents of each reaction are shown in Table 10. The plates were cleared of air bubbles, sealed to prevent evaporation during the experiment and then placed in the PCR machine where the protocol was run. The run was a melt protocol which evolved from 20 °C to 95 °C at 1 °C per minute.

The protein structure will denature as the temperature of the PCR machine increases. As this happens, the SYPRO orange dye in the reaction can then bind to more exposed hydrophobic regions and emit fluorescence. This fluorescence is then picked up by the PCR machine and recorded. The change of this fluorescence over the increasing temperature of the PCR machine produces a melting curve for each reaction on the plate. The raw data from this experiment is then analysed using the Protein Thermal Shift^{TM} software. Every thermal melt curve and melting temperature (T_m) is compared to appropriate controls to identify potential interactions between the protein and a ligand. For each protein used, the ligands used in each set of experiments were the same. However, the contents of the reaction were appropriate to the protein used (shown in Table 10). Five plates were created for each protein used in this work, all with the same format except for the ligands added. An increase in T_m suggests that the compound interacts with and stablilises the protein while decreases in T_m suggest the opposite with destabilisation of the protein. Any deviation of the T_m greater than 0.5 °C (positive or negative) after all corrections using the appropriate controls have been made will be considered to suggest an interaction and will be included in discussion.

Table 10: DSF buffer contents for the three proteins used in this work

DSF Reaction for *Sau*-MenD	**DSF Reaction for *Ec*-MenD**	**DSF Reaction for *Smeg*-MenD**
5 µM *Sau*-MenD	5 µM *Ec*-MenD	5 µM *Smeg*-MenD
20 µM HEPES pH 8.0	20 µM HEPES pH 8.0	20 µM HEPES pH 8.0
150 µM NaCl	75 µM NaCl	150 µM NaCl
1 mM $MgCl_2$	1 mM $MgCl_2$	1 mM $MgCl_2$
5× SYPRO orange	5× SYPRO orange	5× SYPRO orange
Varying Concentration of Ligands	Varying Concentration of Ligands	Varying Concentration of Ligands

2.10 Intrinsic Fluorescence Quenching (IFQ)

Intrinsic protein fluorescence is an effective tool used to study both protein conformation and protein-ligand interactions. The technique specifically looks at the most predominant fluorescent amino acid tryptophan, which absorbs at a wavelength of 280 nm and emits in a range from 300-350 nm depending on environment polarity [65]. The fluorescence of tryptophan is capable of being strongly influenced by residues/compounds found adjacent to the tryptophan, which makes it an effective detection strategy for binding occurring near the residue. In addition to this, the overall rarity of tryptophan in protein structure adds to the ability to measure conformational changes based upon the observed fluorescence and quenching. IFQ was used in favour of other fluorescence techniques due to the ability to detect the fluorescence without the need to covalently modify the molecule which could result in further unintended conformational or other changes.

The IFQ experiment was conducted using an assay buffer shown in Table 11. This buffer was added to quartz cuvettes with 10 mm path length. 1-2 µM concentration of protein was added to these cuvettes as well as any additional ligands added. These additional ligands used were DHNA, ThDP, TCEP and oxoglutarate which could be added in various ways. The setup of these experiments is shown in Table 11. 45-minute incubation stages were required for certain experiments which involved compound and protein interactions. These compounds were not the main focus of the experiment instead being an additive necessary for the appropriate reaction to be observed. The ligand DHNA had to be prepared through addition to DMSO solution. This also required an incubation time of 45 minutes, which when possible was prepared alongside any other incubation stages.

The experiment utilised a Cary Eclipse Fluorescence Spectrophotometer where the reactions were run at an excitation wavelength of 290 nm and measured an emission at 340 nm. Fluorescence excitation at 290 nm and not 280 nm was done to ensure the tryptophan emission spectrum would be dominant over other amino acid fluorescence from tyrosine and phenylalanine. Two readings were made as a ligand was titrated into the cuvette at increasing volume (and concentration) over time. The A_{290} and emission reading at 340 nm were recorded and analysed using the analysis package designed by Allison *et al*. Fluorescence intensity versus ligand concentration were plotted and fitted to determine the K_d.

Table 11: Experimental set up for all IFQ experiments for all three proteins. Specific buffer conditions also included.

IFQ Buffer for *Sau*-MenD & *Smeg*-MenD	**IFQ Buffer for Ec-MenD**	**Exp 1 & 2**	**Exp 3 & 4**	**Exp 5 & 6**	**Exp 7 & 8**	**Exp 9 & 10**
20 µM HEPES pH 8.0	20 µM HEPES pH 8.0	Buffer	Buffer	Buffer	Buffer	Buffer
150 µM NaCl	75 µM NaCl	1-2 µM Protein	1-2 µM Protein	1-2 µM Protein	1-2 µM Protein	1-2 µM Protein
1 mM $MgCl_2$	1 mM $MgCl_2$	Titrated: DHNA (1) ThDP (1)	2.5 mM TCEP	100 µM ThDP	100 µM ThDP	100 µM ThDP
				2.5 mM TCEP (6)	100 µM Oxoglutarate (8)	2.5 mM TCEP
			Titrated: DHNA (3) ThDP (4)	Titrated: Oxoglutarate	Titrated DHNA	100 µM Oxoglutarate
						Titrated: DHNA

Fluorescence quenching arises from several different mechanisms which can be collected under two main classifications. These are dynamic quenching (collisional encounters between fluorophores and quenchers) and static quenching (ground-state complex formation between fluorophores and quenchers) [66]. Dynamic quenching includes proton and electron transfer and long range energy transfer, which involve the excited fluorophore colliding with ions and returning to ground state in non-radiative manners, whereas static quenching such as conformational changes and intramolecular interactions occur when the fluorophore and quencher form a ground state complex which prevents excitation of molecules [67].

2.11 Inner Filter Effect

The absorbance or optical dispersion of light at the excitation of emission wavelength by a compound in the fluorescence assay is known as the inner filter effect (IFE). This can affect fluorescence experiments in a negative way, providing false positives or misinformation shown as non-linearity of fluorescence intensity and fluorophore connection [68]. While one option is to ignore the IFE if absorbances are negligible [69], in the case of this work an attempt to estimate the inner filter effect and correct for it has instead been done using the following equation.

$$F_{i\ corr} = F_{i\ dil} \times 10^{\left[\frac{(A_{ex}+A_{em})}{2}\right]}$$

Where $F_{i\ corr}$ is the corrected value of fluorescence intensity at the titration point, $F_{i\ dil}$ is the dilution corrected fluorescence intensity measured, A_{ex} is the absorbance of sample at excitation wavelength and A_{em} is the absorbance of sample at emission maximum [68].

By first determining the absorbance of ligands being added to the cuvette, these absorbances can be used in the equation to account for the ligand presence and provide a more accurate representation of the fluorescence quenching occurring.

Chapter 3. Protein Purification

3.1 Origin and Purification of Proteins

Table 12: Information pertaining to each protein used in this work outlining the level of purification completed.

Protein	**Construct**	**Histidine tag location/Cleaved or not cleaved**	**Source of cells from expression work**	**Purification steps done in this work**
Sau-MenD	pET30a	N-terminal and C-terminal histidine tag. N-Terminal thrombin cleavage site. Cleaved from Protein via rTEV	Obtained purified protein from Dr Stanborough	No purification steps done. Purified protein obtained from Dr Stanborough
Mtb-MenD	pYUB28b-TEV	N-terminal histidine tag. TEV cleavage site replacing thrombin cleavage	Obtained purified protein from Dr Ho	No purification steps done. Purified protein obtained from Dr Ho
Ec-MenD	pET19	N-terminal histidine tag.	Obtained cells from Dr Ho	IMAC purification SEC purification
Smeg-MenD	pYUB28b-TEV	N-terminal histidine tag. TEV cleavage site replacing thrombin cleavage	Obtained cells from Dr Ho and Dr Stanborough	IMAC purification rTEV Cleavage Reverse IMAC purification SEC purification

3.2 *Ec*-MenD

In this work *Ec*-MenD was purified using the methods described in Chapter 2; briefly the pellets containing over-expressed MenD were lysed using a cell disruptor then purified via immobilised metal affinity chromatography (IMAC) and size exclusion chromatography (SEC). The N-terminal hexa-histidine tag was linked to MenD via short sequence containing a thrombin cleavage site and was not cleaved.

3.2.1 *Ec*-MenD IMAC

IMAC purification of *Ec*-MenD successfully separated the desired protein from the protein mix found in the cell pellet. As shown in Figure 10, purification of *Ec*-MenD was highly specific, with only one major elution peak (fractions 6-8) observed during the IMAC purification process.

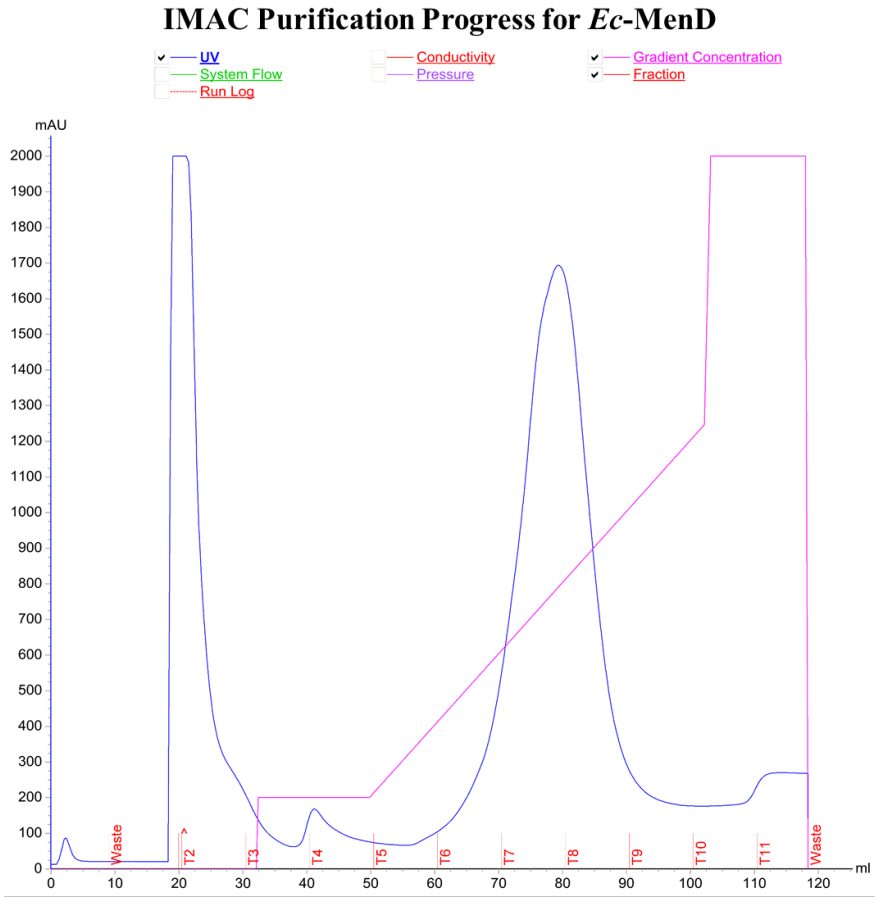

Figure 10: *Ec*-MenD IMAC chromatogram. Blue line is the UV absorbance at 280 nm with one major peak observed from fractions 6-8.

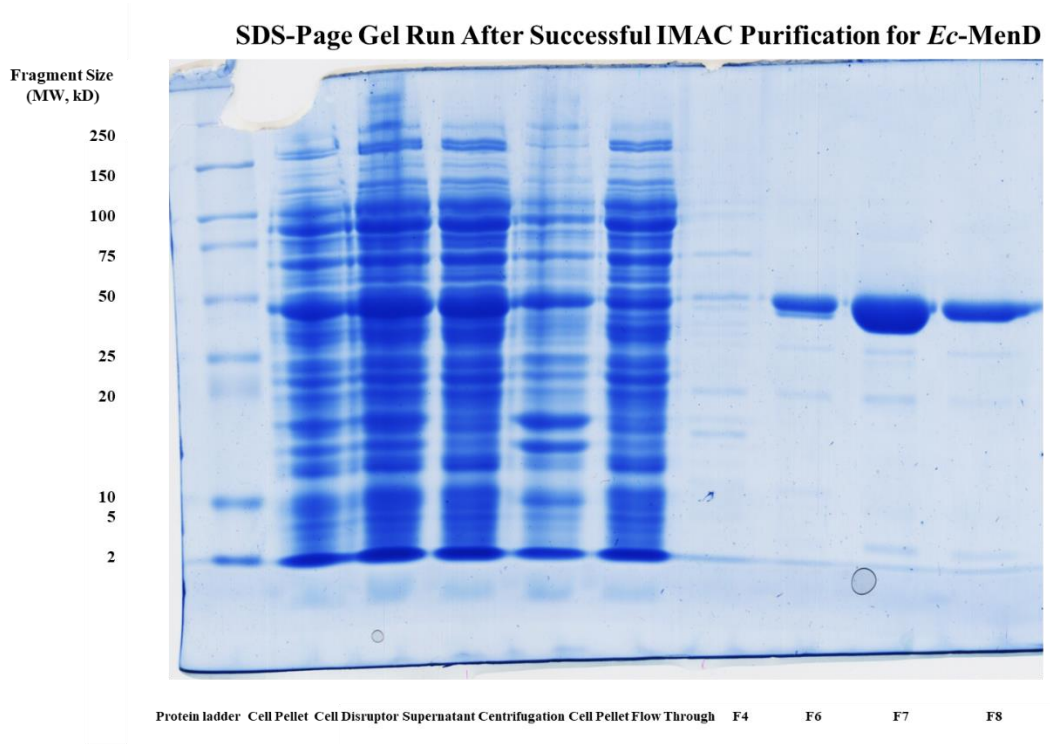

Figure 11: SDS-PAGE showing progression from before and including IMAC purification. From left to right the lanes are: protein standard, cell pellet and lysis buffer, cell pellet after cell disruptor, supernatant after centrifugation, cell pellet after centrifugation, protein flow through, fraction 4, fraction 6, fraction 7, fraction 8.

3.2.2 *Ec*-MenD SEC

Based on the results from the SDS-PAGE, fractions 6-8 were pooled and concentrated for further purification by size exclusion chromatography on a S200 16/600 column. This column contains a void volume of 20 mL. Void volume is a reference to the liquid phase volume that is contained inside a column. The void volume of a column varies depending on the size of the column as well as the volume of support moleules found inside the column. The protein was purifed in one run, and demonstrated a single large peak starting at approximately 35 mL after protein injection. All fractions in this peak (B3 – C5) were considered important in terms of protein presence, however not all could be included on the SDS-PAGE gel and so every second fraction was analysed by SDS-PAGE.

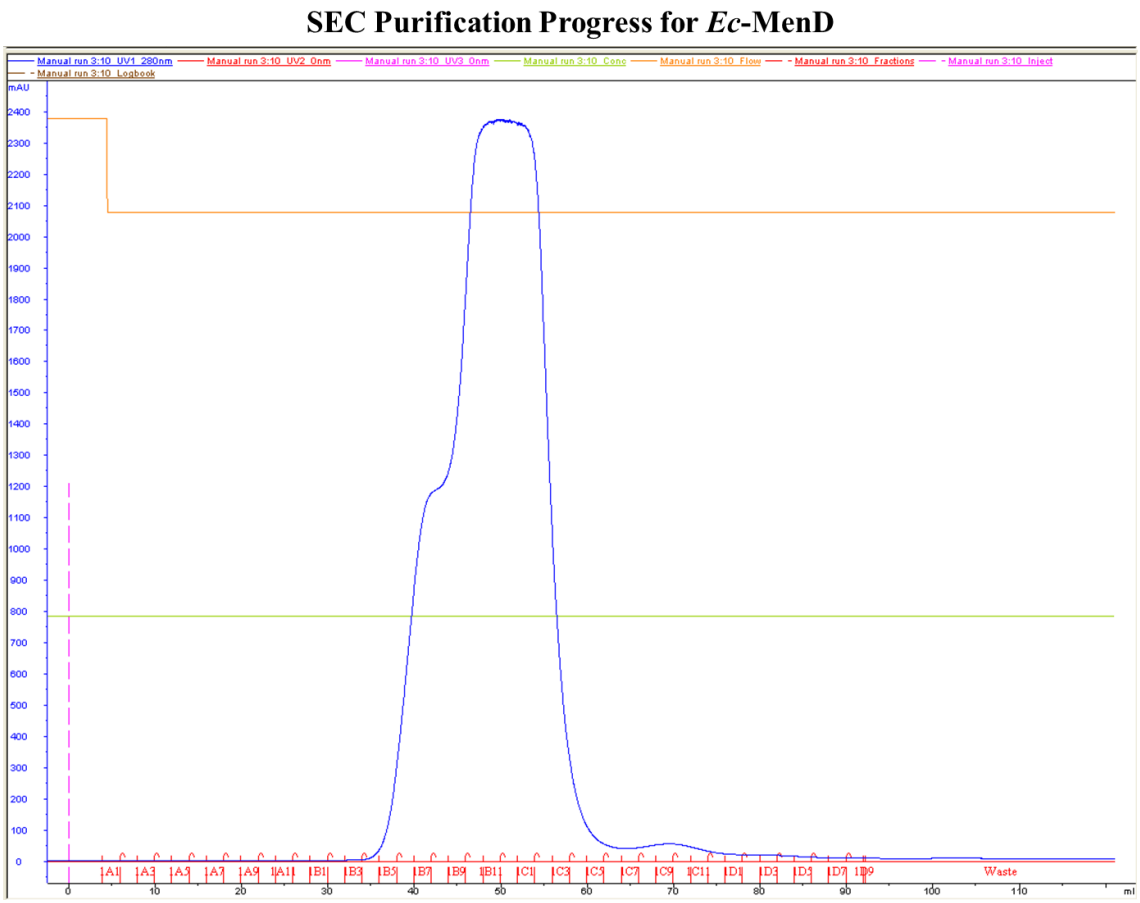

Figure 12: *Ec*-MenD SEC chromatogram. Blue line shows UV absorbance at 280 nm. One major broad peak observed between 30-60 mL.

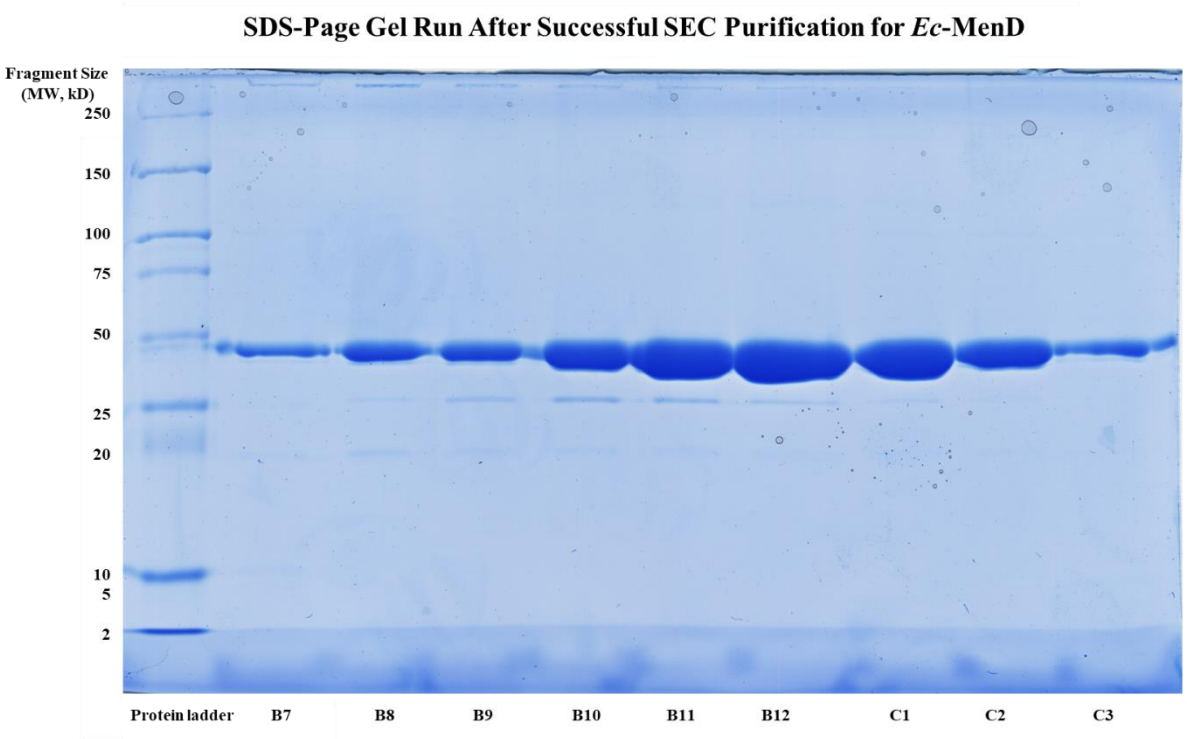

Figure 13: SDS-PAGE demonstrating progression of SEC purification. From left to right: Protein standard, fraction B7, B8, B9, B10, B11, B12, C1, C2, C3. Fractions B9-B12 appear to have a second smaller band below the protein.

3.3 *Smeg*-MenD

The N-terminal hexa-histidine tag on the *Smeg*-MenD protein was removed using rTEV (rTEV site which was incorporated into the *Smeg*-MenD protein was utilised) and hence this protein purification required additional steps compared to *Ec*-MenD. This is detailed in chapter 2 (sections 2.5, 2.6).

3.3.1 IMAC Step 1

IMAC purification successfully separated *Smeg*-MenD in the cell pellet from the protein mix found. Figure 14 demonstrates a progressive protein separation throughout the purification process with the majority of *Smeg*-MenD found at fractions 4-7.

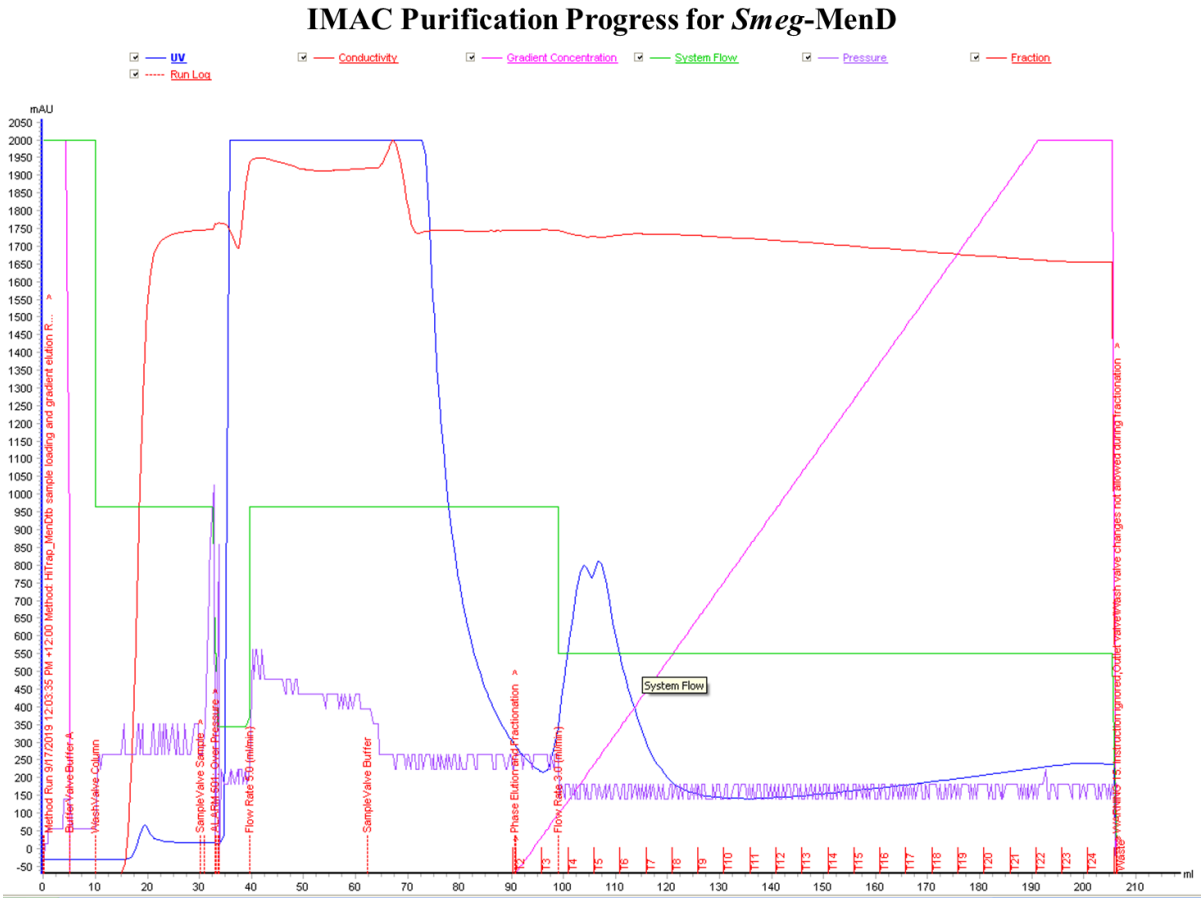

Figure 14: IMAC of *Smeg*-MenD chromatogram. The blue line highlights the UV readings of the protein with higher UV recordings likely correlating to protein presence.

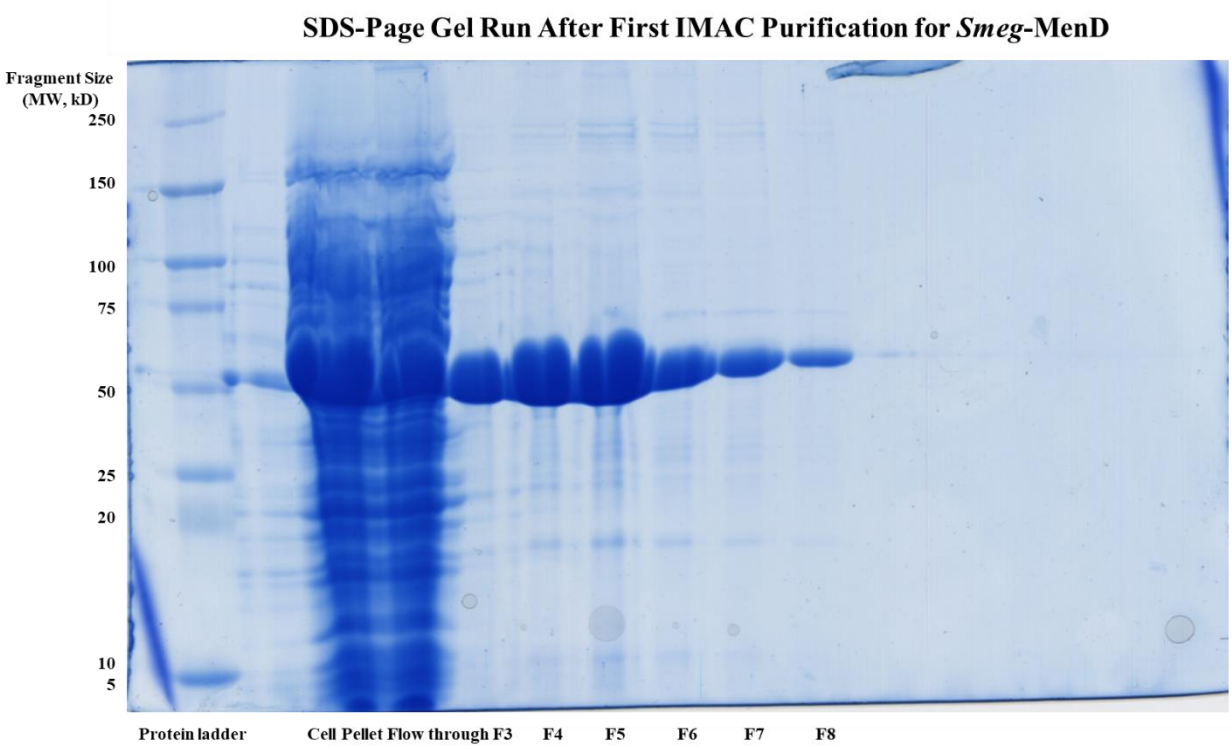

Figure 15: SDS-PAGE including both progression from before and including IMAC purification. From left to right these are; Standard/gel ladder, blank space, Cell pellet after centrifugation, flow through from IMAC, fraction 3, 4, 5, 6, 7, 8.

3.3.2 Cleavage with rTEV and Reverse IMAC

Fractions with positive confirmation of purified protein were pooled for dialysis (50 mL). These fractions were placed in dialysis tubing and set in a non-imidazole containing buffer for dialysis. Prior to dialysis, 500 µL of rTEV protein was added to the protein fractions to remove the histidine tag (as mentioned in chapter 2). The dialysis setup was placed at 25 ˚C overnight.

SDS-PAGE analysis of the initial cleavage suggested that the tag had not completely cut (Figure 16). A reverse IMAC was undertaken to check for any completely cleaved protein. A broad region of low absorbance was observed in the flowthrough followed by two more standard peaks (fractions 4-5 and then 6-7). The fractions were analysed on an SDS-PAGE gel, which suggested only one band was present. As these had stuck to the IMAC column it was considered likely they still retained their tag. At the time of this work the flowthrough observation was not thought to contain protein and so was not used in further purification however after further purification work it has been noted that this was likely a significant amount of cut protein.

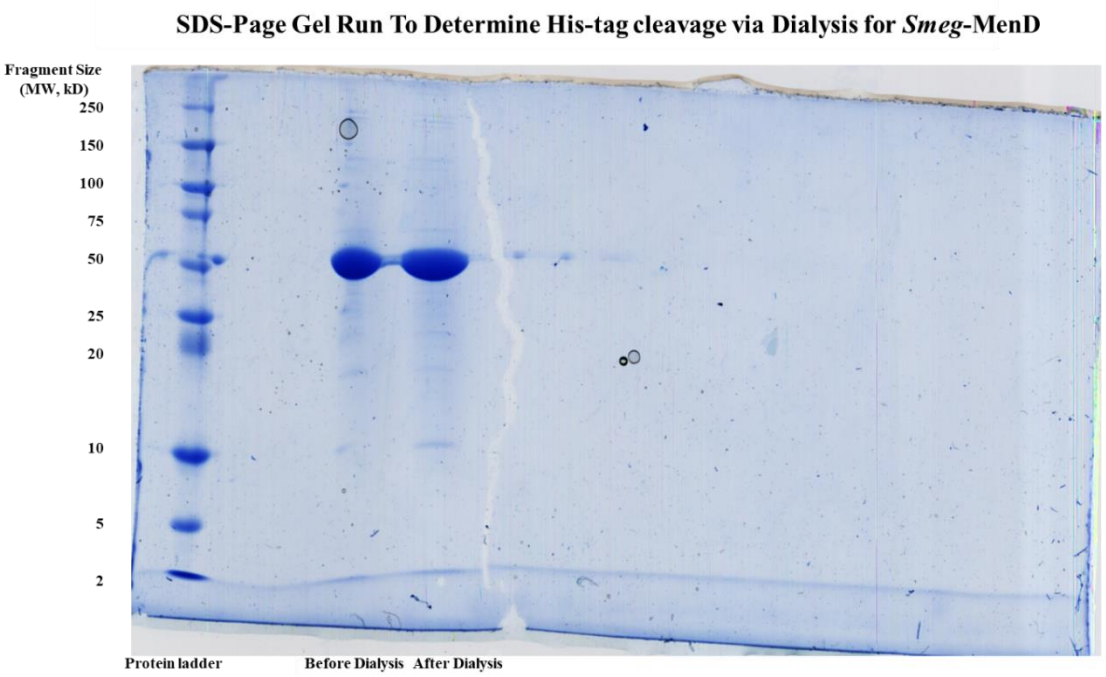

Figure 16: SDS-PAGE from first *Smeg*-MenD dialysis (His-tag cleavage) experiment. From left to right; protein standard, protein before dialysis, protein after dialysis. The small yet distinct band at the bottom of this well is likely the rTEV protein presence.

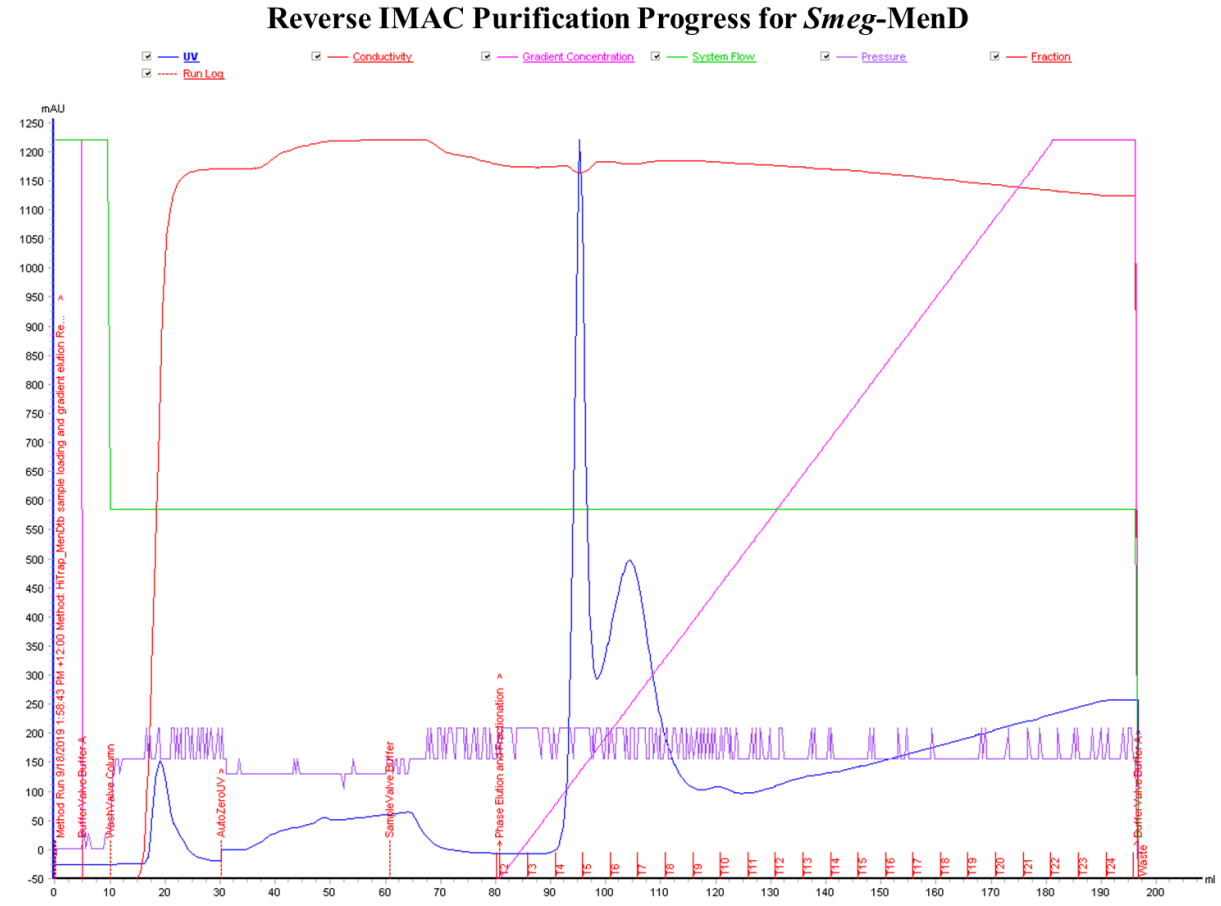

Figure 17: *Smeg*-MenD reverse IMAC chromatogram. Unlike the first IMAC experiment the UV peaks are more specific and cover a smaller range of volume, implying higher specificity in the protein than previous.

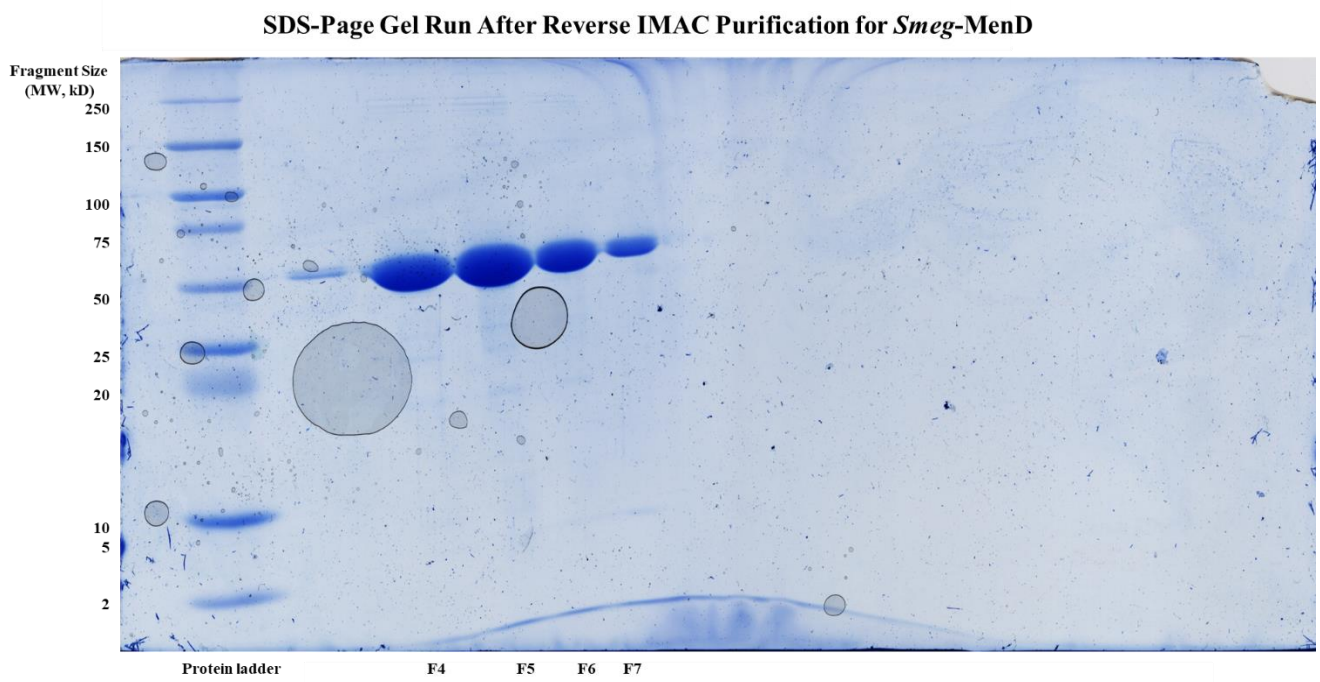

Figure 18: Gel run focusing on the fractions from the reverse *Smeg*-MenD IMAC experiment. From left to right; protein standard, space, fraction 4, 5, 6, 7.

Fractions 4-5 were pooled as were 6-7 and a higher concentration of rTEV (1 mL of 500 µM for 30 mL) was added. The two pooled proteins were dialysed at 37˚C for 5 hours followed by 4˚C for 3 days. A gel was run again to confirm if successful cleavage had occurred in either case. However, the amount of protein used to check appeared to be overloading the wells and made it difficult to determine the presence of two different bands. A second gel run with less protein present in the wells was also completed and this distinctly displayed successful cleavage of the histidine tag on *Smeg*-MenD (seen in Figure 19, 20).

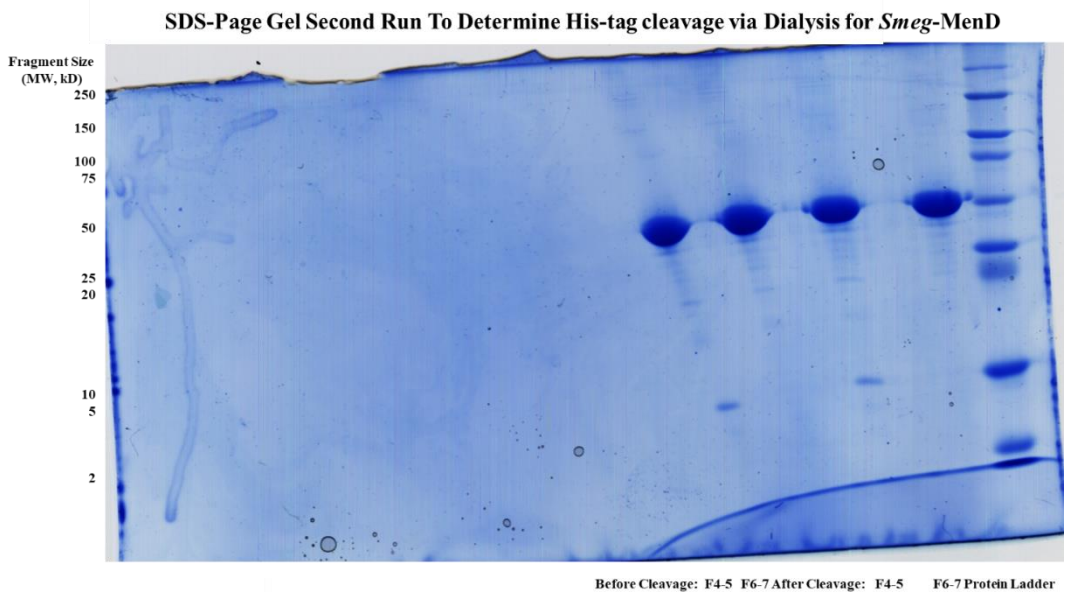

Figure 19: SDS-PAGE from the second *Smeg*-MenD dialysis (His-tag cleavage) experiment. From left to right, fractions 4-5 before cleavage, fractions 4-5 after cleavage, fractions 6-7 before cleavage, fractions 6-7 after cleavage, protein standard. Both fractions before cleavage display a band at a much lower molecular weight, which is likely to correspond to rTEV.

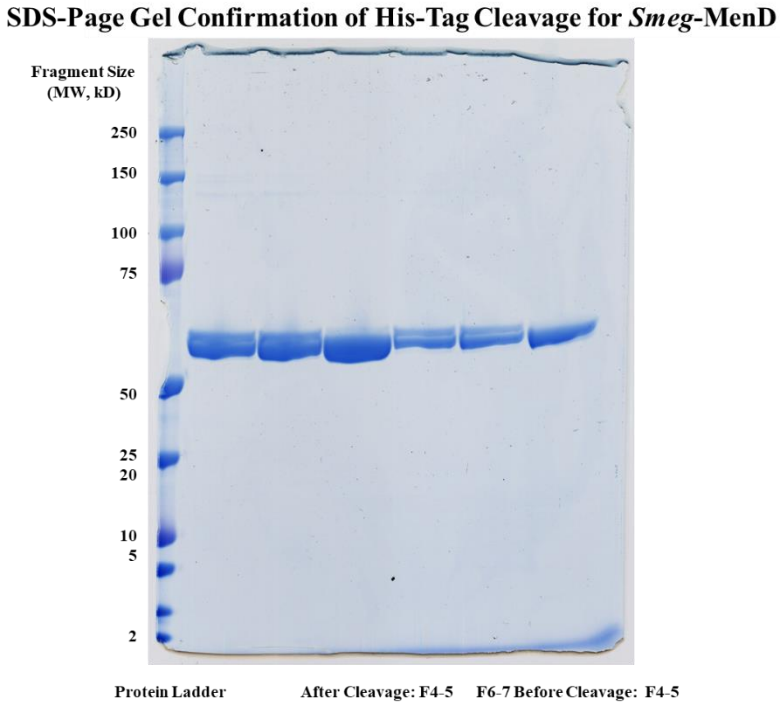

Figure 20: Second SDS-PAGE for second *Smeg*-MenD dialysis with reduced protein volume for better identification of the two protein bands. The only relevant bands for this gel run are the 4th, 5th, and 6th from the right as these are pooled fractions 4-5 after cleavage, pooled fractions 6-7 after cleavage and fraction 4-5 before cleavage.

3.3.3 *Smeg*-MenD SEC

The protein from the second rTEV cleavage attempt was not further purified by reverse IMAC. Instead the protein was purified by size exclusion chromatography using S200 10/30. Protein was concentrated and purified in three runs. As seen in Figure 21, each protein load provided an identical purification reading, with peaks of interest at 1-2 and 4-6 for A, B and C. Of the most interest were the peaks at 4-6 as the protein was expected to take 10-12 mL of buffer run through the column before the protein would then come off. Any peaks observed before 10-12 mL of buffer were considered void volume. This void volume generally contains any aggregated protein. Above this volume it is less likely that any peaks are of aggregated protein because this is consistent with the observed tetramer elution found with *Mtb*-MenD purification These were then loaded onto a SDS-PAGE gel for further confirmation of protein presence. All three runs of the SEC column demonstrated similar results as seen on the gel in Figure 22.

SEC Purification Progress for *Smeg*-MenD

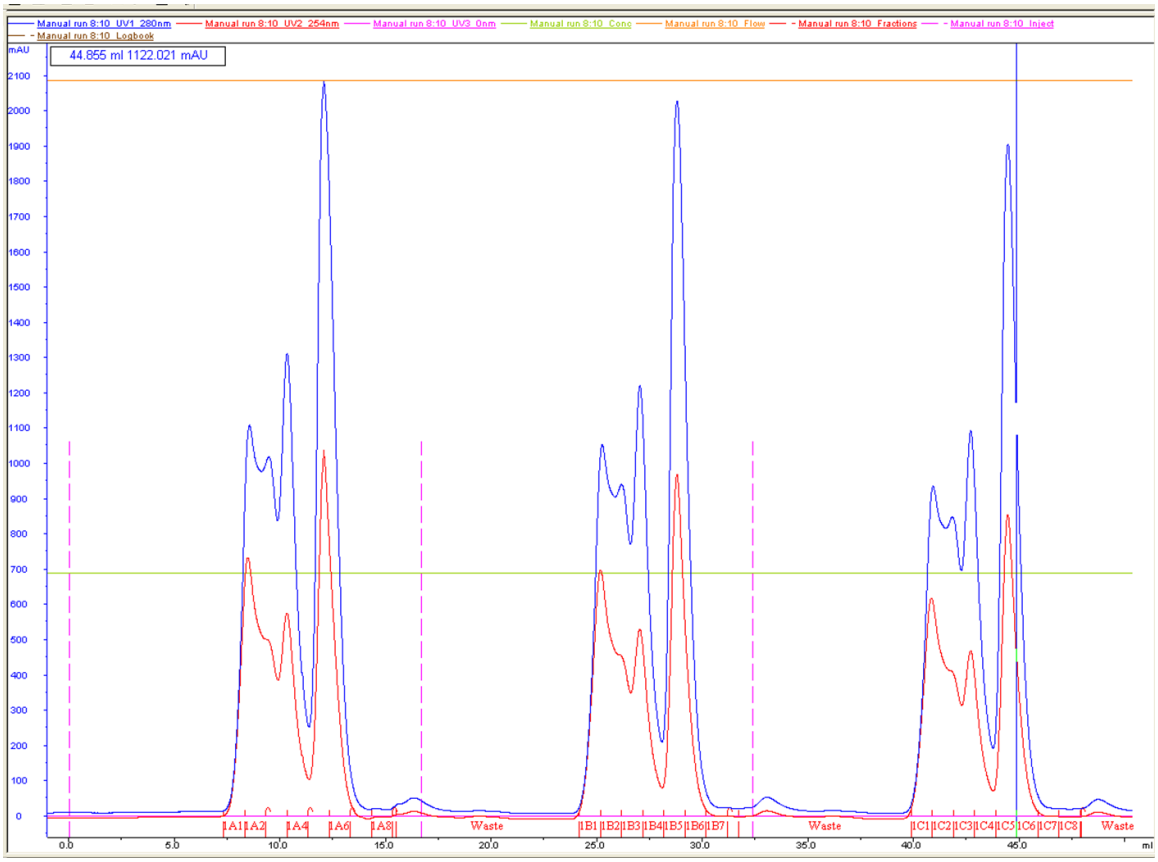

Figure 21: *Smeg*-MenD SEC purification chromatogram. The blue line represents the UV absorbance readings at 280 nm and the red line represents UV absorbance readings at 254 nm. The overall trends are seen repeated between all three runs.

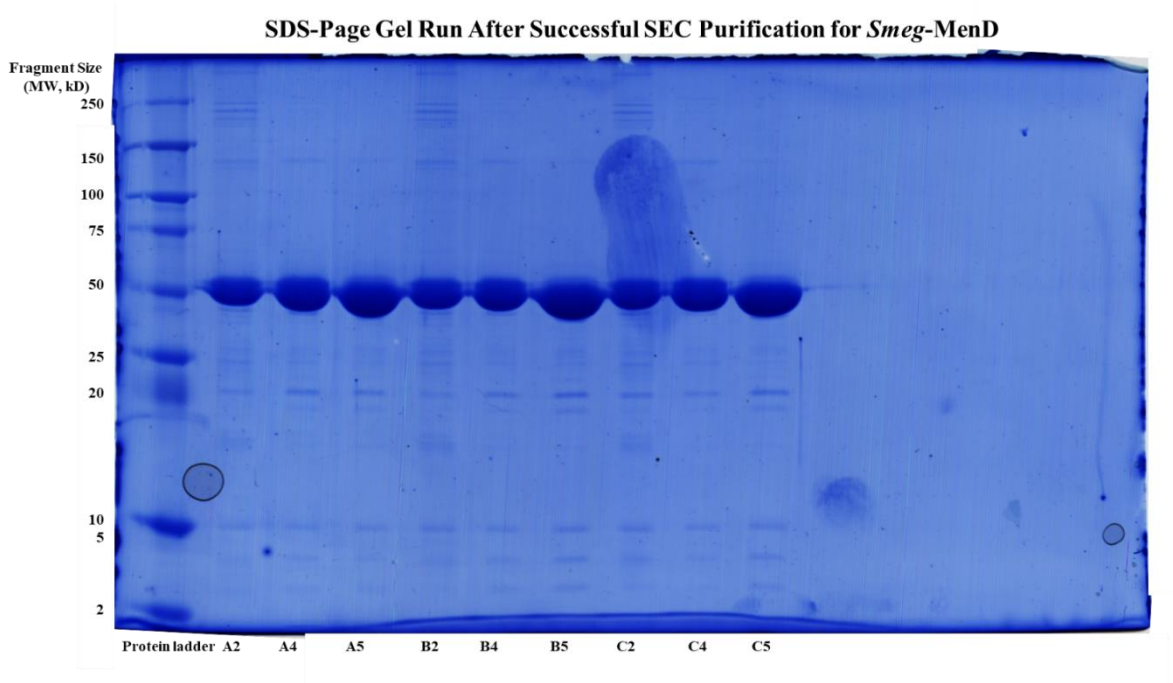

Figure 22: SDS PAGE after successful SEC purification. From left to right: Protein standard, Fraction A2, A4, A5, B2, B4, B5, C2. C4, C5. Each well shows additional bands below the protein, with the second band below the protein likely to correspond to the TEV protein.

Chapter 4. Intrinsic Fluorescence Quenching Measurements of Ligand and Substrate Binding to MenD from *S. aureus*, *E. coli*, and *M. smegmatis*

4.1 Introduction

4.1.1 Background and Overall Goals

The main goal of the work presented in this chapter was to determine the binding affinity of various MenD substrates and ligands. This goal had two primary aims:

- The determination of whether DHNA binds, and binds with a similar affinity, in MenD enzymes from three different species as it does to *Mtb*-MenD. If DHNA does bind equivalently between these MenD enzymes this suggests that inhibitors that bind preferentially over DHNA will do so in all enzymes, and consequentially would bind equally to all disease-relevant MenD enzymes, such as *Mtb*-MenD.
- An investigation into the binding of ThDP, and 2-oxoglutarate. ThDP and 2-oxoglutarate are the co-factor and substrate of MenD, respectively, so determining and comparing the binding strength of these compounds between MenD enzymes from different species is beneficial information for drug design.

The three compounds used in these experiments were DHNA, ThDP, and 2-oxoglutarate. ThDP, or thiamine diphosphate is the co-factor essential to the ability of the enzyme to decarboxylate 2-oxo acids. ThDP binds in the active site in a divalent metal-ion dependent manner.

2-Oxoglutarate is the ligand responsible for the formation of SEPHCHC by MenD. When bound to ThDP, 2-oxoglutarate undergoes a decarboxylation reaction which then prepares the ligand to interact with isochorismate, with which it will then form a new carbon-carbon bond. Like ThDP, 2-oxolgutarate binds to the active site of MenD.

By contrast, DHNA does not bind to the active site of MenD, instead binding to an allosteric site. DHNA is the product of MenI, an enzyme further along in the menaquinone biosynthesis pathway, and is a negative feedback regulator for the biosynthetic cycle in *M. tuberculosis*.

4.1.2 Intrinsic Fluorescence Quenching for Measuring Binding Interactions

A range of different methods are available to detect small molecule binding to proteins. These methods include but are not limited to: surface-plasmon resonance, isothermal titration calorimetry, differential scanning fluorimetry, and mass spectrometry. Each technique provides its own unique strengths and weaknesses in this characterisation process, which can often depend on the system under study and the binding parameters which are capable of being measured.

One method to detect small molecule binding to proteins is the use of intrinsic fluorescence quenching assays (IFQ). These assays use naturally occurring tryptophan residues present in the proteins in question to investigate the binding of any ligand that could cause changes in the fluorescent properties of these tryptophan residues. By measuring fluorescence as a function of ligand concentration, binding curves can be generated that show proportional changes in fluorescence correlated to ligand binding in a protein. These binding curves can be fitted with equations for binding to derive dissociation constants that describe the strength of binding interaction.

Several research groups have previously used this method for characterising the binding of ThDP to ThDP-dependent enzymes [68, 70]. Assuming that any ligand binding (including ThDP) to either the active site of MenD or an allosteric site will result in a change of fluorescence, IFQ can be a useful technique for measuring binding affinities for MenD ligands. A major advantage of using IFQ is the relatively small amount of protein consumed in experimental work, as well as the technique being label-free, producing results with less potential for interference or artefacts.

4.1.3 Prior IFQ-based Studies of *Mtb*-MenD

Previously completed work in this field has established the *Mtb*-MenD allosteric site [41]. This site contains several key conserved residues, namely Tyr95, Arg97, Arg277, Arg303 and Trp304. These residues are key to binding the inhibitor DHNA, with the residue of highest interest for this work being the Trp304 [41]. The main structure of the allosteric site of *Mtb*-MenD is an arginine 'cage' made up of Arg97, Arg277 and Arg303 (Figure 23) [41]. These three arginine residues surround DHNA in its binding site and all interact directly with DHNA. In addition, these arginine residues are potential candidates for signalling between the allosteric and active site of *Mtb*-MenD. The residue Trp304 is of particular interest in relation to IFQ experiments due to the high level of intrinsic fluorescence this amino acid contains and the proximity of this particular tryptophan residue to the allosteric site. Any changes observed in the intrinsic fluorescence of the enzyme are likely going to contribute at least in part to an effect upon this residue specifically.

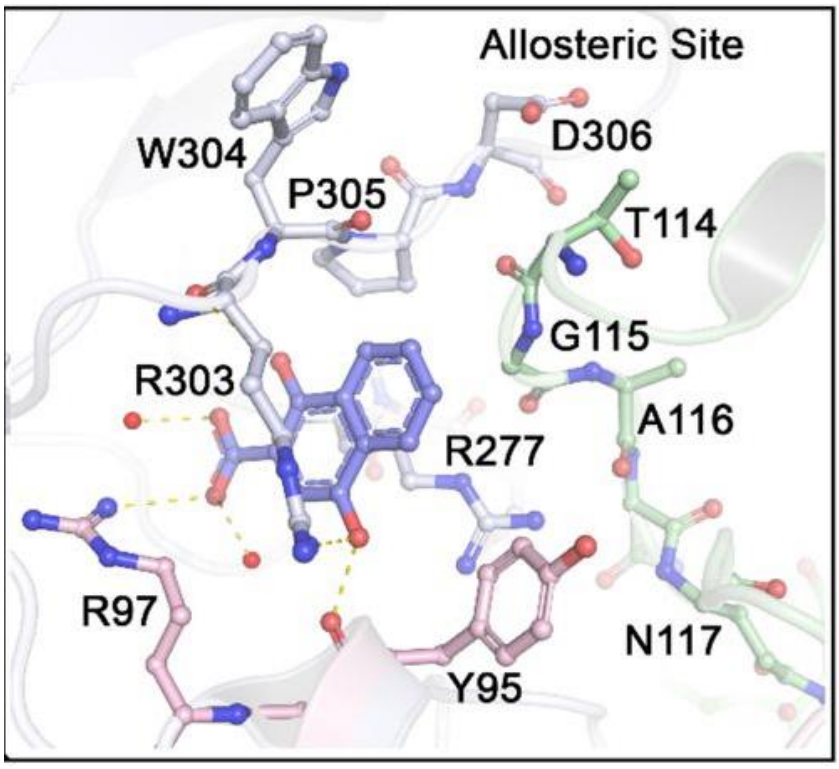

Figure 23: Allosteric site from *Mtb*-MenD with the conserved and important residues labelled. Three arginine residues make up the cage (Arg97, Arg277, Arg303) while the most fluorescently important (Trp304) is near the allosteric site. Image adapted from[41].

In previous IFQ work on *Mtb*-MenD conducted by Dr Thu Ho and Dr Tamsyn Stanborough, ThDP binding was not able to be measured due to binding not causing any change in fluorescence after inner filter effect corrections were applied. However, this technique was discovered to be suitable for measuring DHNA binding and could prove to be useful for 2-oxoglutarate as well.

4.1.4 Active and Allosteric Sites of *Ec*-MenD, *Sau*-MenD and *Smeg*-MenD

The sequence alignment shown in Appendix 1 demonstrates a large degree of conserved residues in all four MenD species, in particular those residues also located in the active site for *Mtb*-MenD. The key residue Glu55 is found to be conserved, alongside both an Asp and Arg residue before and after respectively. Similarly, the His445 residue is also found to be conserved in three of the four MenD enzymes, with *Ec*-MenD replacing this with a Tyr instead. All four enzymes however have a conserved Asp residue directly following this residue, suggesting some degree of conservation present. The remaining two key residues found in the active site, Ile404 and Ala402 are found conserved in all proteins for Ile, and only in *Smeg*-MenD and *Mtb*-MenD for Ala402. The residues which make up the allosteric site for *Mtb*-MenD have been determined, but these don't appear highly conserved across all MenD enzymes from other species, and in general domain II, where the allosteric site resides, is the least conserved of the domains. Experimental work such as IFQ which manipulates the intrinsic fluorescence of residues such as Trp can provide information on if MenD enzymes from other species can bind to the allosteric effector DHNA despite the lack of conservation. This can be determined based upon the amount of fluorescence present in the protein and how large of an effect the binding of DHNA has on this signal. Table 13 shows the number of Trp residues present in each of the MenD enzymes, with a secondary count of which of these Trp residues are not conserved between at least three of the proteins. It is immediately clear that *Ec*-MenD is expected to exhibit the most fluorescence activity of all the proteins, with 17 Trp residues present. The remaining three proteins have only four Trp residues, with *Mtb*-MenD and *Smeg*-MenD observed to have identical Trp residue locations. There is only one Trp residue that is conserved between all four proteins, Trp 328. This is neither in the allosteric site nor the active site but is not too far from the 299-310 region that contributes to the allosteric site. The Trp304 in the allosteric site of *Mtb*-MenD is not conserved in any other protein but *Smeg*-MenD. In addition, because the proteins are known to be conformationally flexible when binding to their co-factor and substrates even in the absence of a Trp directly in the active site there is a possibility that there will be quenching detectable from even remote Trp's on ligand binding.

Table 13: Count of tryptophan (Trp) residues present in each MenD protein.

	Number of Trp Residues	Number of Non-conserved Trp
Mtb-MenD	4	1
Smeg-MenD	4	1
Ec-MenD	17	13
Sau-MenD	4	2

4.2 IFQ Experiments with *Sau*-MenD

For all IFQ experiments no replicates were completed due to time constraints. This limits the interpretation of the results as they are yet to be replicated. Future work requires these IFQ experiments to be replicated for any publications to be made from this work.

4.2.1 ThDP

The magnitude of quenching intensity observed in the ThDP binding experiments with *Sau*-MenD was modest, yet the signal was sufficient to show clear binding (Figure 24) with an estimated K_d in the micromolar range both in the presence and absence of 2.5 mM TCEP (Table 14). The presence of TCEP appeared to increase the K_d but also changed the shape of the curve which fitted better to the bimodal equation implemented in the Allison *et al* IFQ analysis package used to create the graphs. Both results are within the micromolar range and the absence of replicates leads us to be unable to draw conclusions on any significance in the differences with TCEP added.

Table 14: K_d values of *Sau*-MenD under various ThDP conditions

	K_d with $MgCl_2$ added (µM)	Sigma	K_d with $MgCl_2$ added (µM)	Sigma
ThDP	47.0	0.4	-	-
ThDP with TCEP Present	79	2	0.06	0.01

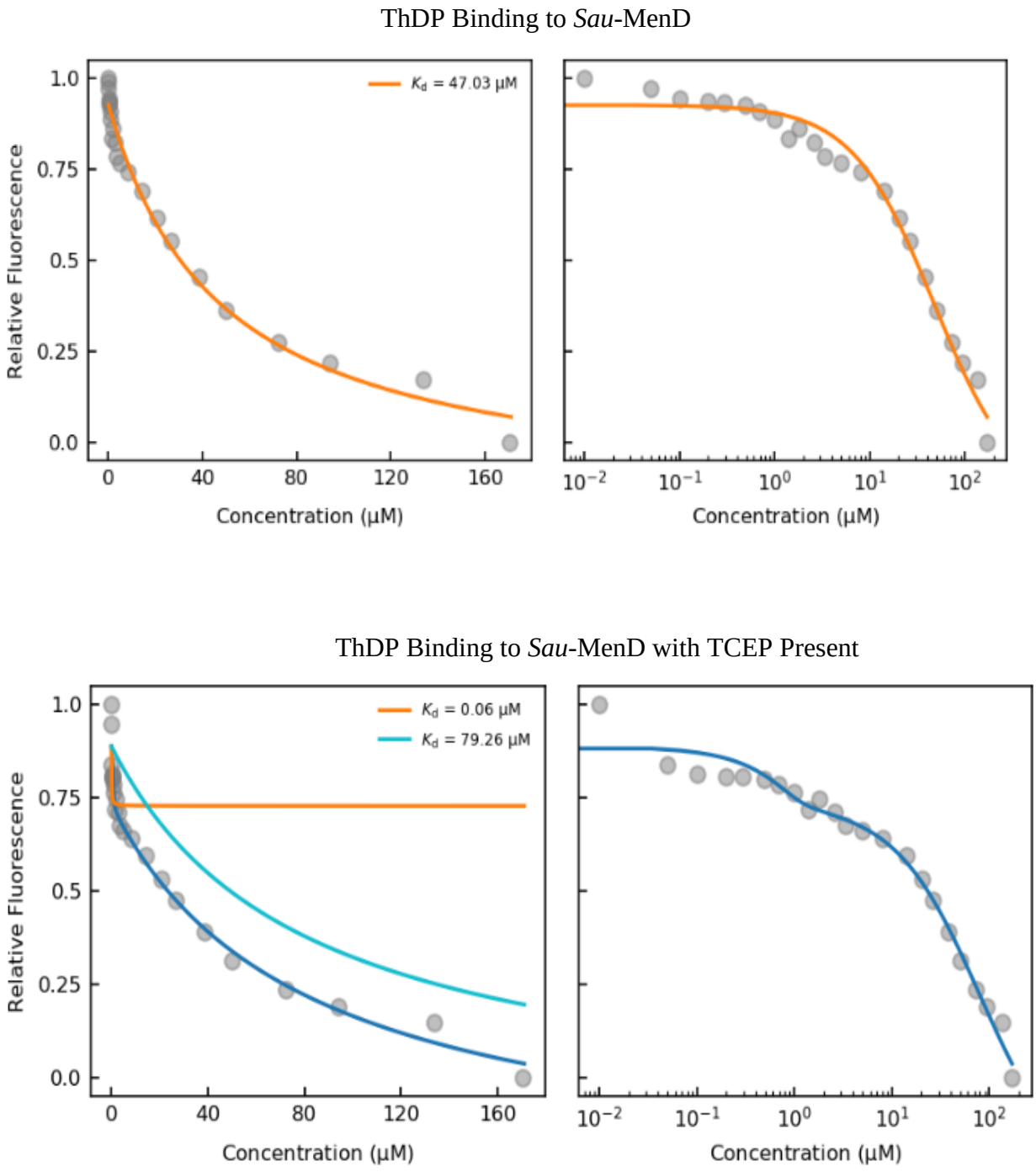

Figure 24: Top (a): ThDP binding to *Sau*-MenD with $MgCl_2$ present. **Bottom (b):** ThDP binding to *Sau*-MenD with $MgCl_2$ and TCEP present.

4.2.2 2-Oxoglutarate

This ligand is a substrate of MenD and will react, so the K_d calculated could be from binding or changes during reaction or a combination thereof. It therefore is not technically a K_d, but a measure of interaction nonetheless. Due to time constraints this complexity was not explored further in this thesis and for simplicity we have termed it K_d in the following discussion. Experiments involving 2-oxoglutarate addition included 100 µM ThDP in the protein buffer mix and were incubated for an hour to ensure full interaction between protein and ThDP occurred. The experiment involving 2-oxoglutarate and ThDP did not provide useable results from this work and so has been omitted. The 2-oxoglutarate binding in the presence of ThDP and TCEP K_d is estimated to be in the low micromolar region (5.4 µM, Table 15). This suggests tighter binding of 2-oxoglutarate than ThDP with a 10-16-fold lower K_d than that measured for ThDP. However, the 2-oxoglutarate experiments show lower quenching signal and more noise (reflected in the lack of data for TCEP free experiments) so the significance of this would need to be confirmed by replicate experiments. Due to the absence of the experiment without no TCEP, it is difficult to determine what effects TCEP may have on the measured K_d and magnitude of binding of 2-oxoglutarate.

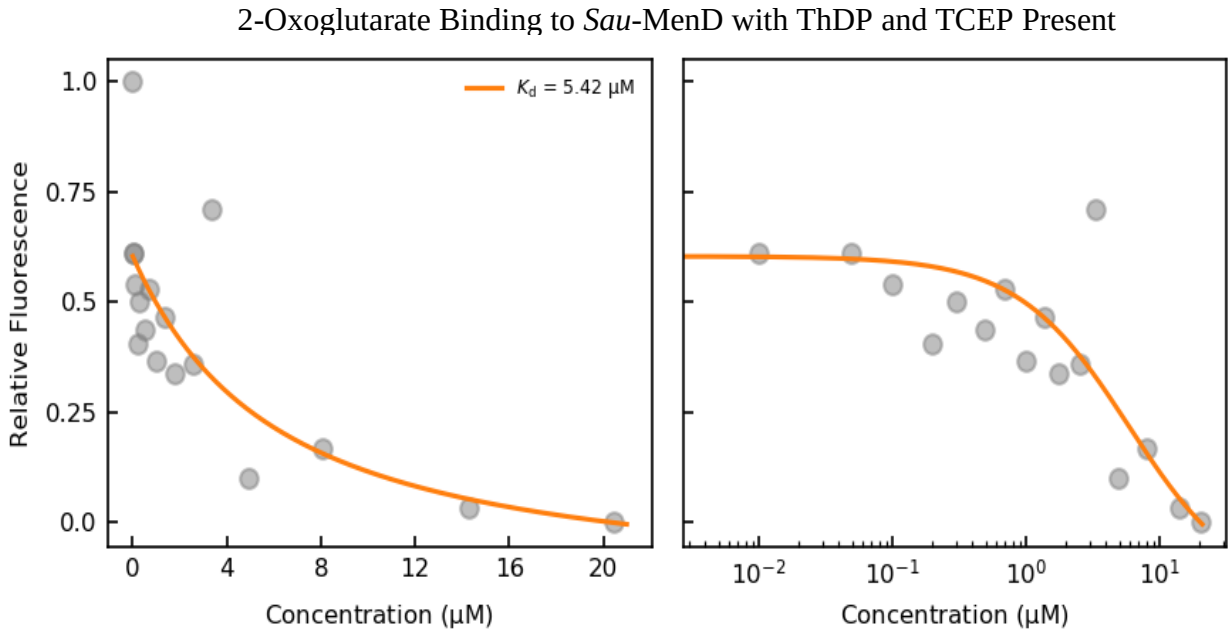

Figure 25: 2-Oxoglutarate binding to *Sau*-MenD with $MgCl_2$, ThDP and TCEP present.

Table 15: K_d values of *Sau*-MenD with $MgCl_2$, ThDP and TCEP present.

	K_d With $MgCl_2$ Added (μM)	**Sigma**
2-Oxoglutarate with ThDP and TCEP Present	5.4	0.4

4.2.3 DHNA

The majority of the IFQ experiments for all proteins used DHNA, as this inhibitor was of the most interest. Initial experiments looked at the quenching of DHNA in buffer with and without the presence of TCEP. As mentioned before the use of TCEP was due to its strong reducing potential and the ability of DHNA to oxidise during the experiment in its absence. DHNA is also unique compared to the previous ligands as it is an allosteric inhibitor rather than being found at the active site.

Binding of DHNA to the protein in the presence and absence of 2.5 mM TCEP produced almost identical results (Figure 26 a and b) with a K_d of ≈1 μM (Table 16) suggesting tight binding and supporting the idea that this allosteric regulator does bind and could have a similar allosteric inhibition as observed in *Mtb*-MenD.

Experiments involving DHNA binding with 100 µM ThDP present in the buffer suggests a lower binding affinity for DHNA with an estimated K_d about 50-fold less (of 57 µM, Figure 26c, Table 16) compared to solely DHNA binding. When ThDP and TCEP is present the curve fitting that appears to fit best is bimodal, suggesting a higher and lower affinity DHNA binding site may be present. The higher binding site being tighter than that seen in the apo protein DHNA binding experiments (1 µM versus <0.03 µM, Figure 26d, Table 16) while the second site is lower (171.3 versus 1 µM, Table 16, Figure 26d). This is an interesting finding which may suggest an interaction or a conformational change of *Sau*-MenD when ThDP is bound which interferes or affects DHNA binding, and hints that this could affect the symmetry of the four potential DHNA binding sites in the tetramer. The significance of the differences between the experiments with and without TCEP is unclear, however TCEP keeps DHNA reduced so the clearer results with TCEP present may reflect the ability of TCEP to keep DHNA in an oxidation state that is preferred for binding. It may also be the bimodal nature of the ThDP without TCEP binding curves was missed in this analysis (which would affect the K_d estimated here) and indeed close inspection of the graphs suggests this may be bimodal as well. Experiments measuring the binding of DHNA to protein where both 100 µM ThDP and 2-oxoglutarate were present, show similar binding K_d estimates to the apo protein, while with TCEP fitted best to the bimodal curve fitting with a tight and weaker binding affinity site. These experiments were not done in replicate so any firm conclusion is pre-emptive, nonetheless these findings confirm DHNA binds consistently to the protein in many different catalytic states and may show differences when co-factor is bound. This preliminary finding is interesting and well worth exploring further with additional replicate experiments.

DHNA Binding to *Sau*-MenD

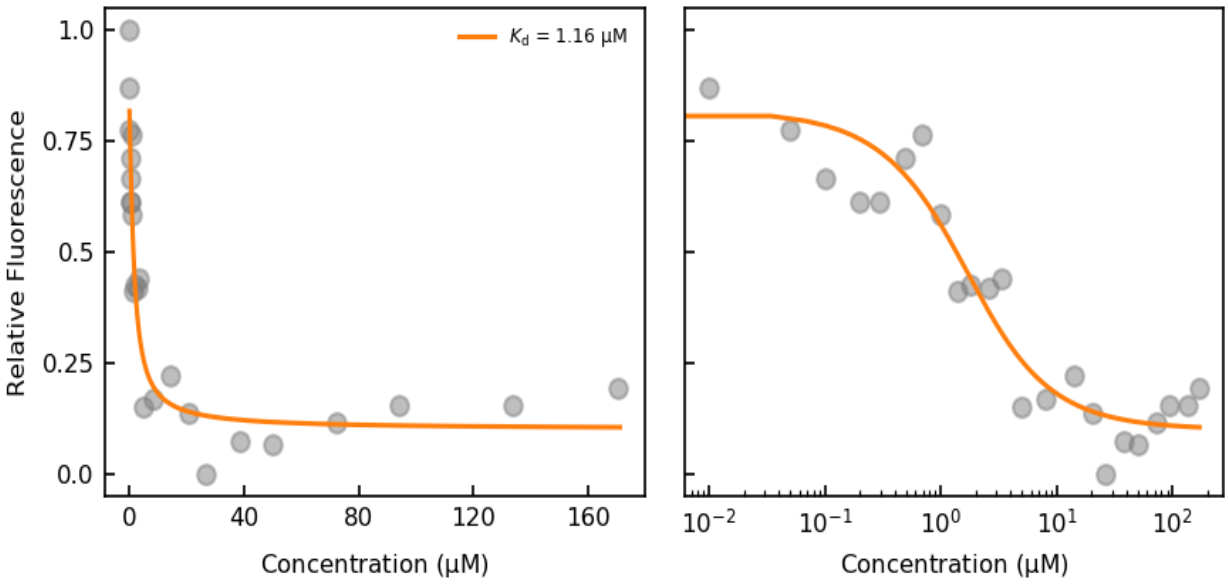

DHNA Binding to *Sau*-MenD in the presence of ThDP

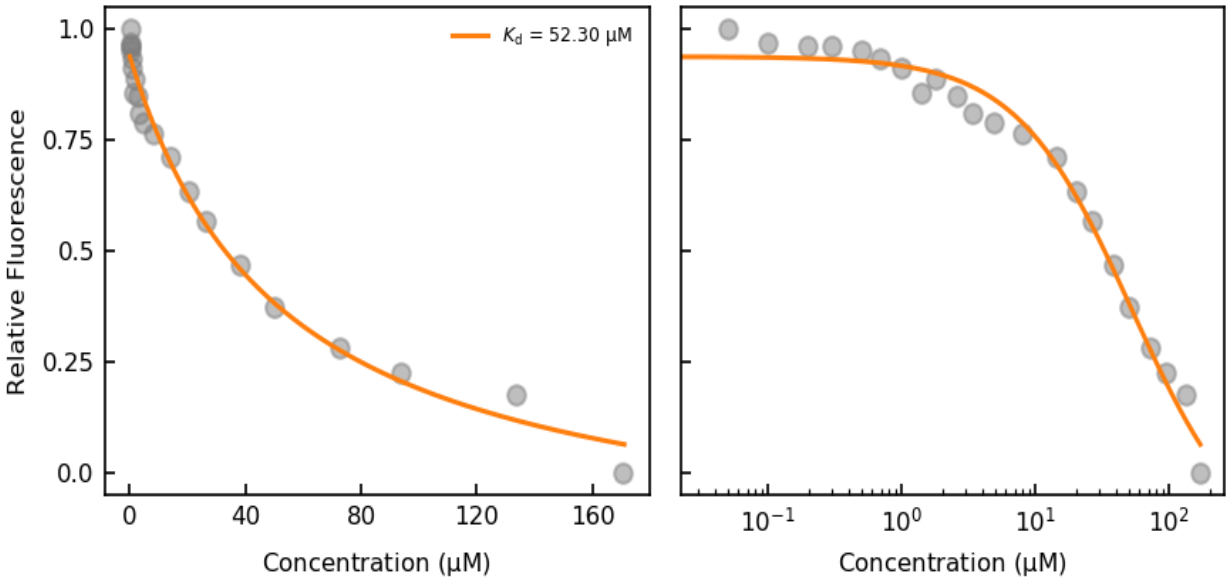

DHNA Binding to *Sau*-MenD in the presence of TCEP

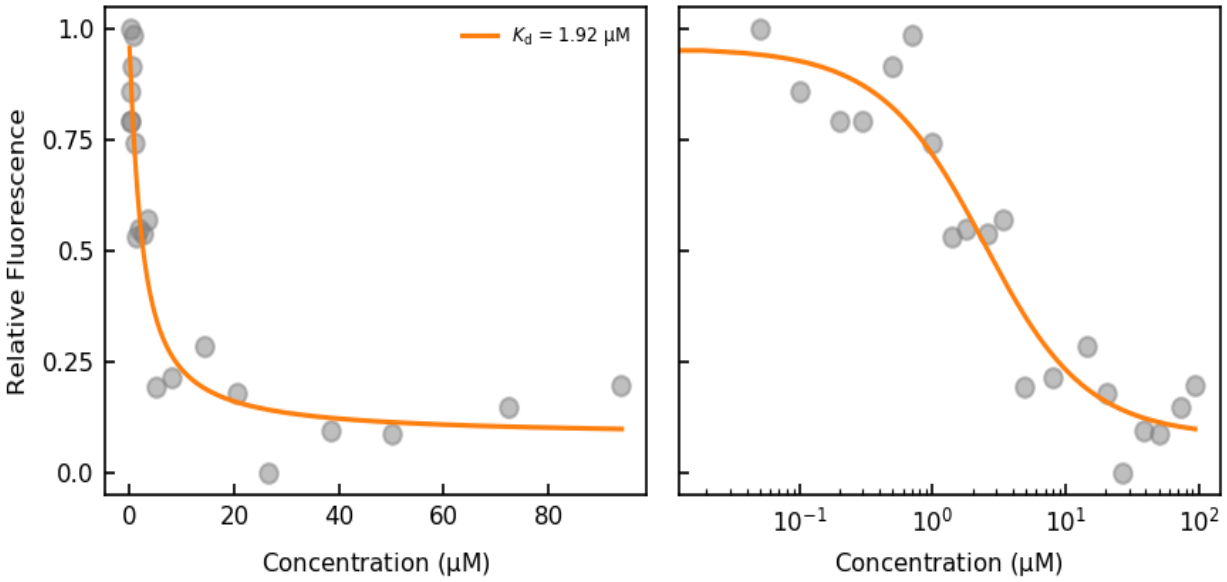

DHNA Binding to *Sau*-MenD in the presence of ThDP and TCEP

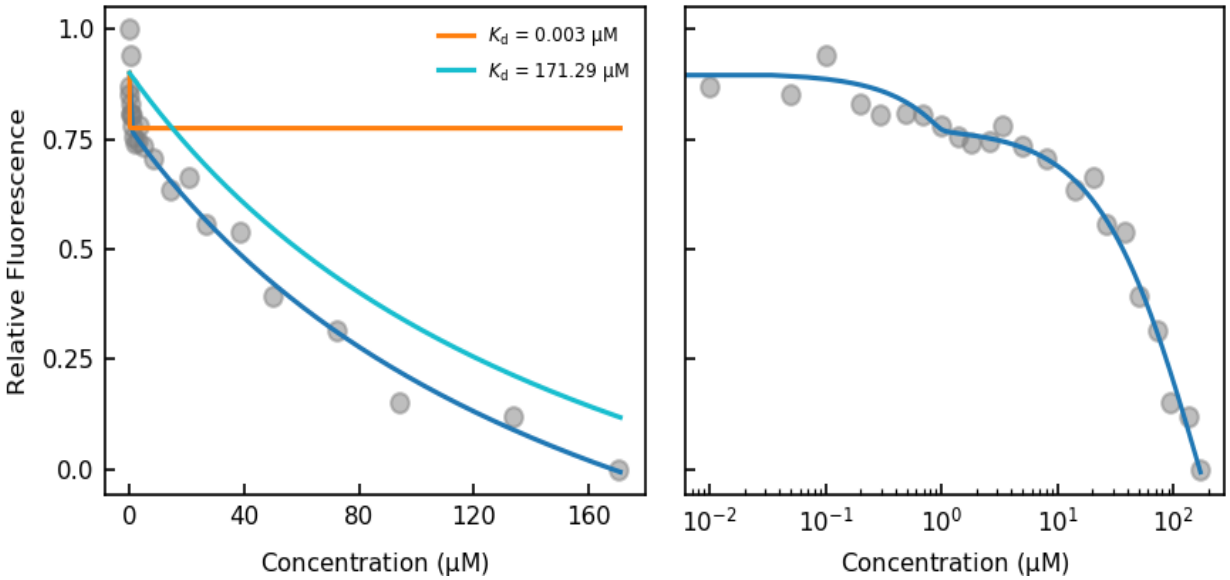

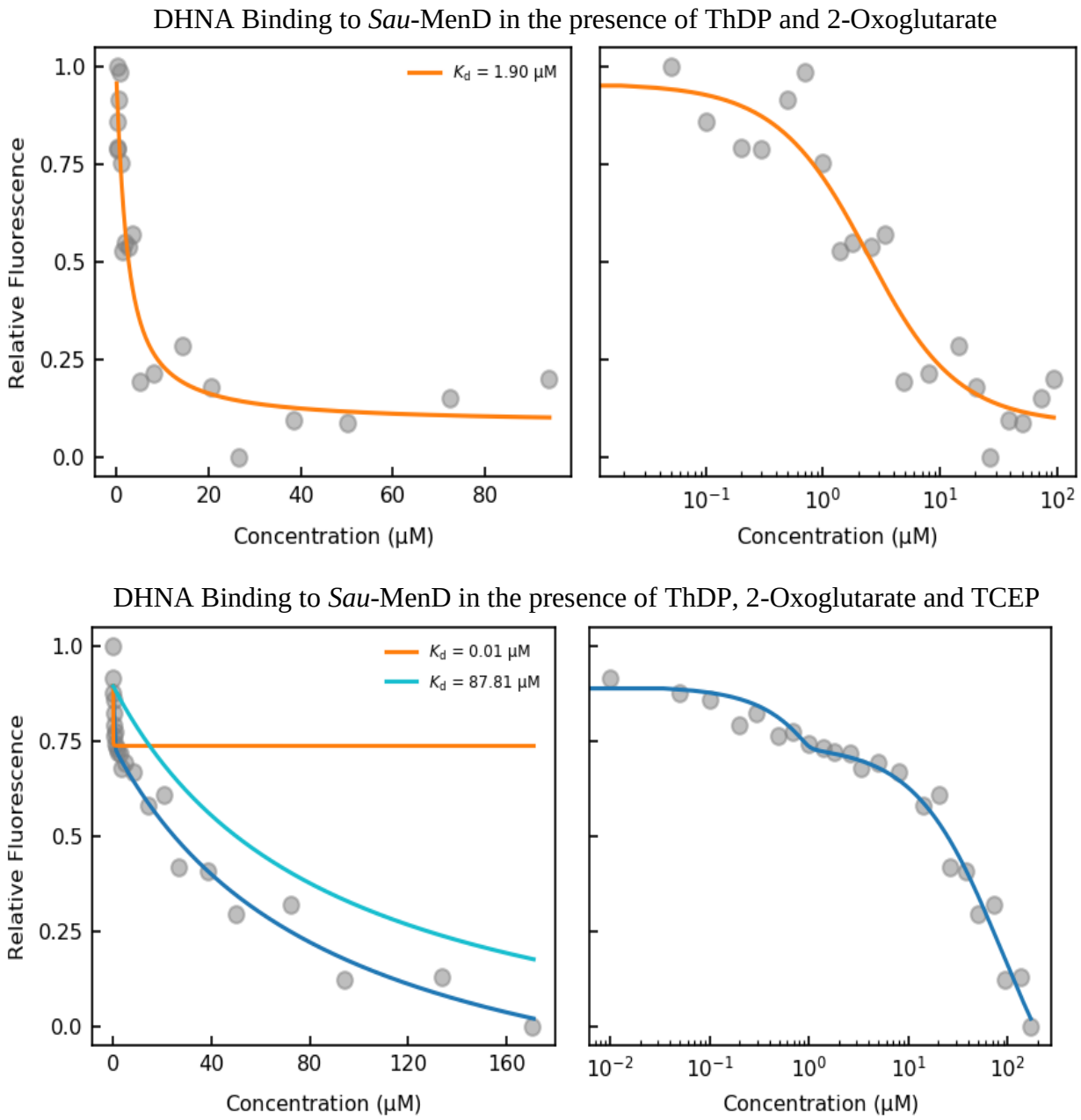

Figure 26: DHNA binding to *Sau*-MenD under various conditions. **1st Row (a):** $MgCl_2$ present. **2nd Row (b):** $MgCl_2$ and TCEP present. **3rd Row(c):** $MgCl_2$ and ThDP present. **4th Row(d):** $MgCl_2$, ThDP and TCEP present. **5th Row(e):** $MgCl_2$, ThDP and 2-oxoglutarate present. **6th Row(f):** $MgCl_2$, ThDP, 2-oxoglutarate and TCEP present.

Table 16: K_d values of *Sau*-MenD under various DHNA binding conditions

	K_d With $MgCl_2$ Added (µM)	**Sigma**	**K_d With $MgCl_2$ Added (µM)**	**Sigma**
DHNA	1.2	0.04	-	-
DHNA with TCEP Present	1.9	0.04	-	-
DHNA with ThDP Present	52.3	0.8	-	-
DHNA with ThDP and TCEP Present	0.003	0.000	171	3
DHNA with ThDP and 2-Oxoglutarate Present	1.90	0.02	-	-
DHNA with ThDP, 2-Oxoglutarate and TCEP present	0.01	0.00	88	2

4.3 IFQ Experiments with *Ec*-MenD

4.3.1 ThDP Binding

The binding of ThDP to *Ec*-MenD appears to fit the bimodal equation for curve fitting favourably. This suggests that there is a higher and lower affinity ThDP binding site for *Ec*-MenD, with a significant difference observed between these sites (K_d of 0.003 µM in tight binding site versus 119 µM, Table 17). These results are found in the nanomolar range and the micromolar range respectively, however there is enough of a difference to consider this a significant observation. The presence of TCEP both changed the shape of the curve as it no longer fit best to the bimodal equation and increased the K_d (Table 17). Clear binding of ThDP to *Ec*-MenD was observed in both experiments (Figure 27), however due to the absence of replicates no further conclusions about the effect of TCEP to the binding of ThDP can be made.

Table 17: K_d values of *Ec*-MenD under various ThDP conditions.

	K_d With $MgCl_2$ Added (µM)	**Sigma**	**K_d With $MgCl_2$ Added (µM)**	**Sigma**
ThDP	0.003	0.001	119	4
ThDP with TCEP Present	34.8	0.3	-	-

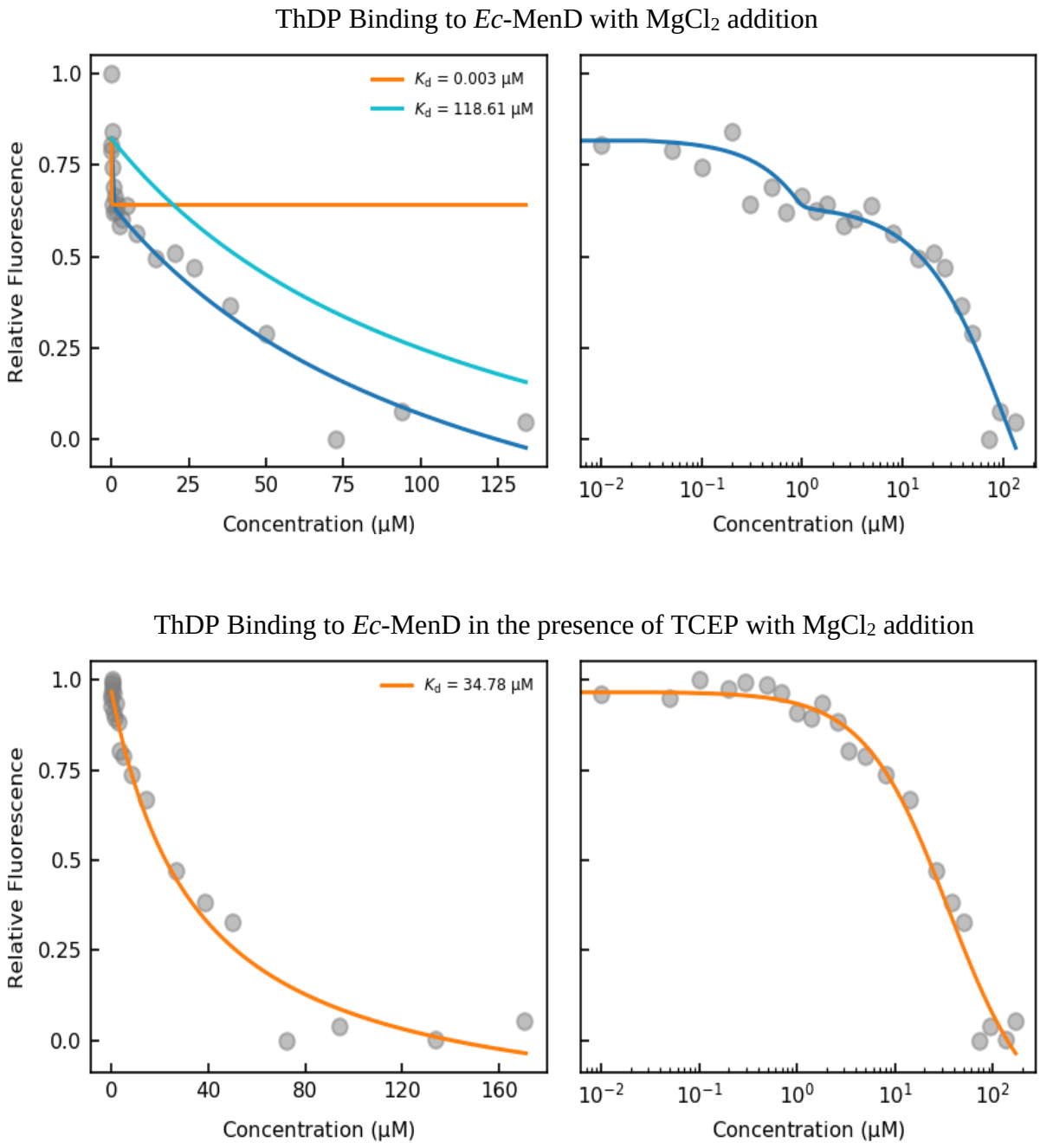

Figure 27: ThDP binding to *Ec*-MenD under various conditions **Top (a):** $MgCl_2$ present. **Bottom (b):** TCEP and $MgCl_2$ present.

4.3.2 2-Oxoglutarate Binding

Experiments involving 2-oxoglutarate addition included 100 µM ThDP in the protein buffer mix and were incubated for an hour to ensure full interaction between protein and ThDP occurred. Binding of 2-oxoglutarate in the presence and absence of TCEP provided nearly identical results (Figure 28), each with incredibly steep decreases in fluorescence over a very minor 2-oxoglutarate concentration increase suggesting tight binding of 2-oxoglutarate to *Ec*-MenD in the presence of ThDP. Only upon further inspection of the respective K_d for these experiments can it be seen that in the absence of TCEP 2-oxoglutarate binds slightly tighter to *Ec*-MenD (Table 18) but this is in likely experimental variation given the lack of replicate experiments. In TCEP presence the K_d of 2-oxoglutarate is observed to be 20-fold lower than the previous ThDP binding experiment (1.68 versus 34.78 µM, Figure 28b, Table 17), however due to the difference in curve fitting equations between non-TCEP addition experiments for ThDP and 2-oxoglutarate no direct comparisons can be made between these results (Figure 27a, Table 16).

Table 18: K_d values of *Ec*-MenD under various 2-oxoglutarate conditions

	K_d With $MgCl_2$ Added (µM)	**Sigma**
2-Oxoglutarate with ThDP Present	0.470	0.001
2-Oxoglutarate with ThDP and TCEP Present	1.68	0.05

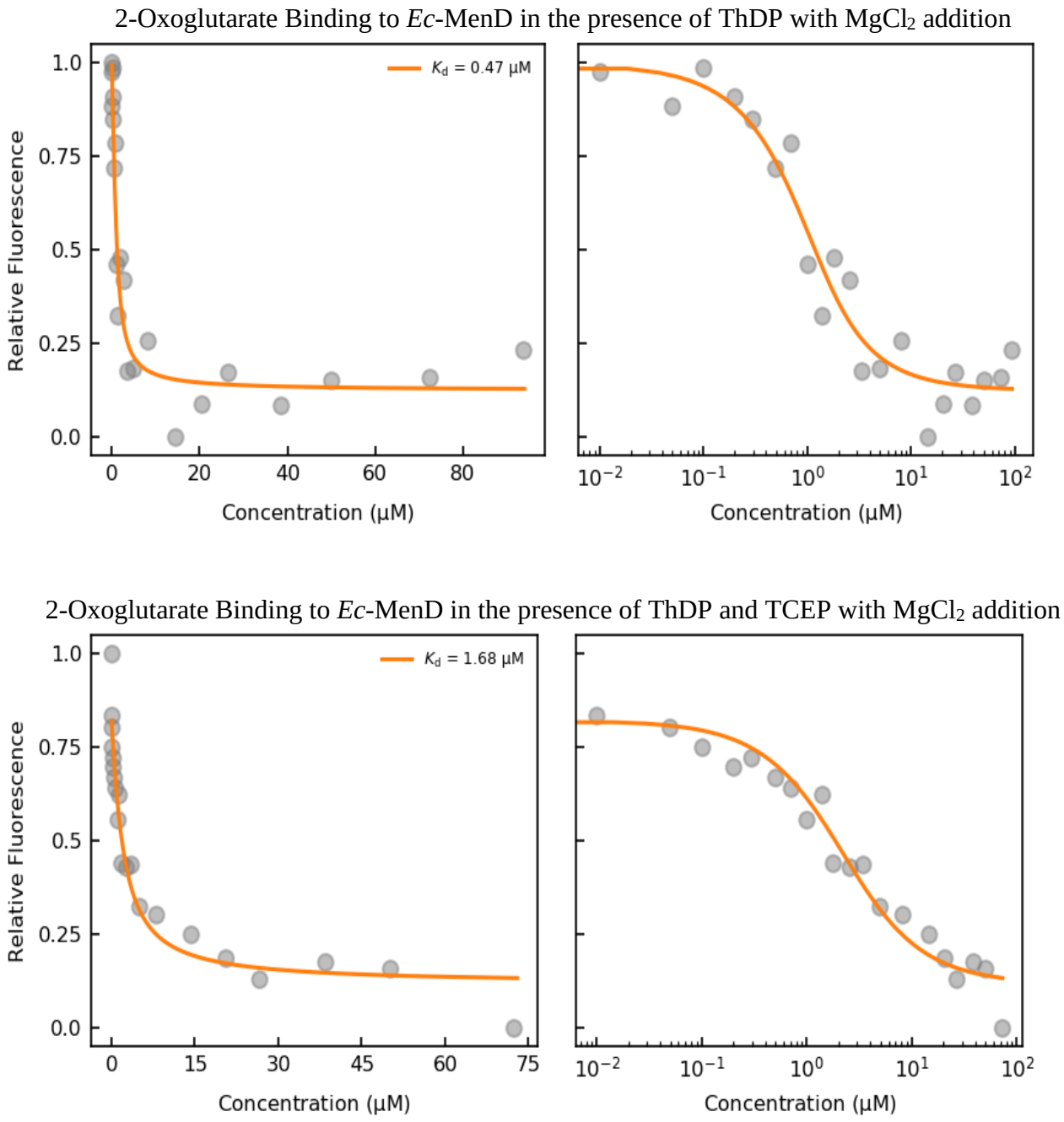

Figure 28: 2-Oxoglutarate binding to *Ec*-MenD under various conditions. **Top (a):** ThDP and $MgCl_2$ present. **Bottom (b):** ThDP, TCEP and $MgCl_2$ present.

4.3.3 DHNA Binding

Experiments involving DHNA addition in the presence and absence of 2.5 mM TCEP support binding of DHNA to *Ec*-MenD (Figure 29 a and b). The DHNA to apo *Ec*-MenD protein and DHNA to *Ec*-MenD protein in the presence of ThDP and 2-oxoglutarate (with and without TCEP) fitted best to the single binding model. While DHNA binding to apo *Ec*-MenD where TCEP was present and to *Ec*-MenD with ThDP present (with or without TCEP) appeared to fit best to a bimodal model suggesting potentially in these cases a higher and lower affinity binding site for DHNA and by extension suggests an effect upon the symmetry upon the potential binding sites of DHNA. Further replicates need to be done to ensure that bimodal binding has not been missed for the other experiments and is not an over interpretation. Examination of the results suggests that the binding of DHNA is the weakest in the apo *Ec*-MenD protein with no co-factor (ThDP), substrate (2-oxoglutarate) or reducing agent (TCEP) present (Table 19, Figure 29a). It is harder to directly compare dissociation constants between bimodal and single curve fitting experiments but it appears that binding in the presence of co-factor or reducing agent results in significantly tighter binding if the assumption that there are two binding sites with different affinity in the enzyme is correct (Table 19, Figure 29c, d). If you compare apo *Ec*-MenD with TCEP versus *Ec*-MenD with ThDP and TCEP (Table 19, Figure 29b, d), both of which are fitted to a bimodal equation, the dissociation constants for the tightest fit is similar. This makes it hard to determine if the TCEP or ThDP is having an effect, or if the effect is the difference in bimodal versus monomodal fitting. More replicates will be needed to work this out. In the presence of co-factor and substrate where a single binding curve is fitted (Figure 29e, f, Table 19) the K_d is slightly lower than apo protein alone (Figure 29a, Table 19) (and similar with and without TCEP) suggesting DHNA binding may be tighter in enzyme with co-factor and substrate present. The differences in curve fitting (bimodal versus single fitting) make it harder to directly compare and suggest more replicates are needed. However, we can conclude from these experiments the idea that DHNA does bind to *Ec*-MenD and a potential allosteric inhibition could be observed which has not been previously observed as the *Ec*-MenD structure shows the allosteric site is not well conserved. Further investigation into viewing this allosteric site is recommended to confirm the presence.

DHNA Binding to *Ec*-MenD

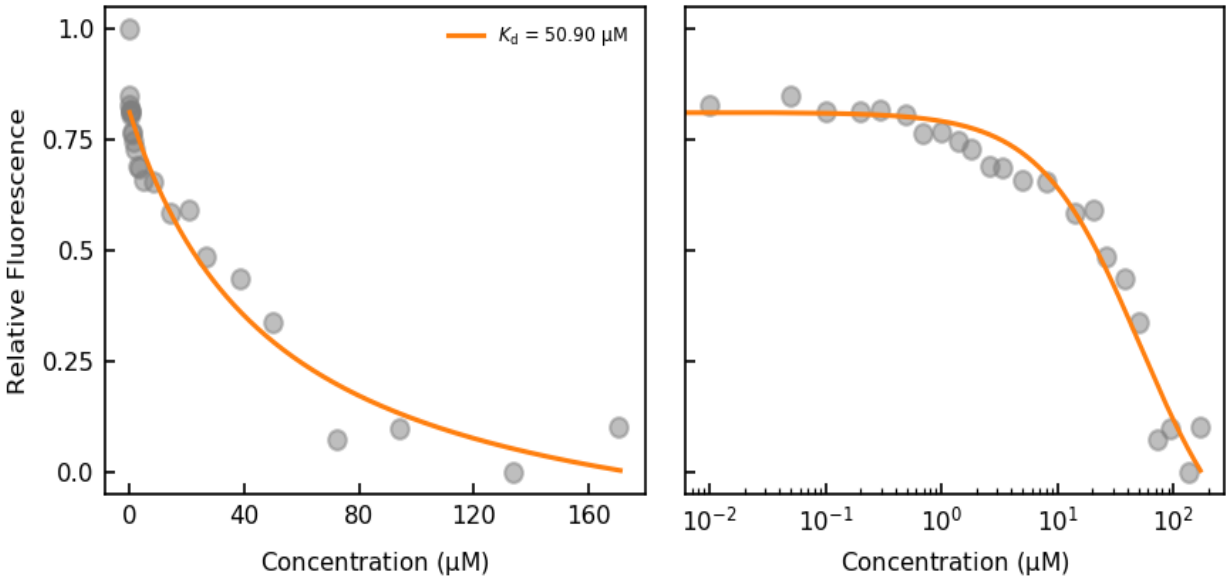

DHNA Binding to *Ec*-MenD in the presence of TCEP

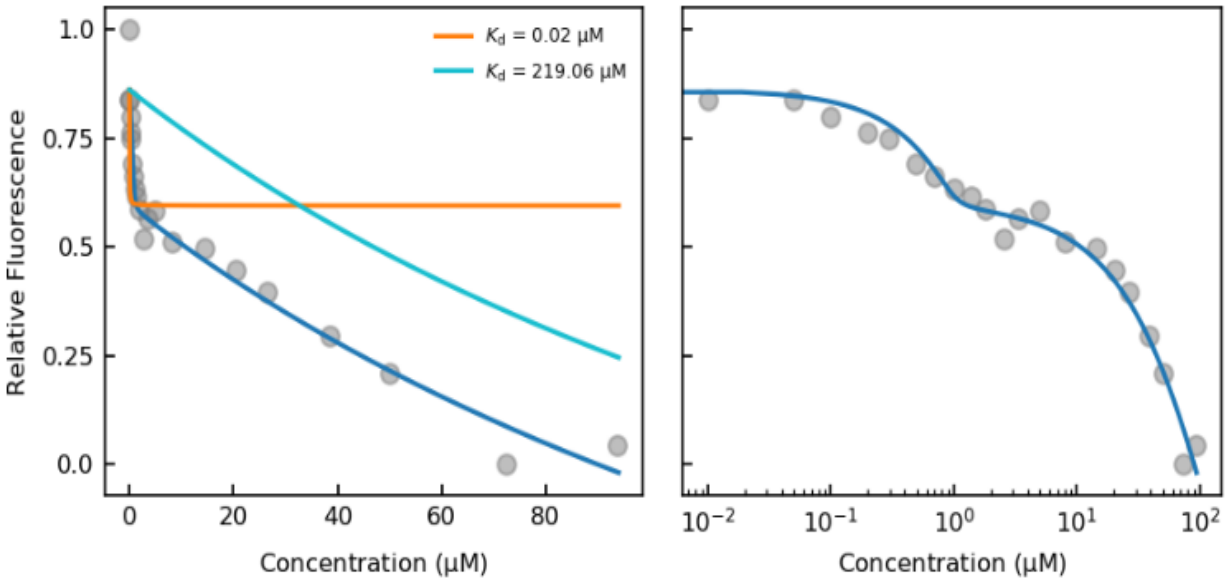

DHNA Binding to *Ec*-MenD in the presence of ThDP

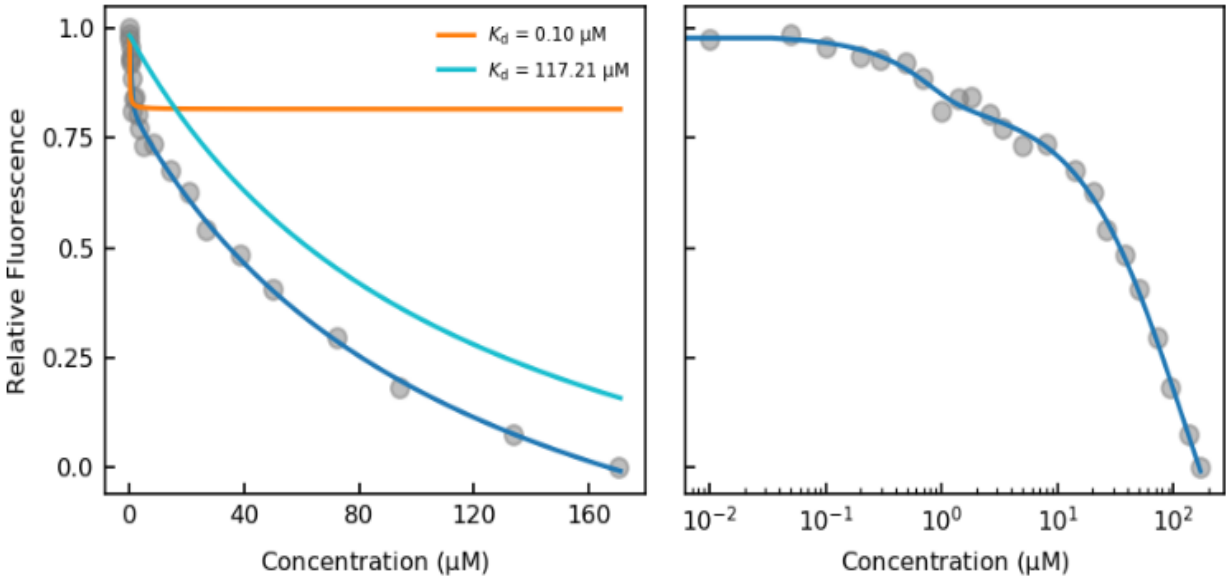

DHNA Binding to *Ec*-MenD in the presence of ThDP and TCEP

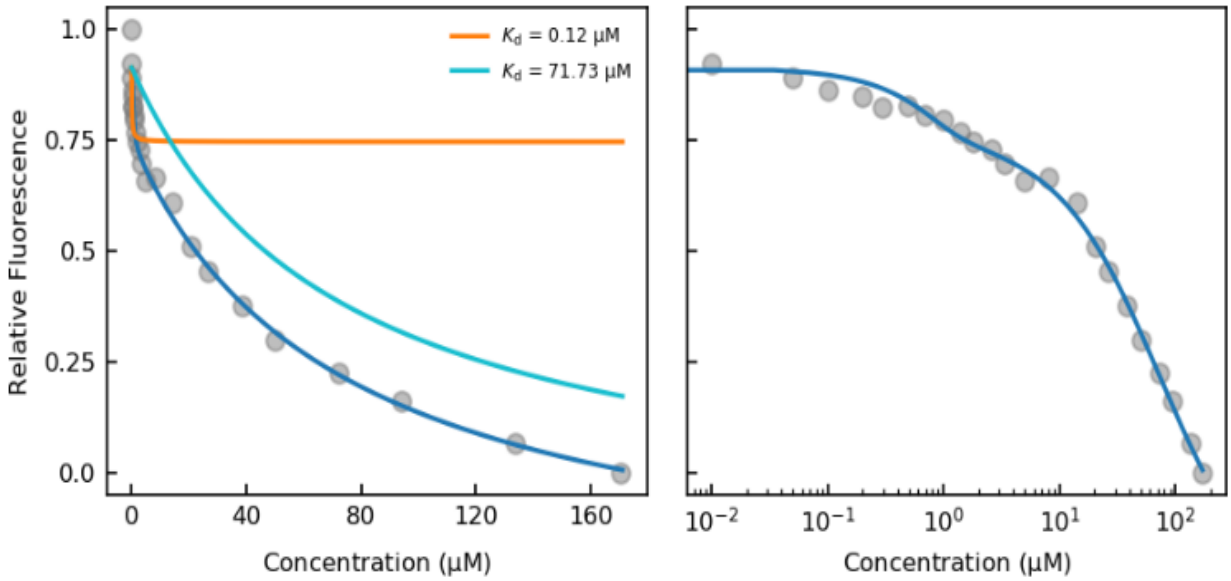

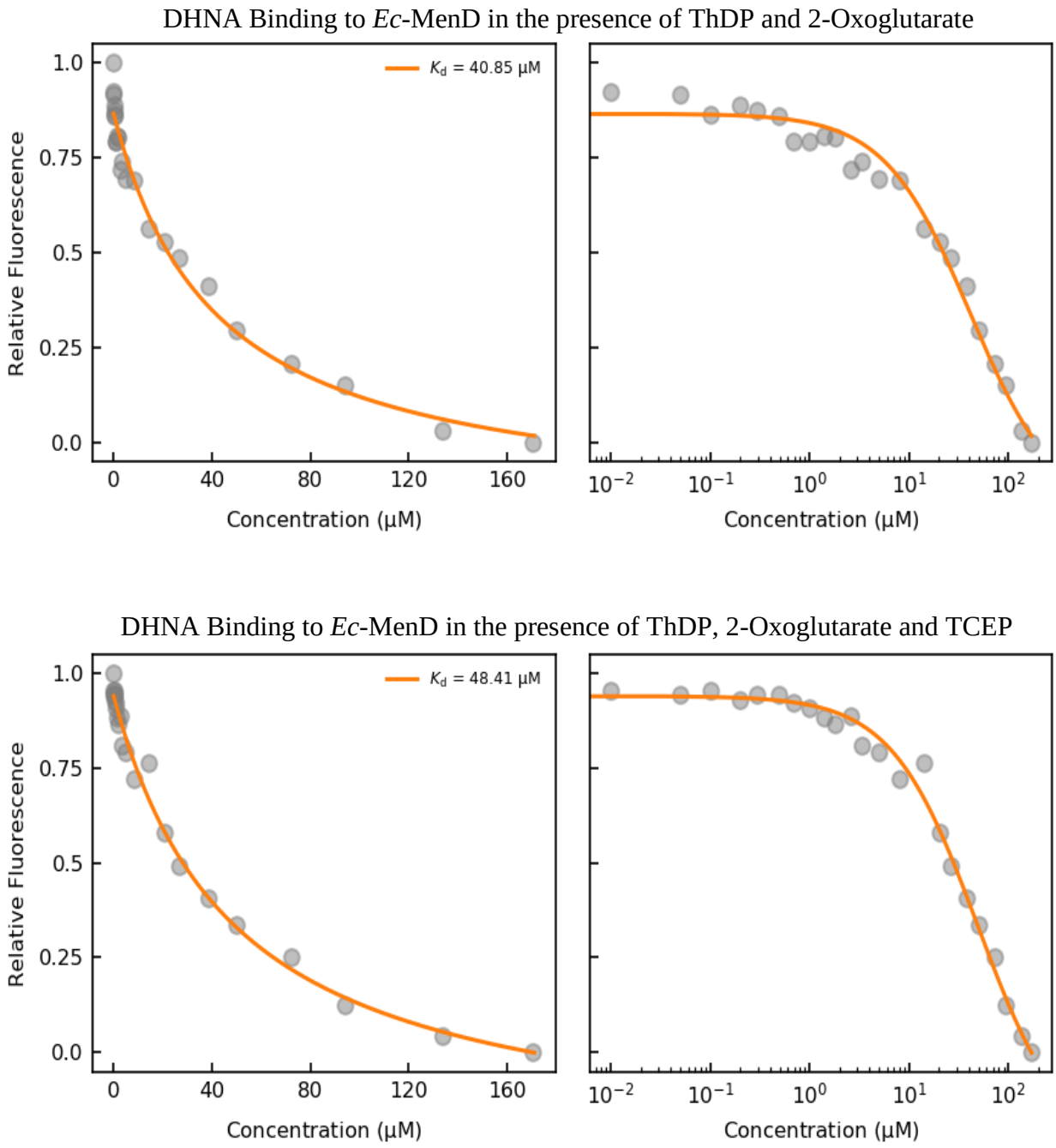

Figure 29: DHNA binding to *Ec*-MenD under various conditions. **1st Row(a):** $MgCl_2$ present **2nd Row (b):** TCEP and $MgCl_2$ present. **3rd Row(c):** ThDP and $MgCl_2$ present. **4th Row (d):** ThDP, TCEP and $MgCl_2$ present. **5th Row(e):** ThDP, 2-oxoglutarate and $MgCl_2$ present. **6th Row(f):** ThDP, 2-oxoglutarate, TCEP and $MgCl_2$ present.

Table 19: K_d values of *Ec*-MenD under various DHNA binding conditions

	K_d With $MgCl_2$ Added (µM)	**Sigma**	**K_d With $MgCl_2$ Added (µM)**	**Sigma**
DHNA	50.9	1.3	-	-
DHNA with TCEP Present	0.016	0.001	219.1	131.7
DHNA with ThDP Present	0.10	0.01	117.2	1.4
DHNA with ThDP and TCEP Present	0.12	0.01	71.7	0.5
DHNA with ThDP and 2-Oxoglutarate Present	40.9	0.4	-	-
DHNA with ThDP, 2-Oxoglutarate and TCEP Present	48.4	0.3	-	-

4.4 IFQ Experiments with *Smeg*-MenD

4.4.1 ThDP Binding

Binding of ThDP to *Smeg*-MenD with the presence and absence of 2.5 mM TCEP displayed almost identical results. Clear binding is observed with both experiments fitting better to the bimodal equation. The affinity to the two binding sites is both within the same value ranges as each other, with the higher affinity binding site dissociation constants of 0.05 and 0.23 µM respectively and the lower affinity binding site K_d at 47.0 and 48 µM (Figure 30, Table 20). In conjunction with these differences being too insignificant to note, the lack of replicates in these experiments means that conclusions cannot be made.

Table 20: K_d values of *Smeg*-MenD under various ThDP conditions

	K_d With $MgCl_2$ Added (µM)	**Sigma**	**K_d With $MgCl_2$ Added (µM)**	**Sigma**
ThDP	0.05	0.01	47.0	0.5
ThDP with TCEP Present	0.23	0.01	48	2

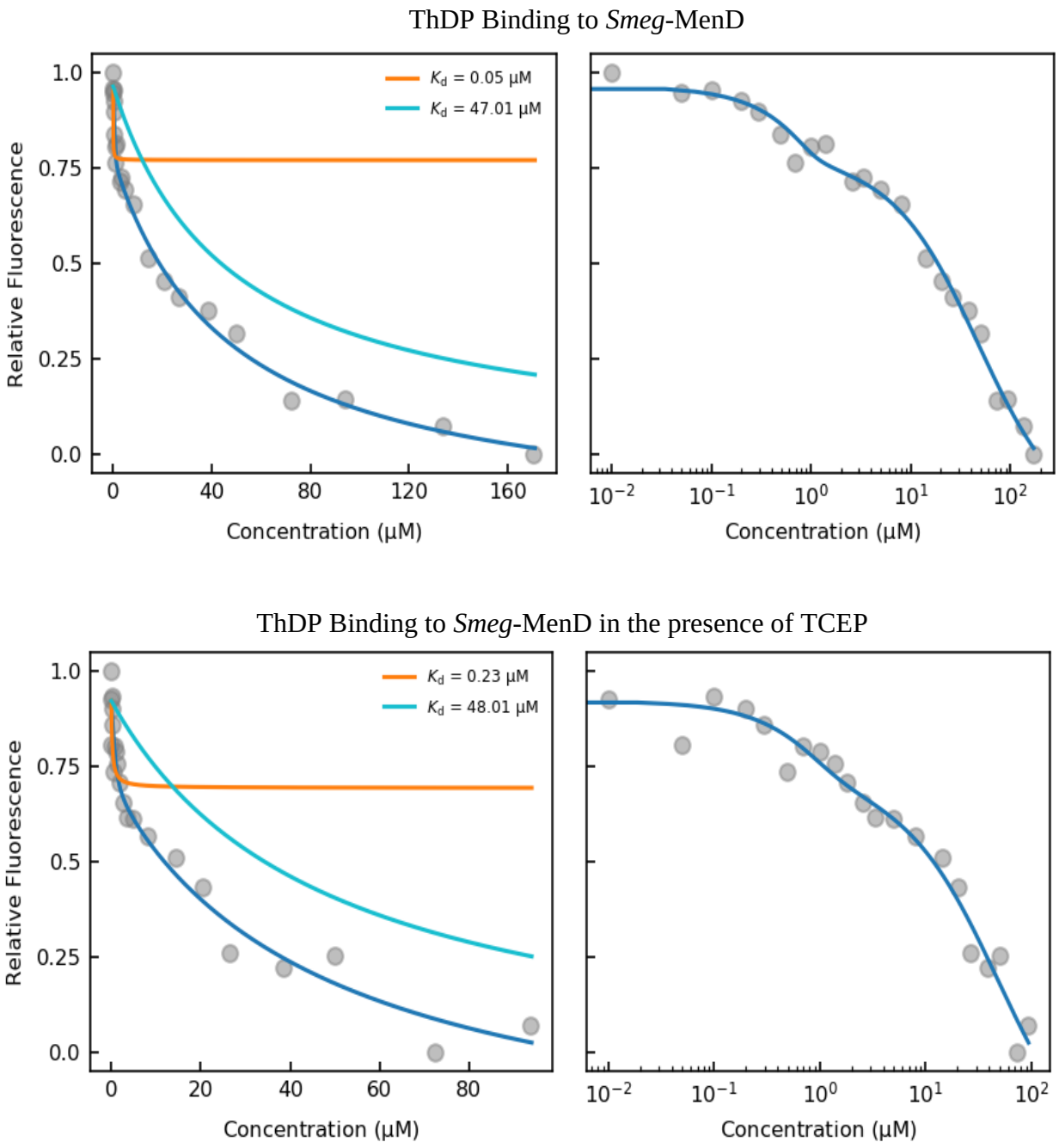

Figure 30: ThDP binding to *Smeg*-MenD under various conditions. **Top (a):** $MgCl_2$ present. **Bottom (b):** TCEP and $MgCl_2$ present.

4.4.2 2-Oxoglutarate Binding

Experiments involving 2-oxoglutarate with 100 µM ThDP presence in the protein buffer mix were again conducted in the presence and absence of 2.5 mM TCEP. In the absence of TCEP, 2-oxoglutarate was observed to fit better to the bimodal equation with binding affinities very similar to the observed binding of ThDP (Figure 31a, Table 20). In the presence of TCEP, the bimodal equation no longer fits the binding curve best, however the single binding curve is not a perfect fit, suggesting bimodal binding might also be present here but not as clearly able to be fitted (Figure 31b). Both experiments demonstrate in the presence of ThDP the substrate 2-oxoglutarate can bind relatively strongly to *Smeg*-MenD (0.18/47 µM and 2.89 µM Table 21).

Table 21: K_d values of *Smeg*-MenD under various 2-oxoglutarate conditions

	K_d With $MgCl_2$ Added (µM)	**Sigma**	**K_d With $MgCl_2$ Added (µM)**	**Sigma**
2-Oxoglutarate with ThDP Present	0.18	0.01	47	3
2-Oxoglutarate with ThDP and TCEP Present	2.89	0.05	-	-

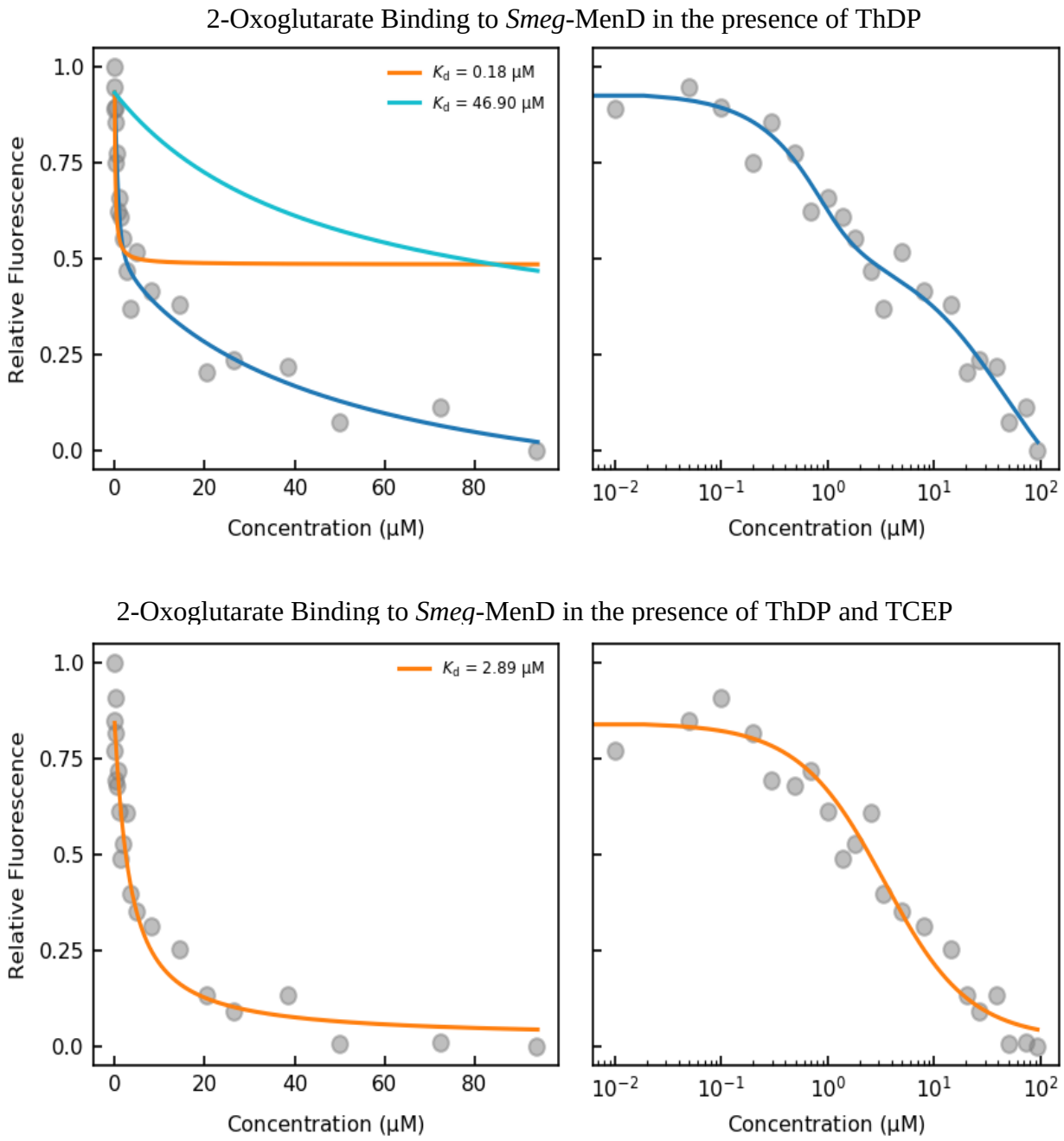

Figure 31: 2-Oxoglutarate binding to *Smeg*-MenD under various conditions **Top (a):** ThDP and $MgCl_2$ present. **Bottom (b):** ThDP, TCEP and $MgCl_2$ present.

4.4.3 DHNA Binding

Binding experiments of DHNA to *Smeg*-MenD provided identical results in both the presence and absence of TCEP (Figure 32 a and b). With K_d values of 5.62 and 5.54 µM respectively, tight binding of DHNA to the *Smeg*-MenD can be confirmed. Due to a lack of replicate experiments, no major changes in enzyme activity due to TCEP presence can be proven or disproven. These results support the idea that DHNA successfully binds as an allosteric regulator similar to what is observed in *Mtb*-MenD.

Further experimental work involving *Smeg*-MenD bound to ThDP (100 µM ThDP in the protein buffer mix) confirmed this theory. Without 2.5 mM TCEP presence DHNA binding fits best to the bimodal curve fitting equation, while in the presence of TCEP and in all other situations with ThDP present it appears to fit a single curve best. As we observe DHNA slowly oxidises over the course of the experiment this bimodal nature is hard to define as it could come from the enzyme which can exhibit asymmetry or the presence of oxidized forms of DHNA without TCEP. If we compare the non-bimodal experiment only, at a K_d of 4.69 µM, 1 µM less than the previous DHNA binding experiment with TCEP presence slightly tighter binding can be observed. Due to the lack of replicates and the value range between K_d still being in the micromolar range no firm conclusions can be made.

The most significant differences observed in the DHNA experiments between TCEP absence and presence is observed with 100 µM ThDP and 2-oxoglutarate presence in the protein buffer mix. Without TCEP presence the K_d observed is 28.33 µM, approximately 5-fold higher than apo protein DHNA binding With TCEP presence, the K_d value experiences a 10-fold decrease to 2.84 µM (Figure 32f), indicating tighter binding to *Smeg*-MenD with TCEP presence. Due to the lack of replicates, it is difficult to confirm this is the case and as such further experimentation would be required for more supporting evidence. What can be concluded from all the DHNA binding experiments for *Smeg*-MenD however is the successful binding of the allosteric regulator to *Smeg*-MenD. This provides a new outlet for investigation of allosteric inhibitors and the characteristics of the MenD enzyme in all species.

DHNA Binding to *Smeg*-MenD

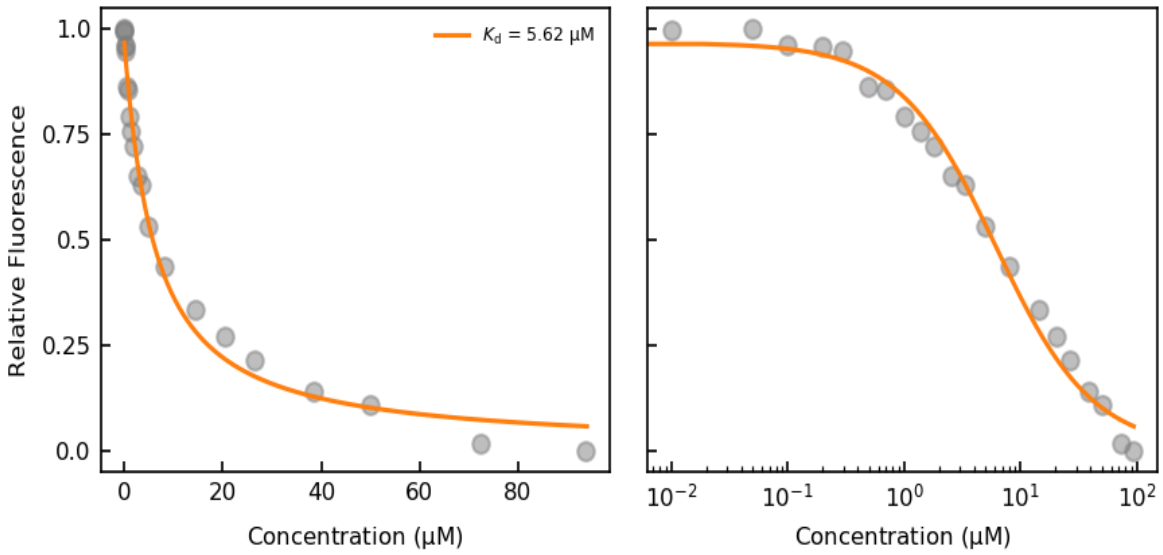

DHNA Binding to *Smeg*-MenD in the presence of TCEP

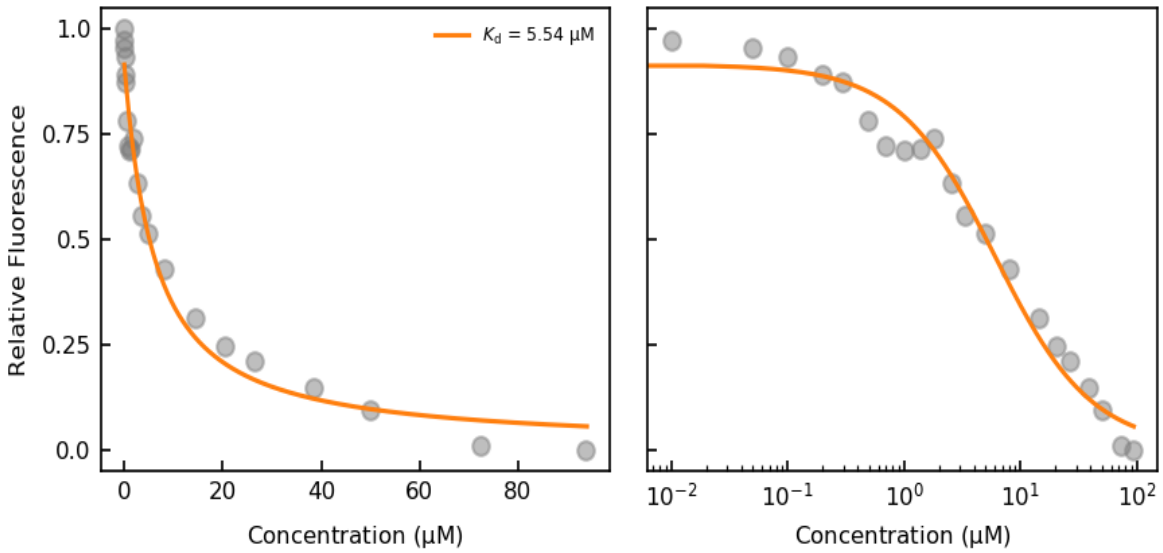

DHNA Binding to *Smeg*-MenD in the presence of ThDP

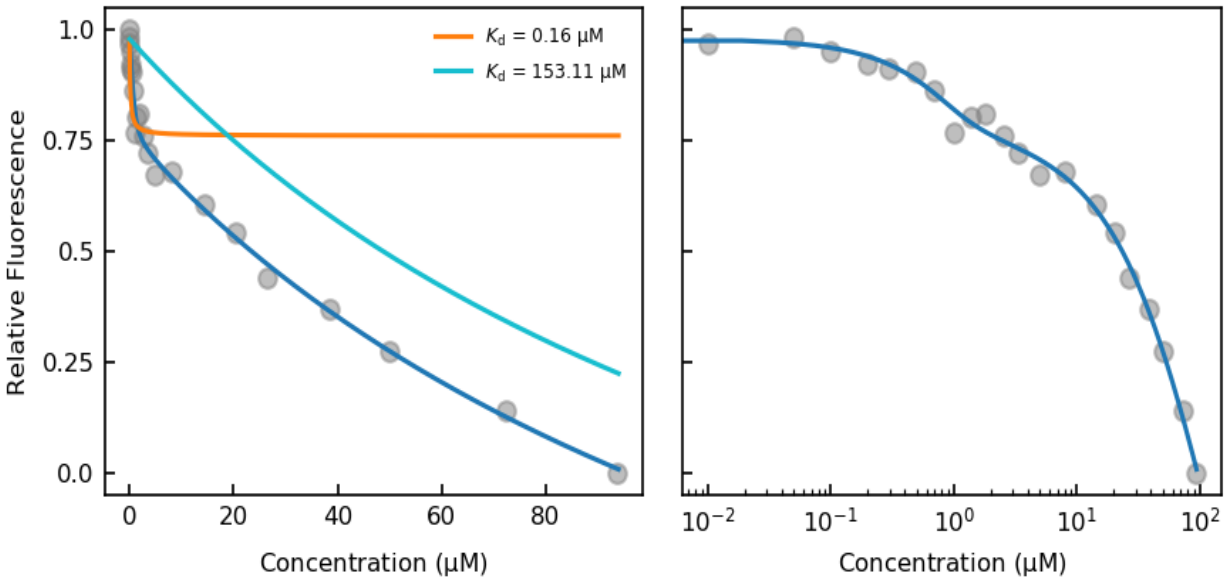

DHNA Binding to *Smeg*-MenD in the presence of ThDP and TCEP

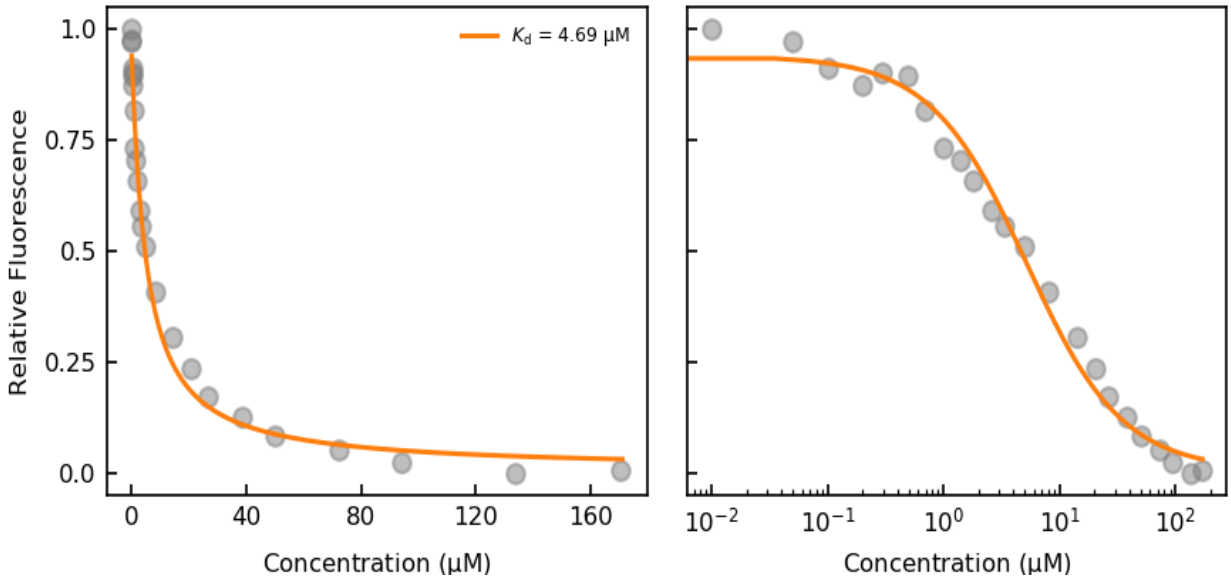

DHNA Binding to *Smeg*-MenD in the presence of ThDP and 2-Oxoglutarate

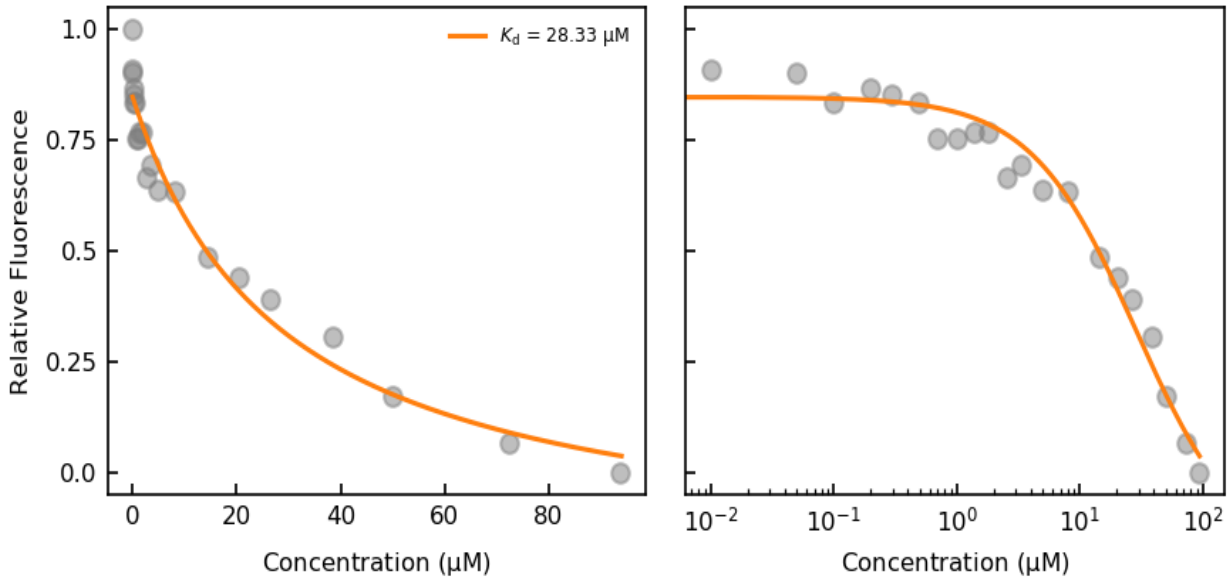

DHNA Binding to *Smeg*-MenD in the presence of ThDP, 2-Oxoglutarate and TCEP

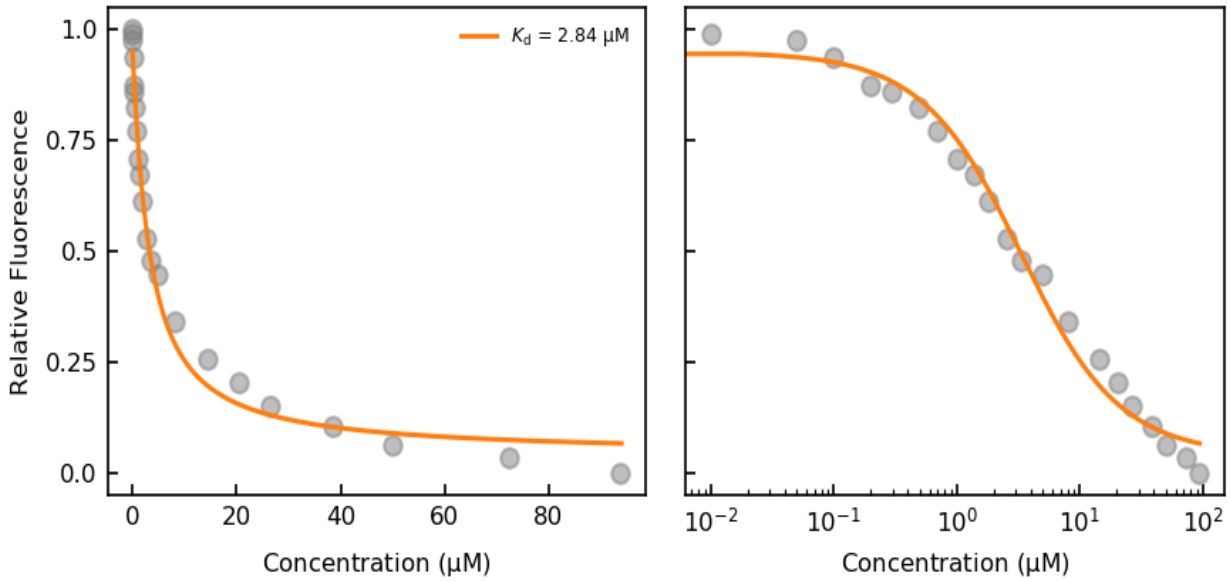

Figure 32: DHNA binding to Smeg-MenD under various conditions. **1st Row(a):** MgCl2 present **2nd Row(b):** TCEP and MgCl2 present. **3rd Row(c):** ThDP and MgCl2 present. **4th Row(d):** ThDP, TCEP and MgCl2 present. **5th Row(e):** ThDP, 2-oxoglutarate and MgCl2 present. **6th Row(f):** ThDP, 2-oxoglutarate, TCEP and MgCl2 present.

Table 22: K_d values of *Smeg*-MenD under various DHNA conditions

	K_d With $MgCl_2$ Added (µM)	**Sigma**	**K_d With $MgCl_2$ Added (µM)**	**Sigma**
DHNA	5.62	0.04	-	-
DHNA with TCEP Present	5.54	0.08	-	-
DHNA with ThDP Present	0.16	0.02	150	10
DHNA with ThDP and TCEP Present	4.69	0.03	-	-
DHNA with ThDP and 2-Oxoglutarate Present	28.3	0.3	-	-
DHNA with ThDP, 2-Oxoglutarate and TCEP present	2.84	0.04	-	-

4.5 Comparison of Binding Affinities Between Enzymes

4.5.1 ThDP Binding

None of the three MenD enzymes appear to display the exact same binding patterns as each other, but all three do have a confirmed high binding affinity condition for ThDP expected for a ThDP-dependent enzyme. If we compare the K_d for ThDP (without TCEP) the binding affinity appears to be strongest for *Smeg*-MenD. This is because despite having a bimodal fit for the curve, considering the difference for both K_d values the higher K_d value is equal to the monomodal K_d observed from *Sau*-MenD. This is unlike *Sau*-MenD, *Ec*-MenD and *Smeg*-MenD show bimodal curves for ThDP binding without TCEP.

Table 23: Calculated K_d values of ThDP experiments for MenD enzymes used in this work

	***Sau*-MenD**	***Ec*-MenD**	***Smeg*-MenD**
ThDP	47.0 µM (monomodal)	0.003/118.6 µM (bimodal)	0.05/47.0 µM (bimodal)
ThDP (TCEP)	0.06/79.3 µM (bimodal)	34.8 µM (monomodal)	0.23/48.0 µM (bimodal)

4.5.2 2-Oxoglutarate Binding

Due to the unavailability of one 2-oxoglutarate binding experimental data for *Sau*-MenD, it is more difficult to make direct comparisons between the three enzymes in this case. From the experimental data that is available it can be noted that only 2-oxoglutarate binding experiments of *Smeg*-MenD fit bimodal equation binding curve, specifically without TCEP addition. As there is no available data for the 2-oxoglutarate binding with ThDP presence and TCEP absence, we instead compare the K_d for 2-oxoglutarate binding with ThDP and TCEP presence. All three of these experiments have a monomodal fit for the curve, with the binding affinity between all three in a similar magnitude. This similar magnitude demonstrates consistently moderately tight binding of 2-oxoglutarate to all enzymes.

Table 24: Calculated K_d values of 2-oxoglutarate experiments for MenD enzymes used in this work

	***Sau*-MenD**	***Ec*-MenD**	***Smeg*-MenD**
Oxo (ThDP)	N/A	0.47 µM (monomodal)	0.18/46.9 µM (bimodal)
Oxo (ThDP/TCEP)	5.4 µM (monomodal)	1.68 µM (monomodal)	2.89 µM (monomodal)

4.5.3 DHNA Binding

All three enzymes in this work demonstrated the potential for successful binding of DHNA. There does not appear to be any pattern in the binding between the enzymes despite this observation, such as no consistency in the curve fitting between enzymes. By comparing the K_d for DHNA (without TCEP) we can see that the binding affinity between *Sau*-MenD and *Smeg*-MenD are very similar and are both higher than observed in *Ec*-MenD. The K_d for *Sau*-MenD is 4.5 µM lower than *Smeg*-MenD, however these two values are in the same magnitude and so can be considered almost identical in terms of how tightly they bind DHNA.

Mtb-MenD (carried out by Dr Ho) IFQ experiments done in replicate showed K_d of about 5 µM in to apo protein and increasing tight binding (lowering of K_d) with ThDP (down to ≈1µM) then ThDP and oxoglutarate (down to 0.3 µM). The results were similar with and without TCEP present.

Table 25: Calculated K_d values of DHNA experiments for MenD enzymes used in this work

	***Sau*-MenD**	***Ec*-MenD**	***Smeg*-MenD**
DHNA	1.2 µM (monomodal)	50.9 µM (monomodal)	5.62 µM (monomodal)
DHNA (TCEP)	1.9 µM (monomodal)	0.02/219.1 µM (bimodal)	5.54 µM (monomodal)
DHNA (ThDP)	52.3 µM (monomodal)	0.10/117.2 µM (bimodal)	0.16/153.1 µM (bimodal)
DHNA (ThDP/TCEP)	0.003/171.3 µM (bimodal)	0.12/71.7 µM (bimodal)	4.69 µM (monomodal)
DHNA (ThDP/Oxo)	1.90 µM (monomodal)	40.9 µM (monomodal)	28.3 µM (monomodal)
DHNA (ThDP/TCEP/Oxo)	0.01/87.81 µM (bimodal)	48.4 µM (monomodal)	2.84 µM (monomodal)

4.6 Discussion

4.6.1 Summary and Implications for Enzyme Activity and Regulation

There is always more to learn about all enzymes and their activity, and the MenD enzyme is no different. This experimental work has demonstrated that interactions occurring in the MenD enzymes are diverse and certain binding characteristics that previously were not thought to be present may just require the right conditions to be observed. The binding of DHNA to all enzymes in this work is proof of this circumstance. This work provides key insight into the similarities in the MenD enzymes in terms of activity and binding sites regardless of the type of bacteria investigated (Gram-positive or Gram-negative). As such, regulatory work can also be conducted upon the variants of MenD enzyme and help to determine if any interactions that are observed in *Mtb*-MenD are unique to the enzyme or present in the wider family of MenD enzymes, which by extension can provide valuable target points for drug design.

4.6.2 Limitations

Unfortunately, due to time constraints for this work, none of the IFQ experiments were conducted in duplicate or triplicate. A consequence of this is that none of the results would be able to be published findings until this is done so and the observations made so far can be confirmed. It also means that many of the observations may not provide the actual results of the protein's activity in these conditions. In addition to this, corrections were made for the inner filter effect assuming certain conditions, and as shown from the absence of the 2-oxoglutarate experiment with ThDP present in the buffer, some of the results provided very strange/unusable results. These would need to be revised and adjusted to achieve better results.

4.6.3 Further Research

Further research involving IFQ experimentation would be threefold. Firstly, repeat experiments of each result found in this work would be conducted in at least triplicate or higher to observe any deviations between experiments and firmly conclude the ideas discussed. Secondly, all experiments in this work utilised Mg^{2+} metal ions in the protein buffer mix. By changing the metal ions in the protein buffer mix and conducting the same experiments a clearer picture of the preferred metal ions for each MenD enzyme can be made and optimisation of the technique will be achieved. Finally, the experiments conducted upon the select MenD proteins in this work will be expanded to include additional MenD enzymes. This will help provide further insight into the similarities in activities between all MenD enzymes which will result in better drug design as a follow-on effect.

Chapter 5. Differential Scanning Fluorimetry of MenD from *S. aureus, E. coli and, M. smegmatis*

5.1 Introduction

5.1.1 Background

Differential scanning fluorimetry (DSF) is an experimental technique that can be used to investigate the thermal stability of proteins. It can investigate the effect on the melting temperature (T_m) of various additives to a protein. Detection of a positive (stabilising) or negative (destabilising) shift in the T_m of a protein can support the interaction of a protein with the additive. The amount of the protein and the concentration of the protein required are both low, allowing several experiments to be able to run with ease even in situations where protein aggregation has affected the final purified sample [71].

The thermal unfolding of proteins is frequently monitored by the presence of a fluorescent dye. The most common dye used in DSF experiments is SYPRO orange, though many other dyes can be used as well. The fluorescent dye used in DSF experiments must be highly fluorescent in non-polar environments such as those found in the hydrophobic sites of unfolded proteins compared to the aqueous solution [72]. SYPRO orange is favoured due to its high signal-to-noise ratio, demonstrating high increases in fluorescence in denatured protein compared to aqueous solution. In addition, SYPRO orange has a high excitation wavelength (500 nm) which decreases the chances for small molecule interference with dye fluorescence [71]. DSF is not without limitations, however. Interactions with the dye can occur despite being rare. These interactions can result in quenching of fluorescence intensity and a poor reading of the true T_m for the experiment. In addition, some DSF experiments fail to detect any ligand-protein binding. Despite these shortcomings, DSF is an extremely effective technique at detecting ligand-protein interactions and as such was a focus for the research in this chapter.

In this chapter, DSF was used to assess binding of different ligands and additives to three different MenD proteins (*Sau*-MenD, *Ec*-MenD, *Smeg*-MenD). Five 96-well plates were set up using a combination of natural ligands and substrates as well as some possible inhibitor candidates (Table 26). The use of natural ligands and substrates that are confirmed to bind were used to determine how effective DSF is at detecting the binding of these additives and allows comparisons between the MenD proteins and how these proteins from different species interact with the same additives. Following on from these experiments, the potential inhibitor compounds as well as the natural regulator of *Mtb*-MenD (DHNA) were screened to determine if they bind to these three proteins.

Table 26: All additives used in the DSF experiments with reason for use.

Ligand/Additive Tested	Reason
TCEP	Reducing agent, used to keep DHNA reduced in DHNA binding experiment. Tested by itself to see if it influenced the systems.
DMSO	Used to keep dissolve DHNA and inhibitors in binding experiment. Tested by itself to see if it influenced the systems.
ThDP	Co-factor, needed for reaction with 2-oxoglutarate in the enzyme active site to form intermediate 1. Tested by itself and with a variety of additives to see if it influences their binding.
2-Oxoglutarate	Substrate, reacts with ThDP in the enzyme active site to form intermediate 1, along with the loss of CO_2. Tested by itself and with a variety of additives to see if it influences their binding.
Metal ions	Divalent metal ions required for co-factor to bind to protein. Some metal ions known to completely abolish activity.
CHD	Alternative substrate to the second substrate isochorismate, reacts with intermediate 1 in the enzyme active site, tested with ThDP and 2-oxoglutarate.
DHNA	Allosteric regulator of *Mtb*-MenD, yet to be determined if it regulates other MenD proteins in the same way. Tested by itself and with a variety of additives to see if these influence its binding.
5-Hydroxyinole carboxylic acid	Potential inhibitor candidates. Structurally similar to allosteric regulator DHNA. Expected to bind to allosteric site
1-Hydroxy-2-napthoic acid	
p-Phenylene diacetic acid	
Monobutyl phthalate	
2-Napthtoic acid	
2-Hydroxy-1-napthoic acid	
6-Hydroxy-2-napthoic acid	

5.1.2 General Experimental Considerations and Controls

The interaction of each MenD with various additives were screened across a number of DSF trays each containing 96 conditions. Each condition within the tray was measured in replicate (generally five technical replicates per condition). In addition, for accurate comparison of T_m control conditions were present on each tray (for example apo protein with no additive or protein with ThDP in later trays). This enables the differences in T_m to be measured within the same experimental tray and helped determine if any deviation in the T_m from the same condition occurred between experimental trays.

5.2 DSF Experiments with *Sau*-MenD

5.2.1 Apo with Additives

Between the three identical apo protein experiments with no additives it is apparent that, while the latter two are in close agreement, the initial no additive apo condition has a lower T_m (Figure 33). This suggests some variability is possible between experiments and supports use of the apo control that matches that particular experiment to be used (as shown in Table 27, i.e. no additive (1) compared with additive conditions from the same experiment).

With the addition of 1 mM TCEP a stabilisation effect was observed for *Sau*-MenD compared from the control no additive within that same experiment (no additive 1). However, this is not the case when taking into account T_m calculated from the apo protein without additives in the subsequent experiments (no additive 2 and 3). Experiments with higher concentrations of TCEP (2.5 mM TCEP) gave unclear melt curves with no agreement between the technical replicates and a T_m could not be determined. This may be due to an effect on the protein or an effect of higher levels of reducing agent on the experiment itself (e.g. on the dye used).

DMSO addition does not demonstrate any changes to the T_m of *Sau*-MenD, this is an important control to do for future experiments with ligands dissolved in DMSO as it suggests the presence of DMSO alone does not affect the protein's T_m. With 0.1% DMSO and 2.5 mM TCEP present in the buffer however, a high T_m increase is observed. This is of particular interest due to the lack of data received from the 2.5 mM TCEP experiment, suggesting several possibilities, somehow DMSO may mitigate effects of TCEP either on the protein or to the experimental setup itself.

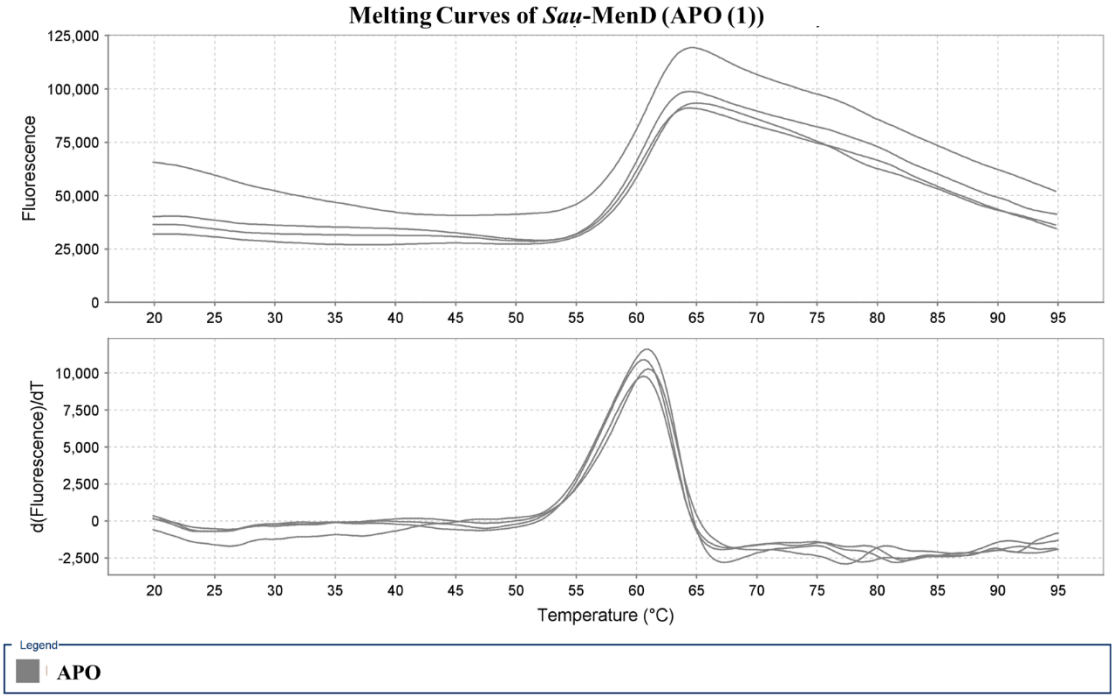

Figure 33: Melting curve of *Sau*-MenD under apo conditions. This is an example of the replicates visualised for each condition during this work. Some experiments have fewer replicates than seen here. The top graph is the raw melt curve and the bottom graph the derivative melt curve.

Table 27: Melting temperature (T_m) of 5 µM *Sau*-MenD in different buffer conditions. The error is the standard error of the mean. [A dash (-) signifies data unavailable due to an unreadable T_m change. T_m and differences are measured in Celsius].

Additive(s)	T_m	Error	Diff.	Rel. To[1]
No additive (1)	59.6	0.1		
No additive (2)	61.0	0.2	1.4	No additive (1)
No additive (3)	60.7	0.3	1.1	No additive (1)
1 mM TCEP	61.1	0.4	1.5	No additive (1)
2.5 mM TCEP	-	-		
0.1% DMSO	-	-		
1% DMSO	60.7	0.3	0.0	No additive (3)
0.1% DMSO, 2.5 mM TCEP	63.4	0.3	2.4	No additive (2)

[1] Compared to no additive conditions from the same experiment tray.

5.2.2 ThDP

Binding of the co-factor ThDP to *Sau*-MenD was probed using DSF over a range of ThDP concentrations from 50–1000 µM in the presence and absence of the reducing agent TCEP (a ratio of between 1:10 protein to co-factor and 1:200 protein to cofactor). As divalent metal ions are required for ThDP to bind, 5 mM of $MgCl_2$ was present in the buffer used for the DSF experiments. All experiments were performed with three to five technical replicates within the same tray and a standard error calculated that suggested in general any change in T_m from the appropriate control that was less than ~0.5 °C was within the noise of the experiment and not considered significant. In some cases, there was higher variability than others which could have arisen from additional factors causing added noise to the experiment. Some of these major causes could have been protein aggregation, pH drift, SYPRO dye affected by the cofactors and air bubbles, all of which would provide more variation in both T_m and standard error.

In general, for ThDP experiments with no other additives we found that the addition of concentrations of less than 250 µM ThDP had very minor effects (maximum of 0.5 °C) on the T_m compared to the co-factor free apo protein control tested in the same experiment (Table 28). Higher concentrations (500 µM and 1000 µM) observed a change in temperature from co-factor free controls that were reproducible.

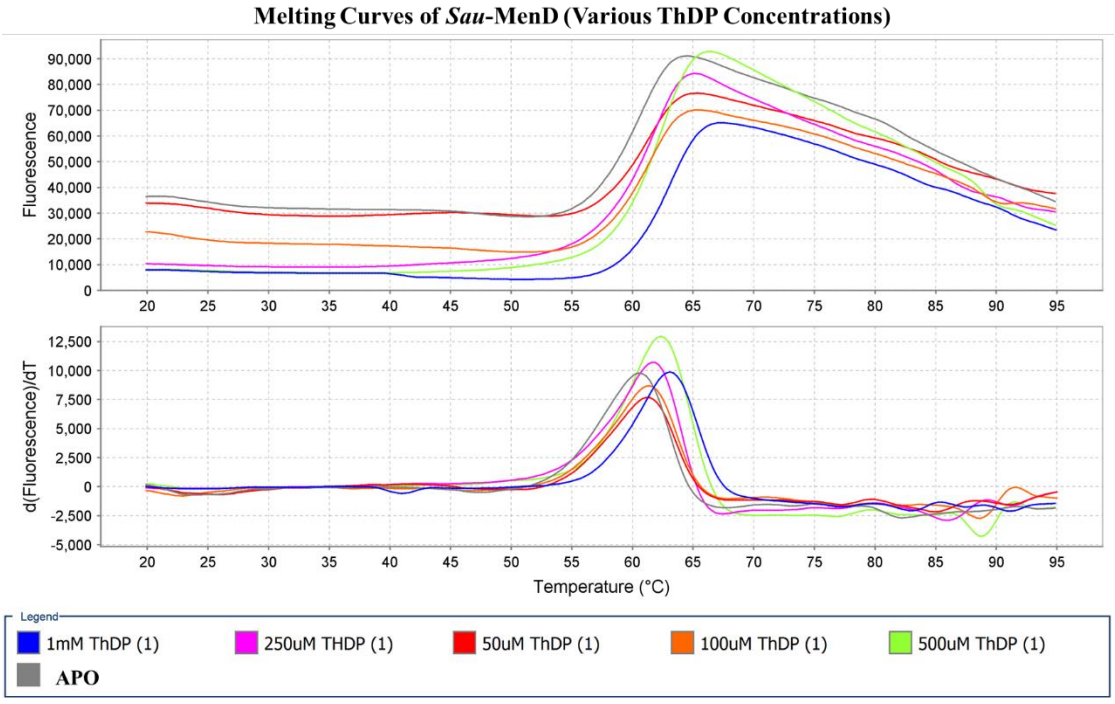

Figure 34: Comparison of all ThDP concentrations present with *Sau*-MenD. As each experiment was conducted in replicate a representative result was selected. Apo condition was included.

The ThDP co-factor at 500 µM was tested in four different experiments (with five technical replicates for the first two experiments and three replicates for the remaining two) and in each case the T_m significantly increased for protein with ThDP added against apo conditions (Table 28). The majority of these experiments observed a T_m increase of 2.5-2.9 °C (with one exception demonstrating a T_m increase of only 1.4 °C (500 µM ThDP (1), Table 28)). This condition however also gave a higher standard error value suggesting variability in the measurement. Inspection of the melt curves for this experiment showed large variation between replicates (Figure 35). Addition of 1000 µM ThDP also demonstrated an increased T_m from the apo protein to a similar magnitude as 500 µM ThDP presence, suggesting saturation of the protein at 500 µM concentration. While a T_m change representing a genuine binding event would be expected to increase with the concentration of ligand it is possible that the binding of the protein is saturated by 500 µM ThDP (protein to ThDP molar ratio of 1:100). It is possible that the concentrations between 250 and 500 µM may have shown this increasing effect but they were not tested in this work.

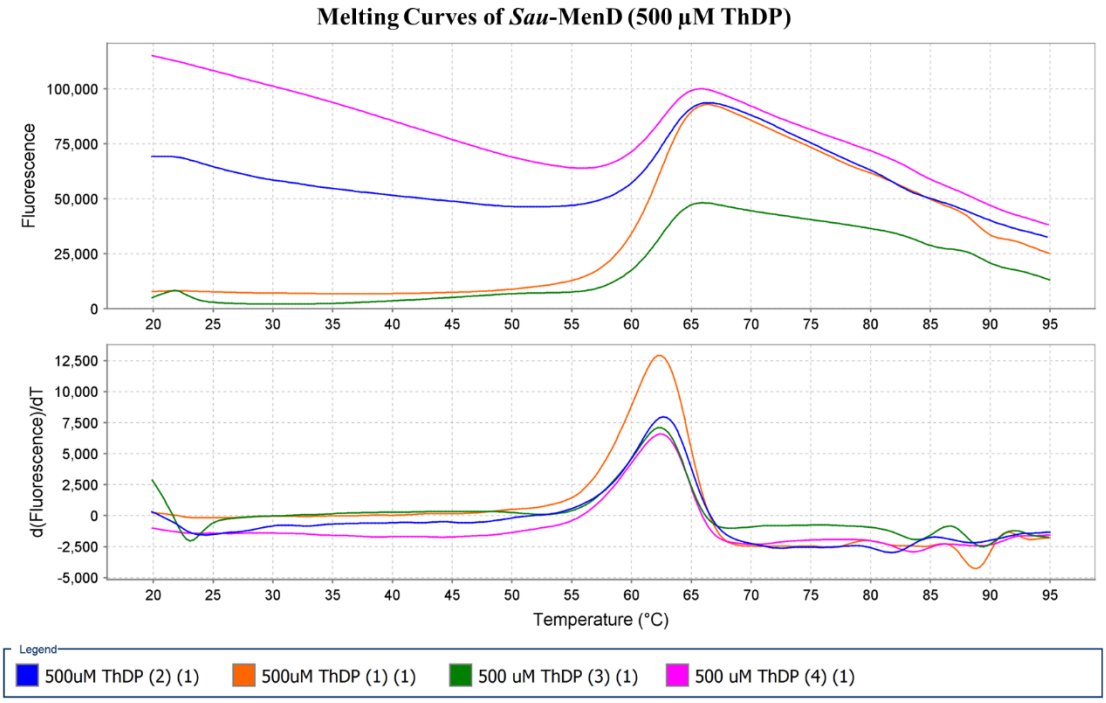

Figure 35: Comparison of 500 µM ThDP addition to *Sau*-MenD in several plates. The binding of 500 µM ThDP was also measured in the presence of reducing agent, TCEP.

The rationale behind this experiment was the need to keep redox active DHNA, which can oxidise over the course of several hours The goal was to see the effect of TCEP at two concentrations; 1 mM as generally used in protein purification buffer and 2.5 mM as used in DHNA experiments where DHNA was being kept in the reduced form. When apo protein with TCEP present at 1 mM was compared to the same condition with 500 µM ThDP added, the temperature showed an increase similar, but slightly less, to that seen in the TCEP free experiments above, supporting the idea that *Sau*-MenD was able to bind to ThDP even when reducing agent was present (1.7 °C, Table 28). At 2.5 mM TCEP due to the variation observed between the replicates and no definitive peak for T_m observed, no temperature difference can be inferred for either apo conditions or with 500 µM ThDP. This result at 2.5 mM could be due to effects on protein or potentially effects on the fluorescent signal from the SYPRO orange dye.

The effect of DMSO in the presence of 500 µM ThDP was also measured. DMSO presence experiments were recorded due to the limited solubility of DHNA requiring it to be dissolved in DMSO. In order to give accurate readings upon the effect of DHNA to T_m, the effect of DMSO presence needs to be recorded for comparisons as well. Two concentrations of DMSO were used and tested, these were 0.1% and 1%. These experiments showed no significant changes to the T_m of *Sau*-MenD as seen in Table 28. An experiment looking at 500 µM ThDP, 0.1% DMSO and 2.5 mM TCEP again showed no significant change. These results perhaps suggest that the TCEP concentration which causes instability is dependent upon other ligand presence or influences the SYPRO orange dye itself. Overall, the main finding that can be determined from these ThDP experiments is that the presence of ThDP stabilises the protein, resulting in the higher T_m.

Table 28: Melting temperature (T_m) of 5 µM *Sau*-MenD in different ThDP conditions. The error is the standard error of the mean. [A dash (-) signifies data unavailable due to an unreadable T_m change. T_m and differences are measured in Celsius].

Additive(s)	T_m	Error	Diff.	Rel. To[1]
No additive (1)	59.6	0.1		
50 µM ThDP	60.0	0.2	0.4	No additive (1)
100 µM ThDP	60.1	0.2	0.5	No additive (1)
250 µM ThDP	59.8	0.2	0.2	No additive (1)
500 µM ThDP (1)	61.0	0.8	1.4	No additive (1)
500 µM ThDP (2)	62.4	0.4	2.8	No additive (1)
500 µM ThDP (3)	62.4	0.1	2.9	No additive (1)
500 µM ThDP (4)	62.0	0.4	2.5	No additive (1)
1000 µM ThDP	62.2	0.1	2.7	No additive (1)
500 µM ThDP, 1 mM TCEP	62.7	0.4	1.7	1 mM TCEP
500 µM ThDP, 0.1% DMSO	62.2	0.5	0.2	500 µM ThDP (2)
500 µM ThDP, 1% DMSO (2)	62.3	0.1	0.1	500 µM ThDP (2)
500 µM ThDP, 0.1% DMSO, 2.5 mM TCEP	62.2	0.5	0.0	500 µM ThDP 0.1% DMSO

[1] Compared to no additive conditions from the same experiment tray.

5.2.3 2-Oxoglutarate

The effect of substrate 2-oxoglutarate, which reacts with the co-factor ThDP to form the first covalent intermediate, was then investigated for the effect upon the thermal stability of *Sau*-MenD. This substrate was investigated at a range of concentrations (50–1000 µM). Most experiments were undertaken in the presence of ThDP (generally at 500 µM) as ThDP is thought to be required for 2-oxoglutarate binding. One experiment investigated the effect of addition of high concentrations (1000 µM) of 2-oxoglutarate to apo protein, finding that there was an increase in T_m of 2.5 °C compared to apo protein. This suggests some possible binding or other stabilisation effects on the *Sau*-MenD protein in the absence of cofactor. When 500 µM ThDP is present with addition of 2-oxoglutarate a destabilising effect on the protein is instead observed, resulting in a consistent decrease in T_m.

Closer inspection of the melt curves for these experiments showed a shoulder region, suggesting multiple melts for the protein as shown in Figure 36. This is less obvious at very high 2-oxoglutarate concentration (1000 µM). This could be due to saturation of the enzyme at this high concentration and turnover is not fast enough. An experiment with 2.5 mM TCEP present in addition to 2-oxoglutarate and ThDP at 500 µM provided results which were inconclusive similar to the ThDP experiment, further reinforcing the idea of excess TCEP causing problems for this experiment.

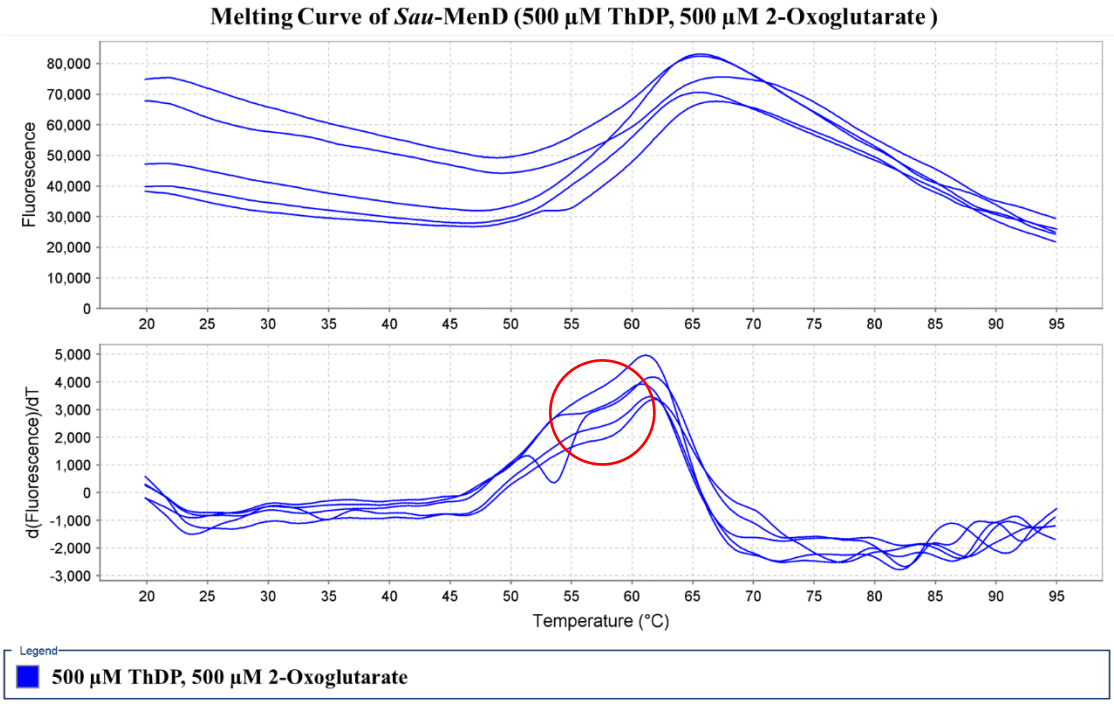

Figure 36: Melting curves of *Sau*-MenD with ThDP and 2-oxoglutarate binding. The shoulder region seen in these replicates demonstrates multiple melting events for the protein in these conditions. Shoulder region highlighted.

An experiment was also conducted with both 0.1% DMSO and 2.5 mM TCEP present in addition to the 2-oxoglutarate and ThDP. There were no significant changes observed in these conditions, which is similar to the observed comparison between 500 µM ThDP, 0.1% DMSO and 2.5 mM TCEP conditions (Tables 28 and 29). The implication from these results is that TCEP activity does not appear to destabilise the reaction or make results difficult to obtain with DMSO present.

Table 29: Melting temperature (T_m) of 5 µM *Sau*-MenD in different 2-oxoglutarate conditions. The error is the standard error of the mean. [A dash (-) signifies data unavailable due to an unreadable T_m change. T_m and differences are measured in Celsius].

Additive(s)	T_m	Error	Diff.	Rel. To[1]
1000 µM 2-oxoglutarate	62.1	0.1	2.5	No additive (1)
500 µM ThDP, 50 µM 2-oxoglutarate	61.0	0.4	-1.4	500 µM ThDP (2)
500 µM ThDP, 100 µM 2-oxoglutarate	57.6	0.9	-4.8	500 µM ThDP (2)
500 µM ThDP, 250 µM 2-oxoglutarate	59.5	0.6	-2.9	500 µM ThDP (2)
500 µM ThDP, 500 µM 2-oxoglutarate	58.8	0.4	-3.6	500 µM ThDP (2)
500 µM ThDP, 1000 µM 2-oxoglutarate	60.5	0.3	-1.9	500 µM ThDP (2)
500 µM ThDP, 500 µM 2-oxoglutarate, 2.5 mM TCEP	-	-		
500 µM ThDP, 500 µM 2-oxoglutarate, 0.1% DMSO, 2.5 mM TCEP	62.7	0.5	-0.1	500 µM ThDP 0.1% DMSO 2.5 mM TCEP (2)

[1] Compared to no additive conditions from the same experiment tray.

5.2.4 2,4-CHD

2,4-Cylcohexadiene (2,4-CHD), an alternative substrate which mimics the highly unstable substrate isochorismate, was also investigated in a small number of experiments. Experiments involved either presence of 2,4-CHD at 500 µM with presence of 500 µM ThDP or the same conditions with 500 µM 2-oxoglutarate in addition. The experiment containing 500 µM ThDP and 500 µM CHD showed a destabilisation effect upon the protein, with a decrease in T_m by 1.4 °C compared to one of the experiments with 500 µM ThDP present (Tables 28 and 30), while the experiment with 500 µM 2-oxoglutarate in addition to the previous substrates had a shoulder present as shown in Figure 37 very similar to what has been observed with the previous 2-oxoglutarate experiments. The large T_m decreases observed for both experiments containing 2,4-CHD (-1.4, -3.8 °C, Table 30) suggests that 2,4-CHD has a destabilising effect upon the protein, however the magnitude of the effect needs to be explored further.

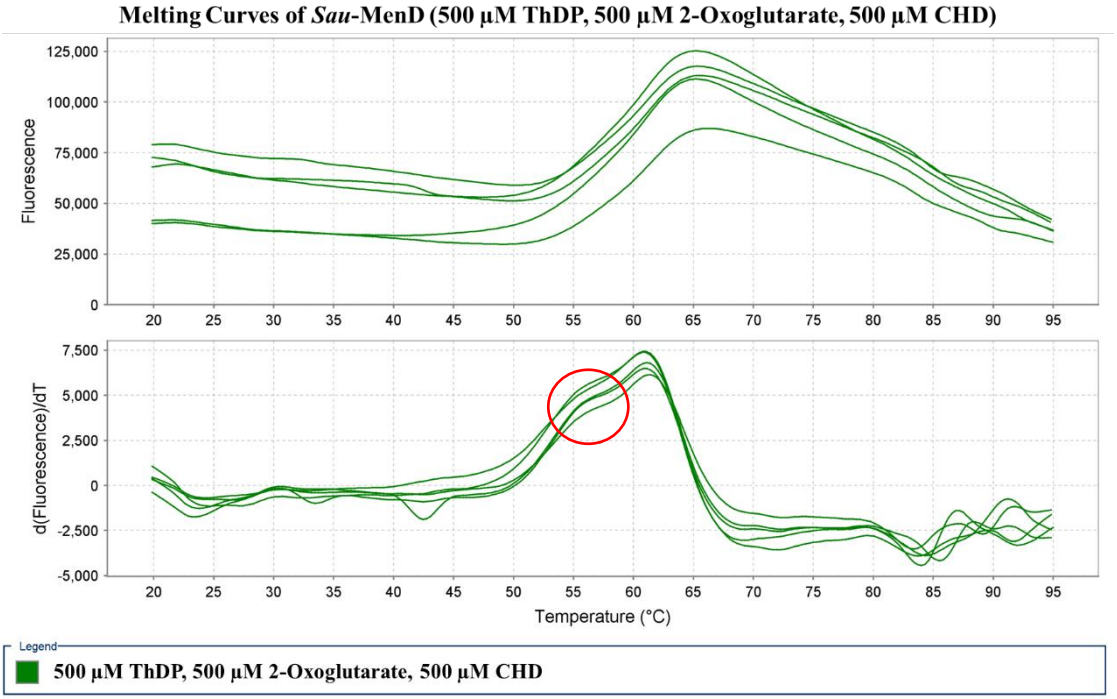

Figure 37: Melting curves of *Sau*-MenD with CHD, ThDP and 2-oxoglutarate. The shoulder region seen in these replicates demonstrates multiple melting events for the protein in these conditions. Shoulder region highlighted.

Table 30: Melting temperature (T_m) of 5 µM *Sau*-MenD in different CHD conditions. The error is the standard error of the mean. [A dash (-) signifies data unavailable due to an unreadable T_m change. T_m and differences are measured in Celsius].

Additive(s)	T_m	Error	Diff.	Rel. To[1]
500 µM ThDP, 500 µM CHD	61.0	0.2	-1.4	500 µM ThDP (2)
500 µM THDP, 500 µM CHD, 500 µM 2-oxoglutarate	58.6	0.2	-3.8	500 µM ThDP (2)

[1] Compared to no additive conditions from the same experiment tray.

5.2.5 DHNA

Exploring the potential binding interactions of MenD with DHNA was a focus of this work. As such, there are many more conditions tested with DHNA present compared to the other ligands. DHNA has some factors which complicate the DSF experimental results, as it has fluorescence of its own and is also not highly soluble. In order to minimise these issues a more modest concentration range from 5–100 µM was tested. The overall trend from DHNA addition was a destabilisation effect on the protein (Figure 38). At 5 µM, the results were inconclusive, however the trend from 10 µM to 100 µM, showed higher concentrations of DHNA resulting in larger decreases in T_m from 2.7–4.9 °C. Interestingly, a DHNA concentration of 50 µM demonstrated a slightly larger decrease in T_m than 100 µM, suggesting an optimal concentration of DHNA. At 30 µM DHNA concentration a 1.9 °C decrease in T_m was observed. This was much less of a T_m decrease than the other DHNA experiments and against the overall trend observed. It is uncertain as to why this is the case, potentially alternative interactions were occurring at this concentration or experimental error is the explanation for this.

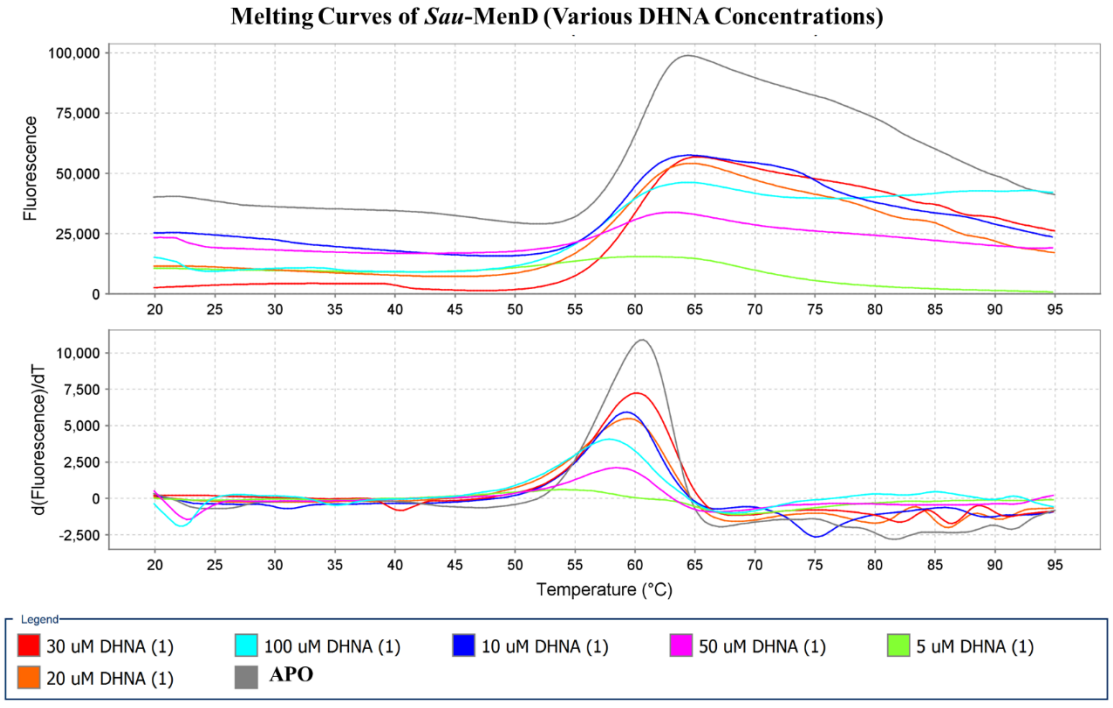

Figure 38: Representative melting curves of increasing DHNA concentrations present with *Sau*-MenD.

Experiments in the presence of the reducing agent TCEP were also carried out. When compared to protein conditions of 2.5 mM TCEP and 0.1% DMSO presence which had already displayed an increased T_m of 2.4 °C compared to apo (2) the increase in T_m was a further 0.8–1.6 depending on the concentration. In these experiments, the lower concentrations of DHNA displayed larger increases than the higher DHNA concentrations (1.6 °C increase at 5 µM DHNA and 0.8 °C from 50 µM DHNA). TCEP helps keep DHNA in a reduced form, so this potentially has an effect somehow on stabilising the protein. However, at the higher concentrations this stabilisation effect lessens and could end with a destabilisation effect gain at a high enough concentration (Figure 39).

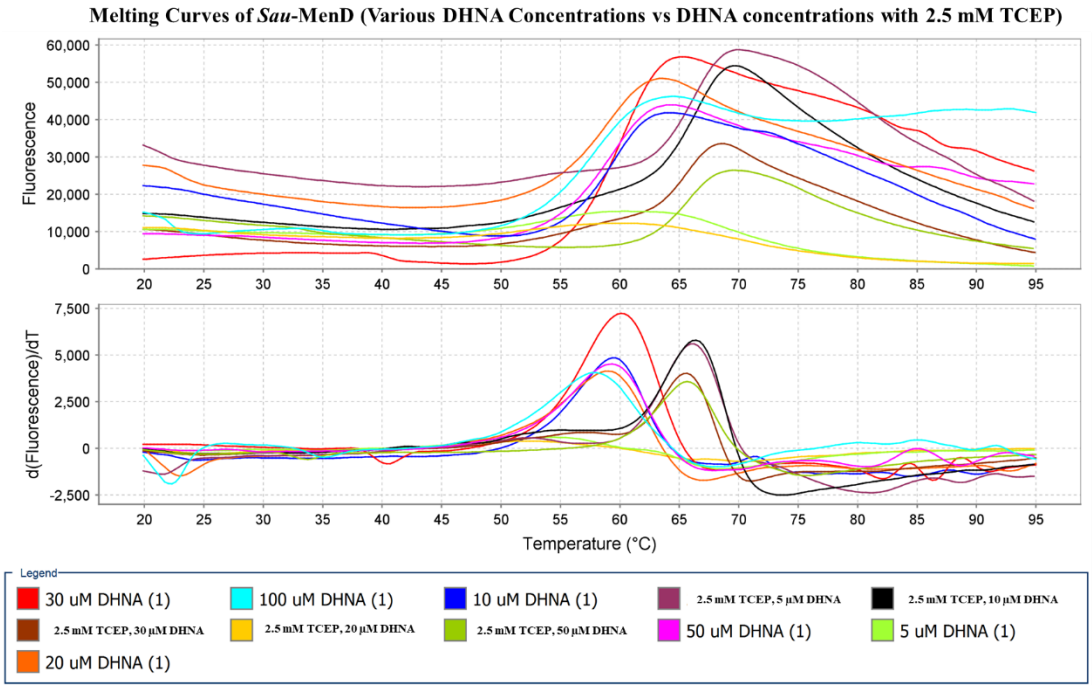

Figure 39: Comparison of melting curves for both DHNA binding and DHNA binding with TCEP presence for *Sau*-MenD.

Experiments in the presence of ThDP (500 µM) with increasing DHNA concentration (5, 10, 50 and 100 µM) were also conducted. With increasing concentration of DHNA and 500 µM ThDP presence a trend of decreasing T_m, and therefore a destabilisation of the protein was observed. These experiments were compared to the experiment containing 500 µM ThDP and 0.1% DMSO. The changes in T_m were high, with the lowest change being with 5 µM DHNA at 3.7 °C (Table 31). Overall it demonstrates that in the presence of ThDP the destabilisation effect of DHNA is still present if not strengthened by ThDP presence.

Interestingly addition of 2.5 mM TCEP to the previous substrates of 500 µM ThDP and increasing DHNA concentration did not show the same destabilisation and in one case showed a stabilisation (100 µM DHNA concentration, showing a T_m increase of 1.8 °C).

Experiments with DHNA involving both ThDP and 2-oxoglutarate at 500 µM being present with the varying concentration of DHNA were also conducted. Again, DHNA presence without TCEP has a destabilisation effect upon the protein, with the decrease in T_m, being as low as 2.9 °C in 10 µM to as high as 4.5 °C in 50 µM (Table 31). At 5 µM the decrease in T_m is much higher than compared to 10 µM at 4.2 °C. It is uncertain as to why this is the case, however it is noted that the graphs for 10 µM have a distinguishable shoulder to the T_m peak, suggesting potential multiple melt sites (Figure 40). This could be further investigated to fully determine. With 2.5 mM TCEP addition to the other ligands, the stabilisation effect is again observed, in this case as an increase of T_m by 1 °C for all three DHNA concentrations.

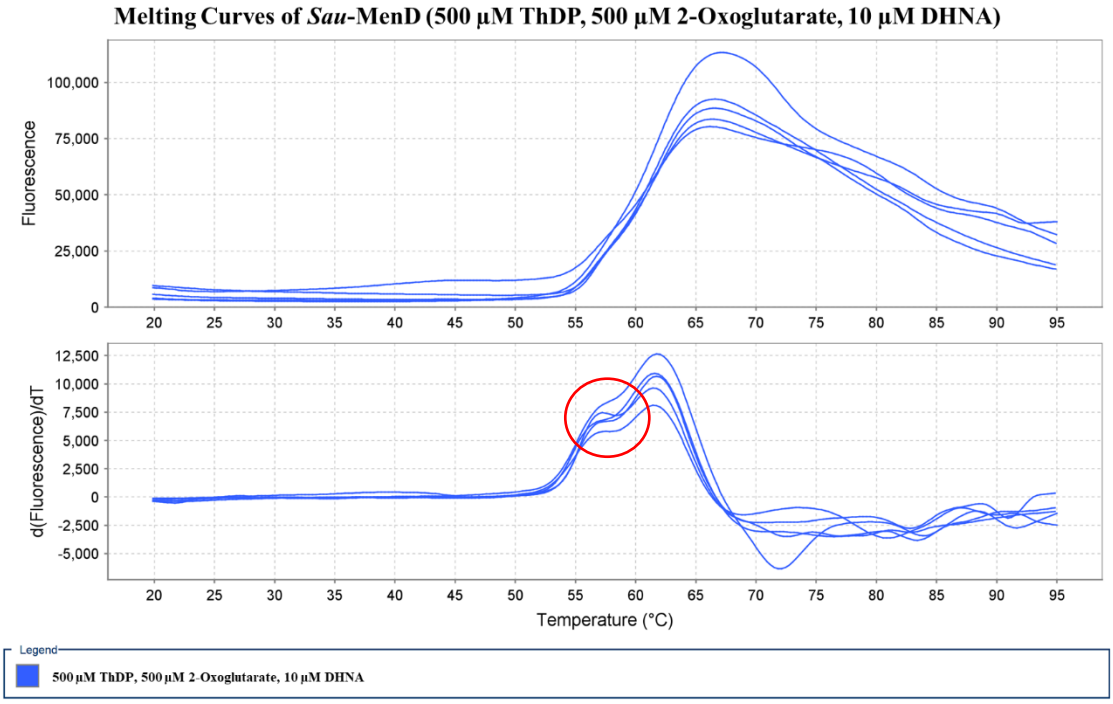

Figure 40: Melting curve of *Sau*-MenD with DHNA, ThDP and 2-oxoglutarate binding. The shoulder region seen in these replicates demonstrates multiple melting sites for the protein in these conditions. Shoulder region highlighted

Table 31: Melting temperature (T_m) of 5 µM *Sau*-MenD in different DHNA conditions. The error is the standard error of the mean. [A dash (-) signifies data unavailable due to an unreadable T_m change. T_m and differences are measured in Celsius. Derivative highlights the use of the derivative melt curves instead of Boltzmann melt curves for situations where the noise from the Boltzmann melt curves is too high].

Additive(s)	T_m	Error	Diff.	Rel. To[1]
No additive (2)	61.0	0.2	1.4	No additive (1)
10 µM DHNA	58.2	0.3	-2.8	No additive (2)
20 µM DHNA	57.7	0.2	-3.2	No additive (2)
30 µM DHNA	59.1	0.2	-1.9	No additive (2)
50 µM DHNA	56.1	0.9	-4.9	No additive (2)
100 µM DHNA	57.0	0.6	-4.0	No additive (2)
5 µM DHNA, 2.5 mM TCEP	65.0	0.5	1.6	2.5 mM TCEP, 0.1% DMSO (2)
10 µM DHNA, 2.5 mM TCEP	64.4	0.8	1.0	2.5 mM TCEP, 0.1% DMSO (2)
30 µM DHNA, 2.5 mM TCEP	63.1	0.6	-0.2	2.5 mM TCEP, 0.1% DMSO (2)
50 µM DHNA, 2.5 mM TCEP	64.2	1.0	0.8	2.5 mM TCEP, 0.1% DMSO (2)
5 µM DHNA, 500 µM ThDP	60.8	0.1	-3.7	500 µM ThDP, 0.1% DMSO (2) (Derivative)
10 µM DHNA, 500 µM ThDP	59.5	0.3	-5.0	500 µM ThDP, 0.1% DMSO (2) (Derivative)
100 µM DHNA, 500 µM ThDP	58.5	0.2	-6.0	500 µM ThDP, 0.1% DMSO (2) (Derivative)
5 µM DHNA, 500 µM ThDP, 2.5 mM TCEP	64.5	0.1	-0.1	500 µM ThDP, 0.1% DMSO, 2.5 mM TCEP (2) (Derivative)
10 µM DHNA, 500 µM ThDP, 2.5 mM TCEP	64.6	0.1	0.1	500 µM ThDP, 0.1% DMSO, 2.5 mM TCEP (2) (Derivative)
50 µM DHNA, 500 µM ThDP, 2.5 mM TCEP	64.6	0.1	0.1	500 µM ThDP, 0.1% DMSO, 2.5 mM TCEP (2) (Derivative)
100 µM DHNA, 500 µM ThDP, 2.5 mM TCEP	66.3	0.3	1.8	500 µM ThDP, 0.1% DMSO, 2.5 mM TCEP (2) (Derivative)
5 µM DHNA, 500 µM ThDP, 500 µM 2-oxoglutarate	60.3	0.1	-4.2	500 µM ThDP, 0.1% DMSO (2) (Derivative)
10 µM DHNA, 500 µM ThDP, 500 µM 2-oxoglutarate	61.6	0.1	-2.9	500 µM ThDP, 0.1% DMSO (2) (Derivative)
50 µM DHNA, 500 µM ThDP, 500 µM 2-oxoglutarate	60.0	0.2	-4.5	500 µM ThDP, 0.1% DMSO (2) (Derivative)
5 µM DHNA, 500 µM ThDP, 500 µM 2-oxoglutarate, 2.5 mM TCEP	65.5	0.1	1.1	500 µM ThDP, 500 µM 2-oxoglutarate, 0.1% DMSO, 2.5 mM TCEP (2) (Derivative)
10 µM DHNA, 500 µM ThDP, 500 µM 2-oxoglutarate, 2.5 mM TCEP	65.4	0.1	1.0	500 µM ThDP, 500 µM 2-oxoglutarate, 0.1% DMSO, 2.5 mM TCEP (2) (Derivative)
50 µM DHNA, 500 µM ThDP, 500 µM 2-oxoglutarate, 2.5 mM TCEP	65.6	0.09	1.1	500 µM ThDP, 500 µM 2-oxoglutarate, 0.1% DMSO, 2.5 mM TCEP (2) (Derivative)

[1] Compared to no additive conditions from the same experiment tray.

5.2.6 Metals

Although $MgCl_2$ was added to the buffer solution for these experiments, three other metals were also investigated via DSF in this work. These metals (the salts $MnCl_2$, $CaCl_2$ and $NiCl_2$) were all tested in apo conditions and in the presence of 500 µM ThDP at 5 mM concentrations. Both the apo conditions and the ThDP present conditions have no significant effects upon the T_m for both $CaCl_2$ and $MnCl_2$. However, $NiCl_2$ demonstrates a significant destabilisation effect in both apo and ThDP conditions, with T_m decreases of 6.9 and 5.9 °C respectively.

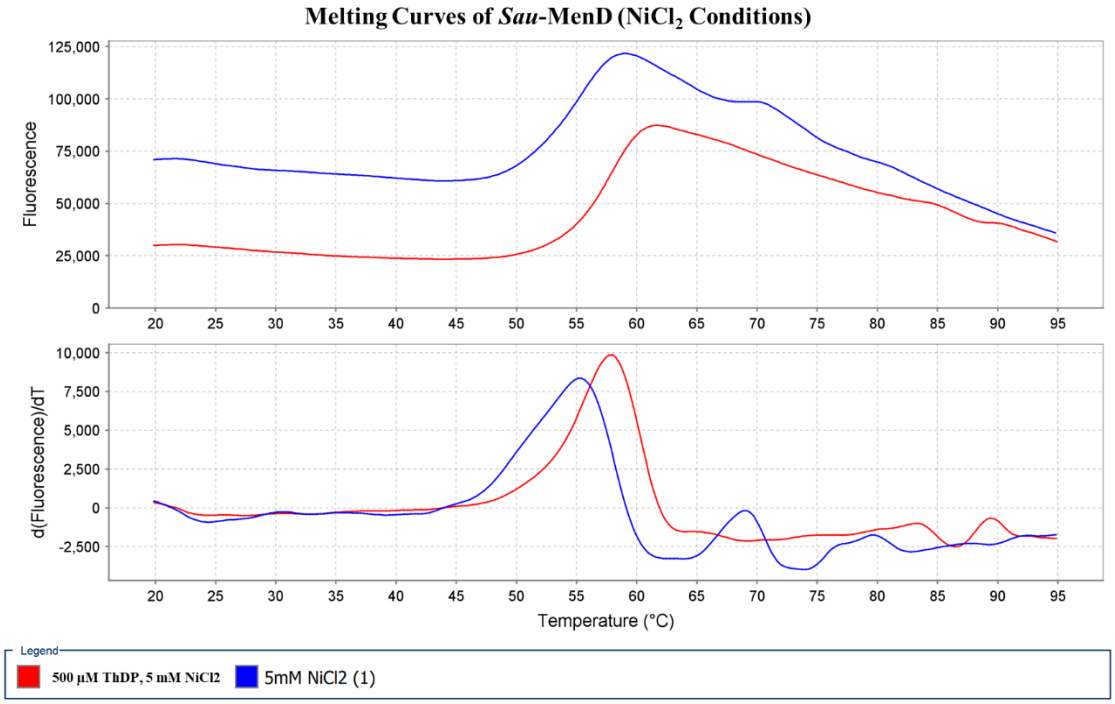

Figure 41: Representative melting curves for both $NiCl_2$ binding experiments conducted with *Sau*-MenD.

Table 32: Melting temperature (T_m) of 5 µM *Sau*-MenD in different Metal conditions. The error is the standard error of the mean. [A dash (-) signifies data unavailable due to an unreadable T_m change. T_m and differences are measured in Celsius].

Additive(s)	T_m	Error	Diff.	Rel. To[1]
5 mM $MnCl_2$	59.3	0.4	-0.3	No additive (1)
5 mM $MnCl_2$, 500 µM ThDP	62.8	0.1	0.4	500 µM ThDP (2)
5 mM $CaCl_2$	59.9	0.4	0.3	No additive (1)
5 mM $CaCl_2$, 500 µM ThDP	62.3	0.2	-0.1	500 µM ThDP (2)
5 mM $NiCl_2$	52.7	0.7	-6.9	No additive (1)
5 mM $NiCl_2$, 500 µM ThDP	56.5	0.2	-5.9	500 µM ThDP (2)

[1] Compared to no additive conditions from the same experiment tray.

5.2.7 Potential Inhibitors

There are seven different potential inhibitors that were investigated in this work. These inhibitors were tested in both low and high concentrations (100 µM and 1000 µM) in both apo conditions and 500 µM ThDP concentration. The general trend of these potential inhibitors was found to be a destabilisation effect on the protein in both apo and ThDP conditions with little variation based on concentration. The most notable inhibitors for *Sau*-MenD appeared to be 2-naphtoic acid, 2-hydroxy-1-naphtoic acid and 6-hydroxy-2-napthoic acid. 2-naphtoic acid showed the largest T_m changes between low concentration and high concentration in apo protein (low concentration T_m decrease of 1.5 °C and high concentration had a T_m increase of 1.2 °C). In addition, the presence of ThDP results in a decrease of 1.2 °C compared to the ThDP control conditions at low concentration. The high concentration results were inconclusive due to the variation between replicates; however, it would be interesting to replicate this experiment to potentially identify a similar effect in ThDP conditions.

2-hydroxy-1-napthoic acid shows destabilisation effects in both apo and ThDP conditions, however in the presence of high concentration and 500 µM ThDP, this effect is much higher than all other conditions for this inhibitor at 1.6 °C.

6-hydroxy-2-napthoic acid has a similar high T_m decrease compared to other conditions at high concentration and 500 µM ThDP at 1.3 °C. This suggests that these conditions may influence the protein, which may make it worth investigating for inhibitory purposes.

Table 33: Melting temperature (T_m) of 5 µM *Sau*-MenD in different Potential Inhibitor conditions. The error is the standard error of the mean. [A dash (-) signifies data unavailable due to an unreadable T_m change. T_m and differences are measured in Celsius].

Additive(s)	T_m	Error	Diff.	Rel. To[1]
100 µM 5-hydroxyinole carboxylic acid	58.3	0.1	-2.4	1% DMSO
100 µM 1-hydroxy-2-napthoic acid	59.9	0.5	-0.8	1% DMSO
1 mM 1-hydroxy-2-napthoic acid	59.7	0.1	-1.0	1% DMSO
100 µM 1-hydroxy-2-napthoic acid, 500 µM ThDP	61.3	0.4	-1.0	500 µM ThDP, 1% DMSO
1 mM 1-hydroxy-2-napthoic acid, 500 µM ThDP	61.6	0.5	-0.8	500 µM ThDP, 1% DMSO (Derivative)
100 µM p-Phenylene diacetic acid	59.8	0.7	-0.9	1% DMSO (Derivative)
1 mM p-Phenylene diacetic acid	60.1	0.4	-0.6	1% DMSO
100 µM p-Phenylene diacetic acid, 500 µM ThDP	61.4	0.2	-0.8	500 µM ThDP, 1% DMSO
1 mM p-Phenylene diacetic acid, 500 µM ThDP	62.4	0.3	0.1	500 µM ThDP, 1% DMSO
100 µM Monobutyl phthalate	59.6	0.7	-1.1	1% DMSO
1 mM Monobutyl phthalate	60.1	0.52	-0.6	1% DMSO
100 µM Monobutyl phthalate, 500 µM ThDP	61.8	0.47	-0.5	500 µM ThDP, 1% DMSO
1 mM Monobutyl phthalate, 500 µM ThDP	62.0	0.5	-0.3	500 µM ThDP, 1% DMSO
100 µM 2-napthtoic acid	60.1	0.1	-1.5	1% DMSO (Derivative)
1 mM 2-napthtoic acid	62.8	0.4	1.2	1% DMSO (Derivative)
100 µM 2-napthtoic acid, 500 µM ThDP	61.1	0.1	-1.2	500 µM ThDP, 1% DMSO
100 µM 2-hydroxy-1-napthoic acid	61.2	0.1	-0.3	1% DMSO
1 mM 2-hydroxy-1-napthoic acid	60.1	0.1	-0.6	1% DMSO
100 µM 2-hydroxy-1-napthoic acid, 500 µM ThDP	62.0	0.1	-0.3	500 µM ThDP, 1% DMSO
1 mM 2-hydroxy-1-napthoic acid, 500 µM ThDP	60.9	0.3	-1.6	500 µM ThDP, 1% DMSO (Derivative)
1 mM 6-hydroxy-2-napthoic acid	60.7	1.3	-0.8	1% DMSO (Derivative)
100 µM 6-hydroxy-2-napthoic acid, 500 µM ThDP	62.2	0.1	-0.3	500 µM ThDP, 1% DMSO (Derivative)
1 mM 6-hydroxy-2-napthoic acid, 500 µM ThDP	60.9	0.2	-1.3	500 µM ThDP, 1% DMSO

[1] Compared to no additive conditions from the same experiment tray.

5.3 DSF Experiments with *Ec*-MenD

5.3.1 Apo Conditions

There were no major differences observed between the three apo condition experiments run unlike those observed in *Sau*-MenD. *Ec*-MenD in general appeared to be more stable upon addition of non-binding compounds to the buffer mix, with no major changes to the T_m observed from either TCEP addition or DMSO addition. The only condition which demonstrated a significant change was with a combination of 0.1% DMSO and 2.5 mM TCEP. A stabilisation effect was observed (1.1 °C, Table 34), suggesting the presence of both compounds having an additive effect upon *Ec*-MenD.

Table 34: Melting temperature (T_m) of 5 µM *Ec*-MenD in different buffer conditions. The error is the standard error of the mean. [A dash (-) signifies data unavailable due to an unreadable T_m change. T_m and differences are measured in Celsius].

Additive(s)	T_m	Error	Diff.	Rel. To[1]
No additive (1)	54.9	0.1		
No additive (2)	55.1	0.0	0.2	No additive (1) (Derivative)
No additive (3)	55.3	0.0	0.4	No additive (1) (Derivative)
1 mM TCEP	55.4	0.1	0.5	No additive (1) (Derivative)
2.5 mM TCEP	55.5	0.1	0.6	No additive (1) (Derivative)
0.1% DMSO	54.6	0.1	-0.5	No additive (2) (Derivative)
1% DMSO	55.0	0.1	-0.3	No additive (3) (Derivative)
0.1% DMSO, 2.5 mM TCEP	56.2	0.1	1.1	No additive (2) (Derivative)

[1] Compared to no additive conditions from the same experiment tray.

5.3.2 ThDP

The overall trend with ThDP concentration increase observed for *Ec*-MenD is one of increasing stabilisation. The T_m increase is very high, with a lowest increase in the experiments with significant changes being 6.6 °C at 50 µM ThDP concentration (Table 35). There is a large difference between the repeated 500 µM ThDP experiments, with small to no change in three of the four experiments (from different trays).

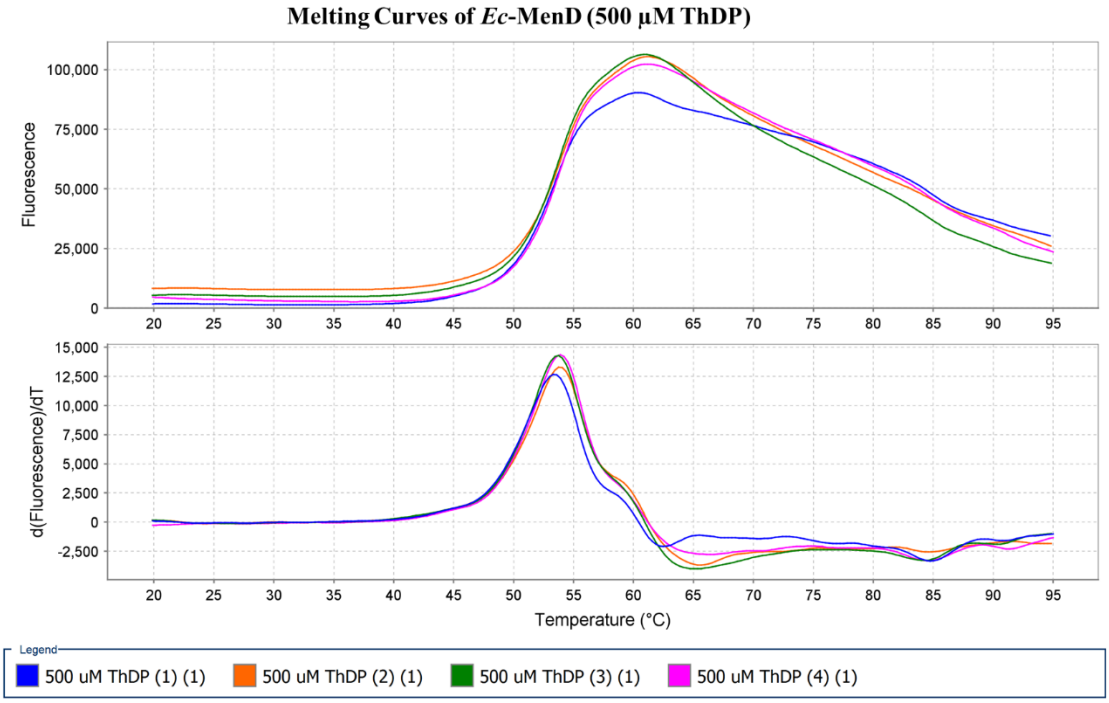

Figure 42: Comparison of melting curves of *Ec*-MenD experiments involving 500 µM ThDP addition from various plates.

TCEP addition does appear to provide a stabilisation effect, although without as significant of an effect on the protein as without ThDP present. While the experimental results for the 1 mM TCEP presence demonstrate a high T_m change, the standard error for this experiment is 6.9 which must be considered as imprecise for the results. Further experimentation work is needed.

DMSO addition to *Ec*-MenD fails to provide any noteworthy effects upon the T_m of the protein, in addition to the condition 2.5 mM TCEP as well as 0.1% DMSO and 500 µM ThDP providing inconclusive results. Further experimentation may be required to investigate any potential interaction between DMSO and *Ec*-MenD.

Table 35: Melting temperature (T_m) of 5 µM *Ec*-MenD in different ThDP conditions. The error is the standard error of the mean. [A dash (-) signifies data unavailable due to an unreadable T_m change. T_m and differences are measured in Celsius].

Additive(s)	T_m	Error	Diff.	Rel. To[1]
No additive (1)	54.9	0.1		
50 µM ThDP	51.3	1.5	6.6	No additive (1)
100 µM ThDP	53.9	0.1	9.2	No additive (1)
250 µM ThDP	53.27	0.03	8.55	No additive (1)
500 µM ThDP (1)	53.3	0.1	8.6	No additive (1)
500 µM ThDP (2)	53.84	0.04	0.54	No additive (1)
500 µM ThDP (3)	53.6	0.10	0.3	No additive (1)
500 µM ThDP (4)	53.9	0.0	0.6	No additive (1)
1000 µM ThDP	53.9	0.1	9.2	No additive (1)
500 µM ThDP, 1 mM TCEP	65.9	6.9	12.6	500 µM ThDP
500 µM ThDP, 2.5 mM TCEP	58.5	0.5	1.9	2.5 mM TCEP
500 µM ThDP, 0.1% DMSO	54.0	0.1	0.5	500 µM ThDP (2)
500 µM ThDP, 1% DMSO	53.5	0.1	-0.4	1% DMSO
500 µM ThDP, 0.1% DMSO, 2.5 mM TCEP	Replicate			500 µM ThDP, 0.1% DMSO

[1] Compared to no additive conditions from the same experiment tray.

5.3.3 2-Oxoglutarate

Addition of 2-oxoglutarate demonstrates a significant T_m increase to both apo and ThDP bound *Ec*-MenD (Table 36). This suggests significant stabilisation effects from the 2-oxoglutarate substrate either during binding or when it reacts to form intermediate I.

With 2.5 mM TCEP, 500 µM ThDP and 2-oxoglutarate present, a stabilisation effect is observed, with an increase of 6.9 °C. However, in the presence of 2.5 mM TCEP due to the large standard error no T_m change of note can be determined.

Table 36: Melting temperature (T_m) of 5 µM *Ec*-MenD in different 2-oxoglutarate conditions. The error is the standard error of the mean. [A dash (-) signifies data unavailable due to an unreadable T_m change. T_m and differences are measured in Celsius].

Additive(s)	T_m	Error	Diff.	Rel. To[1]
1000 µM 2-oxoglutarate	53.0	0.0	8.3	No additive (1)
500 µM ThDP, 50 µM 2-oxoglutarate	54.4	0.1	0.6	500 µM ThDP (2)
500 µM ThDP, 100 µM 2-oxoglutarate	54.5	0.1	0.7	500 µM ThDP (2)
500 µM ThDP, 250 µM 2-oxoglutarate	63.3	0.1	9.4	500 µM ThDP (2)
500 µM ThDP, 500 µM 2-oxoglutarate	55.4	0.0	1.6	500 µM ThDP (2)
500 µM ThDP, 1000 µM 2-oxoglutarate	62.3	0.1	8.4	500 µM ThDP (2)
500 µM ThDP, 500 µM 2-oxoglutarate, 2.5 mM TCEP	62.3	0.2	6.9	500 µM ThDP, 500 µM 2-oxoglutarate
500 µM ThDP, 500 µM 2-oxoglutarate, 0.1% DMSO, 2.5 mM TCEP	56.6	2.0	2.6	500 µM ThDP, 0.1% DMSO, 2.5 mM TCEP (2)

[1] Compared to no additive conditions from the same experiment tray.

5.3.4 CHD

In relation to CHD presence for *Ec*-MenD, in the presence of 500 µM ThDP and CHD a minor T_m increase, and therefore a slight stabilisation effect is observed. Upon 500 µM 2-oxoglutarate addition, no discernible T_m change is observed.

Table 37: Melting temperature (T_m) of 5 µM *Ec*-MenD in different CHD conditions. The error is the standard error of the mean. [A dash (-) signifies data unavailable due to an unreadable T_m change. T_m and differences are measured in Celsius].

Additive(s)	T_m	Error	Diff.	Rel. To[1]
500 µM ThDP, 500 µM CHD	54.8	0.1	0.9	500 µM ThDP (2)
500 µM THDP, 500 µM CHD, 500 µM 2-oxoglutarate	55.1	0.1	0.3	500 µM ThDP (2)

[1] Compared to no additive conditions from the same experiment tray.

5.3.5 DHNA

Many of the DHNA experiments did not provide clear results. This is due to a mixture of unreadable melt curves and replicate experiments not being in agreement with each other (see Appendix 2 for graphs) Most of these experiments will need to be repeated in further work due to this outcome, however some results are still available for discussion.

This work shows that at DHNA concentrations above 10 µM destabilisation effects on *Ec*-MenD are observed. A maximum T_m decrease is observed at 50 µM DHNA concentration (-3.1 °C, Table 38), suggesting an optimal DHNA concentration for *Ec*-MenD. This is supported by the decreasing T_m trend observed from 20-50 µM DHNA and with the lower decrease in T_m observed at 100 µM.

As mentioned previously, many of the DHNA experiments for *Ec*-MenD will need to be repeated, as is the case for DHNA experiments in the presence of 2.5 mM TCEP. The only experiment in this set which provided usable results was at 100 µM DHNA concentration, where a significantly high T_m decrease was observed (19.7 °C, Table 38). while this could suggest the presence of TCEP allowing the redox active DHNA to interact with *Ec*-MenD in its full capacity, the lack of experimental results at lower DHNA concentrations makes it difficult to determine if this destabilization effect is an outlier or part of a trend.

In the presence of 500 µM ThDP, increasing DHNA concentrations have almost no effect upon the T_m of the *Ec*-MenD protein. All four experiments as shown from 5-100 µM DHNA have no notable changes to the T_m. This is a large change from the high decreases of T_m found without 500 µM ThDP presence, implying ThDP's importance to the *Ec*-MenD protein for stabilisation.

Two of the three experiments involving increasing DHNA concentration and 500 µM ThDP and 2-oxoglutarate were also useable. 10 µM and 50 µM DHNA concentrations were recorded and while 50 µM did not have a mentionable T_m change, 10 µM DHNA demonstrated a high stabilisation effect upon *Ec*-MenD (5.8 °C, Table 38). This result is contradictory to the trends observed from all previous DHNA experiments for *Ec*-MenD, however due to the lack of results from most of the experiments it is difficult to determine if this is an outlier or similar to the previous conditions. Further experimentation on these conditions would be required to make appropriate conclusions.

Table 38: Melting temperature (T_m) of 5 µM *Ec*-MenD in different DHNA conditions. The error is the standard error of the mean. [A dash (-) signifies data unavailable due to an unreadable T_m change. T_m and differences are measured in Celsius]. For clarity only the conditions that gave interpretable results are shown in the table.

Additive(s)	T_m	Error	Diff.	Rel. To[1]
10 µM DHNA	52.73	0.04	-0.19	0.1% DMSO
20 µM DHNA	51.3	0.1	-1.7	0.1% DMSO
30 µM DHNA	50.5	0.9	-2.4	0.1% DMSO
50 µM DHNA	49.8	0.1	-3.1	0.1% DMSO
100 µM DHNA	51.5	0.1	-1.5	0.1% DMSO
100 µM DHNA, 2.5 mM TCEP	27.4	0.1	-19.7	100 µM DHNA
5 µM DHNA, 500 µM ThDP	54.2	0.1	0.2	500 µM ThDP, 0.1% DMSO (2) (Derivative)
10 µM DHNA, 500 µM ThDP	54.38	0.03	0.36	500 µM ThDP, 0.1% DMSO (2) (Derivative)
50 µM DHNA, 500 µM ThDP	54.11	0.04	0.09	500 µM ThDP, 0.1% DMSO (2) (Derivative)
100 µM DHNA, 500 µM ThDP	54.5	0.1	0.5	500 µM ThDP, 0.1% DMSO (2) (Derivative)
10 µM DHNA, 500 µM ThDP, 500 µM 2-oxoglutarate	59.8	0.2	5.8	500 µM ThDP, 0.1% DMSO (2) (Derivative)
50 µM DHNA, 500 µM ThDP, 500 µM 2-oxoglutarate	54.5	0.1	0.5	500 µM ThDP, 0.1% DMSO (2) (Derivative)

[1] Compared to no additive conditions from the same experiment tray.

5.3.6 Metals

All three metal ions which were involved in the experiments demonstrated significant stabilisation effects in the absence of 500 µM ThDP. It should be noted that the $NiCl_2$ condition did have a significantly high standard error of 9, meaning this result is not as reliable as the other metals. The result of this high error can be seen in Figure 43. With the presence of 500 µM ThDP, all three metal ions interacted differently. $MnCl_2$ and $NiCl_2$ both demonstrated a destabilisation effect to varying degrees (-0.9 and -12.5 °C respectively, Table 39), while $CaCl_2$ demonstrated a minor T_m increase instead.

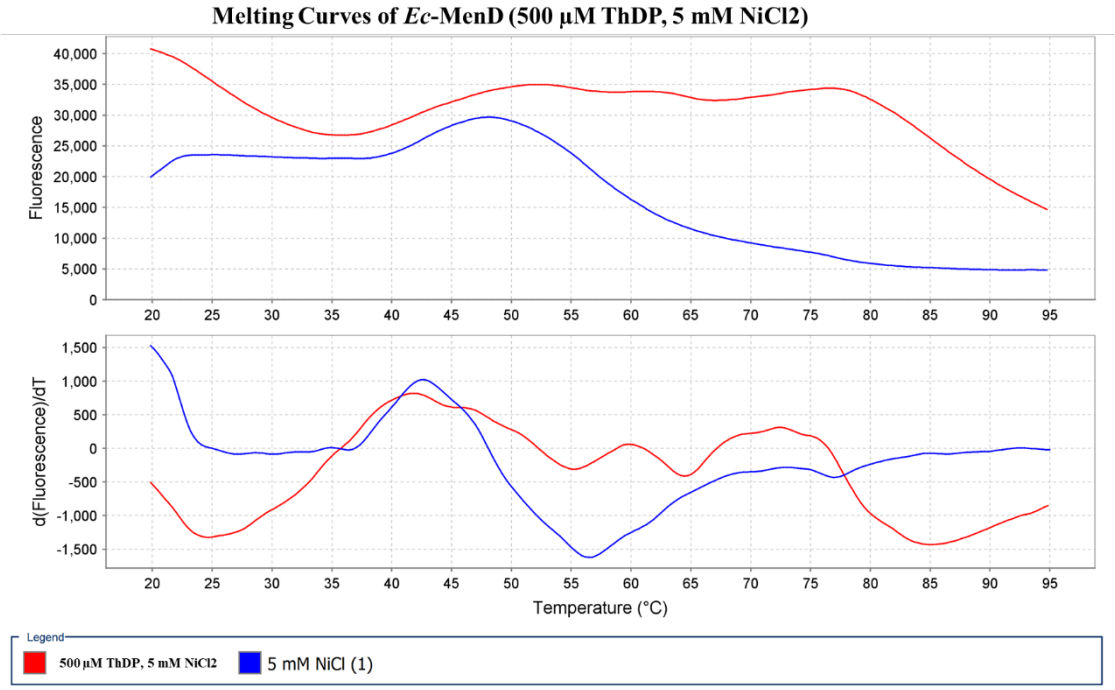

Figure 43: Melting curves of $NiCl_2$ experiments conducted for *Ec*-MenD

Table 39: Melting temperature (T_m) of 5 µM *Ec*-MenD in different Metal conditions. The error is the standard error of the mean. [A dash (-) signifies data unavailable due to an unreadable T_m change. T_m and differences are measured in Celsius].

Additive(s)	T_m	Error	Diff.	Rel. To[1]
5 mM $MnCl_2$	47.7	0.1	3.0	No additive (1)
5 mM $MnCl_2$, 500 µM ThDP	52.9	0.1	-0.9	500 µM ThDP (2)
5 mM $CaCl_2$	53.03	0.04	8.31	No additive (1)
5 mM $CaCl_2$, 500 µM ThDP	54.73	0.04	0.89	500 µM ThDP (2)
5 mM $NiCl_2$	54.7	9.0	10.0	No additive (1)
5 mM $NiCl_2$, 500 µM ThDP	41.4	0.3	-12.5	500 µM ThDP (2)

[1] Compared to no additive conditions from the same experiment tray.

5.3.7 Potential Inhibitors

Most potential inhibitor experiments conducted for *Ec*-MenD did not provide any noteworthy changes. There are three inhibitors with experimental results of interest. 2-hydroxy-1-napthoic acid was observed with two destabilisation effects at both 100 µM and 1 mM 2-hydroxy-1-napthoic acid concentration with 500 µM ThDP concentration present (-1.3 and -1.4 °C, Table 40). At 1 mM p-Phenylene diacetic acid presence, a significantly high T_m decrease is observed which is not consistent with any of the other experiments conducted with this inhibitor. With a low standard error, this condition is worth further investigation as this is the highest T_m change observed from all experiments. Finally, 1 mM 1-hydroxy-2-naphthoic acid with 500 µM ThDP presence demonstrated the only large stabilisation effect observed from the potential inhibitors. (1.1 °C, Table 40). Further experimental work is worthwhile upon these three inhibitors for *Ec*-MenD, as well as investigating the effects upon T_m these inhibitors have upon the different proteins involved in this work.

Table 40: Melting temperature (T_m) of 5 µM *Ec*-MenD in different Potential Inhibitor conditions. The error is the standard error of the mean. [A dash (-) signifies data unavailable due to an unreadable T_m change. T_m and differences are measured in Celsius].

Additive(s)	T_m	Error	Diff.	Rel. To[1]
100 µM 5-hydroxyinole carboxylic acid	52.6	0.3	0.1	1% DMSO (Derivative)
1 mM 5-hydroxyinole carboxylic acid	52.1	0.5	-0.4	1% DMSO (Derivative)
100 µM 5-hydroxyinole carboxylic acid, 500 µM ThDP	54.3	0.1	0.8	500 µM ThDP, 1% DMSO (Derivative)
1 mM 5-hydroxyinole carboxylic acid, 500 µM ThDP	54.0	0.1	0.5	500 µM ThDP, 1% DMSO (Derivative)
100 µM 1-hydroxy-2-napthoic acid	53.0	0.3	0.5	1% DMSO (Derivative)
1 mM 1-hydroxy-2-napthoic acid	52.2	1.0	-0.3	1% DMSO (Derivative)
100 µM 1-hydroxy-2-napthoic acid, 500 µM ThDP	54.4	0.2	0.9	500 µM ThDP, 1% DMSO (Derivative)
1 mM 1-hydroxy-2-napthoic acid, 500 µM ThDP	54.6	0.3	1.1	500 µM ThDP, 1% DMSO (Derivative)
100 µM p-Phenylene diacetic acid	52.8	0.1	0.4	1% DMSO (Derivative)
1 mM p-Phenylene diacetic acid	20.6	0.3	-32.7	1% DMSO (Derivative)
100 µM p-Phenylene diacetic acid, 500 µM ThDP	53.1	0.1	0.6	500 µM ThDP, 1% DMSO (Derivative)

1 mM p-Phenylene diacetic acid, 500 µM ThDP	53.0	0.1	0.5	500 µM ThDP, 1% DMSO (Derivative)
100 µM Monobutyl phthalate	54.2	0.0	0.7	1% DMSO (Derivative)
1 mM Monobutyl phthalate	54.2	0.1	0.7	1% DMSO (Derivative)
100 µM Monobutyl phthalate, 500 µM ThDP	53.0	0.1	0.6	500 µM ThDP, 1% DMSO (Derivative)
1 mM Monobutyl phthalate, 500 µM ThDP	53.0	0.1	0.5	500 µM ThDP, 1% DMSO (Derivative)
100 µM 2-napthtoic acid	54.2	0.0	0.7	1% DMSO (Derivative)
1 mM 2-napthtoic acid	54.0	0.1	0.5	1% DMSO (Derivative)
100 µM 2-napthtoic acid, 500 µM ThDP	53.0	0.1	0.6	500 µM ThDP, 1% DMSO (Derivative)
1 mM 2-napthtoic acid, 500 µM ThDP	52.7	0.4	0.3	500 µM ThDP, 1% DMSO (Derivative)
100 µM 2-hydroxy-1-napthoic acid	54.2	0.0	0.7	1% DMSO (Derivative)
1 mM 2-hydroxy-1-napthoic acid	54.0	0.1	0.5	1% DMSO (Derivative)
100 µM 2-hydroxy-1-napthoic acid, 500 µM ThDP	51.2	0.7	-1.3	500 µM ThDP, 1% DMSO (Derivative)
1 mM 2-hydroxy-1-napthoic acid, 500 µM ThDP	51.0	0.9	-1.4	500 µM ThDP, 1% DMSO (Derivative)
100 µM 6-hydroxy-2-napthoic acid	53.9	0.1	0.4	1% DMSO (Derivative)
1 mM 6-hydroxy-2-napthoic acid	53.9	0.1	0.4	1% DMSO (Derivative)
100 µM 6-hydroxy-2-napthoic acid, 500 µM ThDP	53.1	0.1	0.6	500 µM ThDP, 1% DMSO (Derivative)
1 mM 6-hydroxy-2-napthoic acid, 500 µM ThDP	53.0	0.1	0.5	500 µM ThDP, 1% DMSO (Derivative)

[1] Compared to no additive conditions from the same experiment tray.

5.4 DSF Experiments with *Smeg*-MenD

5.4.1 Apo Conditions

Apo conditions for *Smeg*-MenD showed minimal changes to the T_m between the three conditions. A decrease was observed in the third set of experiments; however, this change was relatively small. Addition of TCEP provided nothing of note at 1 mM TCEP, while at higher concentration of 2.5 mM although a large decrease was observed the standard error for this experiment was sufficiently high to disregard this result due to inaccuracies. DMSO addition provided no T_m changes worth mentioning, while with DMSO and TCEP presence, the standard error was again too high to effectively use this result in this discussion.

Table 41: Melting temperature (T_m) of 5 µM *Smeg*-MenD in different buffer conditions. The error is the standard error of the mean. [A dash (-) signifies data unavailable due to an unreadable T_m change. T_m and differences are measured in Celsius].

Additive(s)	T_m	Error	Diff.	Rel. To[1]
No additive (1)	59.6	0.2		
No additive (2)	59.8	0.0	0.2	No additive (1) (Derivative)
No additive (3)	59.0	0.0	-0.6	No additive (1) (Derivative)
1 mM TCEP	59.6	0.2	0	No additive (1) (Derivative)
2.5 mM TCEP	55.6	2.4	-4	No additive (1) (Derivative)
0.1% DMSO	59.5	0.1	-0.1	No additive (2) (Derivative)
1% DMSO	59.4	0.2	0.4	No additive (3) (Derivative)
0.1% DMSO, 2.5 mM TCEP	57.8	1.1	2	No additive (2) (Derivative)

[1] Compared to no additive conditions from the same experiment tray.

5.4.2 ThDP

It is not until a ThDP concentration of 250 µM is present that a significant T_m change is observed in *Smeg*-MenD. At this concentration a major destabilisation effect occurs for *Smeg*-MenD, which is the most significant change observed from any concentration of ThDP addition. (-18.2 °C, Table 42). It should be noted however that this large decrease in T_m is accompanied by a large standard error of 5 and as such must be observed under some scrutiny on the precision of this result (Figure 44). The remaining experiments with solely ThDP addition to *Smeg*-MenD do not appear to follow any specific stabilisation or destabilisation trend. Of the four repeated experiments at 500 µM ThDP concentration, the only T_m changes of increase are destabilisation results, and only one of these shows a significant change. Conversely, at 1000 µM ThDP concentration a T_m increase comparative to the decrease seen at 500 µM ThDP concentration was observed (-3.1 vs 2.3 °C, Table 42), suggesting no particular trend in the effects of ThDP on *Smeg*-MenD.

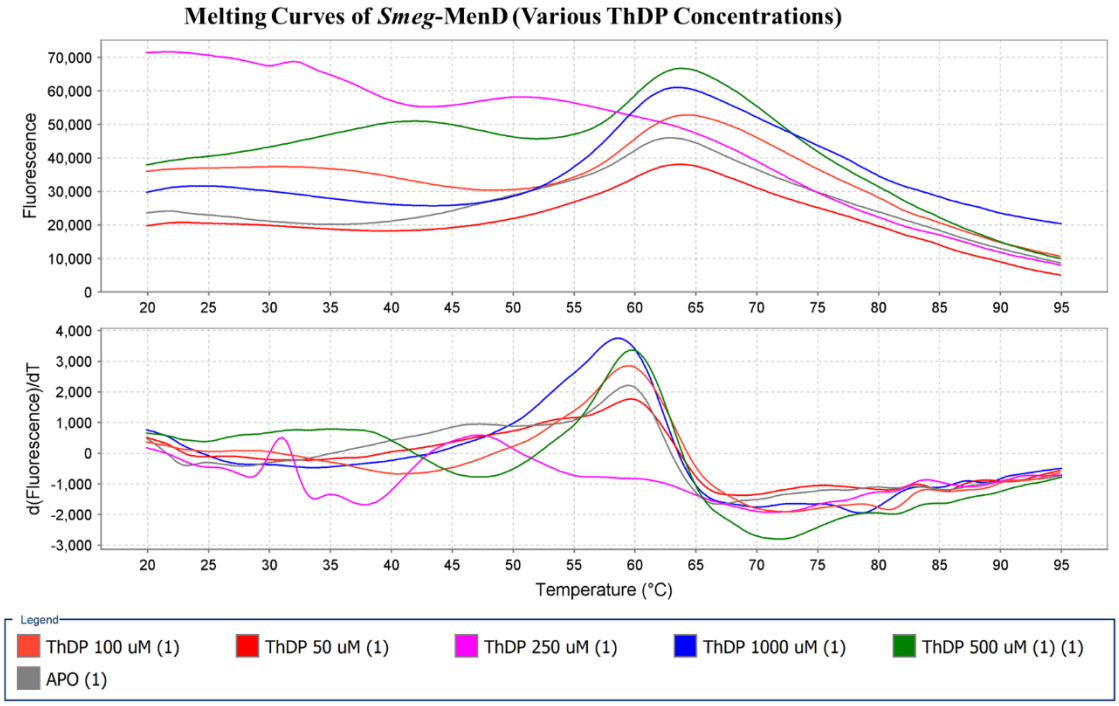

Figure 44: Melting curves of all ThDP concentrations for *Smeg*-MenD. As can be seen the large error observed at 250 µM concentration corresponds accordingly to a melt curve significantly different than the other ThDP concentrations.

A significant change occurs in the 2.5 mM TCEP 500 µM ThDP condition. A destabilisation effect is observed (-2 °C, Table 42). With 1 mM TCEP addition no major changes in T_m are observed. DMSO addition provides interesting results. At 0.1 % DMSO concentration a high T_m increase is observed whilst in the presence of 500 µM ThDP, whereas at a higher concentration of DMSO (1%) this stabilisation effect is absent (3.3 vs -0.9 °C, Table 42). This could be due to an ideal DMSO concentration for *Smeg*-MenD interactions. 2.5 mM TCEP presence does not appear to have any meaningful effect upon the T_m of *Smeg*-MenD.

Table 42: Melting temperature (T_m) of 5 µM *Smeg*-MenD in different ThDP conditions. The error is the standard error of the mean. [A dash (-) signifies data unavailable due to an unreadable T_m change. T_m and differences are measured in Celsius].

Additive(s)	T_m	Error	Diff.	Rel. To[1]
No additive (1)	59.6	0.2		
50 µM ThDP	59.7	0.1	0.1	No additive (1) (Derivative)
100 µM ThDP	59.7	0.2	0.1	No additive (1) (Derivative)
250 µM ThDP	41.4	5.0	-18.2	No additive (1) (Derivative)
500 µM ThDP (1)	58.9	0.9	-0.7	No additive (1) (Derivative)
500 µM ThDP (2)	56.9	0.1	0.2	No additive (1) (Derivative)
500 µM ThDP (3)	59.8	0.1	-3.1	No additive (1) (Derivative)
500 µM ThDP (4)	60.1	0.1	0.5	No additive (1) (Derivative)
1000 µM ThDP	56.2	0.3	2.3	No additive (1) (Derivative)
500 µM ThDP, 1 mM TCEP	59.7	0.1	0.1	1 mM TCEP
500 µM ThDP, 2.5 mM TCEP	57.6	0.8	-2.0	2.5 mM TCEP
500 µM ThDP, 0.1% DMSO	59.8	0.1	3.3	500 µM ThDP (3)
500 µM ThDP, 1% DMSO	59.0	0.2	-0.9	500 µM ThDP (1)
500 µM ThDP, 0.1% DMSO, 2.5 mM TCEP	59.3	0.4	-0.5	500 µM ThDP, 0.1% DMSO

[1] Compared to no additive conditions from the same experiment tray.

5.4.3 2-Oxoglutarate

2-Oxoglutarate does not appear to display much of a change in the T_m of *Smeg*-MenD at any concentration. The most significant change observed in the T_m is observed at 250 µM 2-oxoglutarate concentration with 500 µM ThDP presence. The change observed at this concentration is slightly higher than what is observed with only 1000 µM 2-oxoglutarate presence for *Smeg*-MenD, potentially suggesting a saturation concentration of 2-oxoglutarate while in the presence of ThDP. 2.5 mM TCEP addition also does not provide any noteworthy T_m changes for *Smeg*-MenD, and the significantly high T_m increase seen with ThDP, 2-oxoglutarate, DMSO and TCEP presence is accompanied by an even higher standard error, rendering this result far too inaccurate for use.

The experiment involving 0.1% DMSO addition in addition to 500 µM ThDP and 2-oxoglutarate and 2.5 mM TCEP has a standard error both higher than the T_m difference and the accepted standard error, meaning this experiment has unusable results for this experiment.

Table 43: Melting temperature (T_m) of 5 µM *Smeg*-MenD in different 2-oxoglutarate conditions. The error is the standard error of the mean. [A dash (-) signifies data unavailable due to an unreadable T_m change. T_m and differences are measured in Celsius].

Additive(s)	T_m	Error	Diff.	Rel. To[1]
1000 µM 2-oxoglutarate	60.2	0.1	0.6	No additive (1) (Derivative)
500 µM ThDP, 50 µM 2-oxoglutarate	60.0	0.1	0.3	500 µM ThDP (2) (Derivative)
500 µM ThDP, 100 µM 2-oxoglutarate	59.7	0.1	0.0	500 µM ThDP (2) (Derivative)
500 µM ThDP, 250 µM 2-oxoglutarate	57.8	0.3	0.9	500 µM ThDP (2)
500 µM ThDP, 500 µM 2-oxoglutarate	60.1	0.1	0.4	500 µM ThDP (2) (Derivative)
500 µM ThDP, 1000 µM 2-oxoglutarate	59.9	0.1	0.2	500 µM ThDP (2) (Derivative)
500 µM ThDP, 500 µM 2-oxoglutarate, 2.5 mM TCEP	60.3	0.1	0.1	500 µM ThDP, 1000 µM 2-oxoglutarate
500 µM ThDP, 500 µM 2-oxoglutarate, 0.1% DMSO, 2.5 mM TCEP	64.7	5.5	5.3	500 µM ThDP, 0.1% DMSO, 2.5 mM TCEP (2)

[1] Compared to no additive conditions from the same experiment tray.

5.4.4 CHD

CHD was not a ligand of major focus in this work, but the results provided from the experiments warranted further discussion. In a trend like the results observed from the 2-oxoglutarate experiments the CHD binding experiments demonstrated destabilisation effects in *Sau*-MenD, and stabilisation effects in *Ec*-MenD and *Smeg*-MenD, with a greater stabilisation effect (T_m increase) observed in *Ec*-MenD. This result could be due to the presence of ThDP and 2-oxoglutarate in addition to CHD, however as the T_m differences were compared to ThDP binding experiments with similar concentration this can at least eliminate the possibility that all that is observed is ThDP binding effects. CHD could be affecting the proteins through either binding to the ligands prior to interactions, direct protein interaction, or a mixture of both. Regardless, these results suggest that further CHD experimentation is needed for better characterisation of the MenD enzyme.

Table 44: Melting temperature (T_m) of 5 µM *Smeg*-MenD in different CHD conditions. The error is the standard error of the mean. [A dash (-) signifies data unavailable due to an unreadable T_m change. T_m and differences are measured in Celsius].

Additive(s)	T_m	Error	Diff.	Rel. To[1]
500 µM ThDP, 500 µM CHD	60.1	0.1	0.3	500 µM ThDP (2) (Derivative)
500 µM THDP, 500 µM CHD, 500 µM 2-oxoglutarate	60.0	0.1	-0.1	500 µM ThDP (2) (Derivative)

[1] Compared to no additive conditions from the same experiment tray.

5.4.5 DHNA

Significant changes to the T_m were observed upon addition of increasing DHNA concentrations. These destabilisation effects occurred at 10 µM DHNA concentration through to 100 µM DHNA and as shown in Table 45 ranged from a T_m decrease of 24.4 – 32.7 °C. The presence of 2.5 mM TCEP appears to not only fully negate the destabilisation effects of DHNA seen previously, but also provide stabilisation effects upon *Smeg*-MenD (Figure 45). The only exception is at 30 µM DHNA concentration which maintained a destabilisation effect of -14.9 °C but also had the highest standard error as well. These results are quite supportive of the theory that DHNA requires the presence of TCEP to maintain redox activity, as these two results are drastically different. Further investigation potentially using different reducing agents to determine if this effect is purely due to the DHNA being redox active or the reducing agent is having an additional effect could prove to be useful to this work.

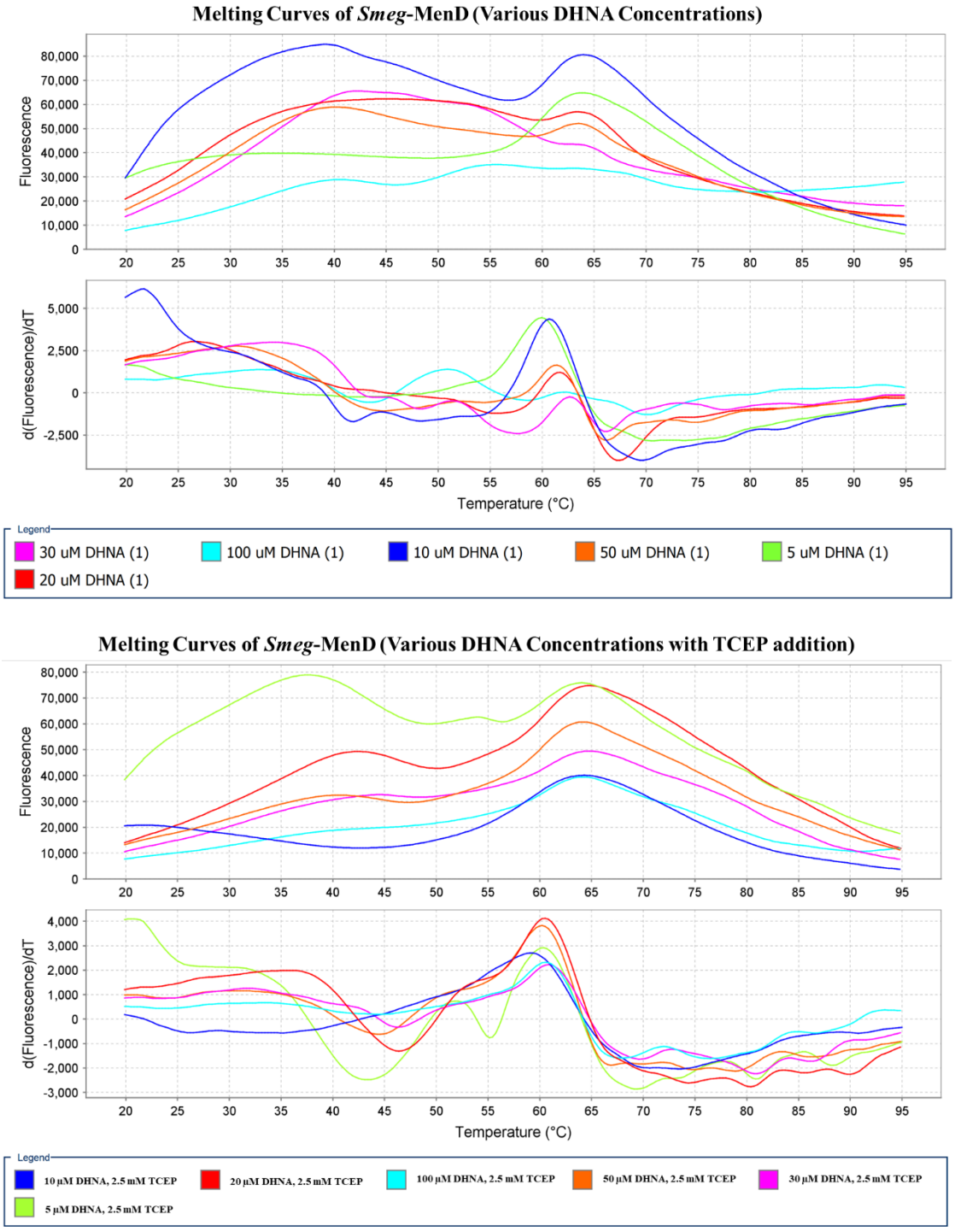

Figure 45: Top (a): Comparisons of melting curves for all DHNA concentrations to *Smeg*-MenD. **Bottom (b):** Comparisons of melting curves for all DHNA concentrations with 2.5 mM TCEP present for *Smeg*-MenD.

The presence of 500 µM ThDP with an increasing DHNA concentration had an interesting effect on the *Smeg*-MenD protein. DHNA concentrations of 5 and 50 µM whilst having large destabilisation effects upon *Smeg*-MenD have equally high standard errors, resulting in unusable results for discussion. At 10 µM and 100 µM DHNA, stabilisation effects of vastly different magnitudes were observed. Due to the incredibly high T_m increase observed at 100 µM DHNA concentration, further experimentation at higher DHNA concentrations would provide more accurate information on the optimal concentration needed for the *Smeg*-MenD protein, and MenD proteins in general. Regardless, it is apparent that higher DHNA presence at this point have only provided more significant changes to T_m and as such finding the upper limit would be beneficial. 2.5 mM TCEP addition follows the same trend as seen before with all concentrations having stabilisation effects, with the T_m increase at 100 µM DHNA being significantly higher.

The presence of 500 µM 2-oxoglutarate has very negative effects upon the experimentation work, resulting in high standard errors in all experiments. This suggests reproducibility between replicates is very poor and as such most of these results cannot be used to discern anything of use. This also appear to be the case for the same experiments with 2.5 mM TCEP presence. Appendix 3 shows the poor reproducibility in replicates. The only exception to this is found at 10 µM DHNA concentration with 2.5 mM presence. At this concentration as low error is observed while a high T_m decrease can be seen. Further experimentation around these conditions need to be done to determine if the presence of 2-oxoglutarate does result in this destabilisation effect observed.

Table 45: Melting temperature (T_m) of 5 µM *Smeg*-MenD in different DHNA conditions. The error is the standard error of the mean. [A dash (-) signifies data unavailable due to an unreadable T_m change. T_m and differences are measured in Celsius].

Additive(s)	T_m	Error	Diff.	Rel. To
5 µM DHNA	60.1	0.1	0.5	0.1% DMSO (Derivative)
10 µM DHNA	25.3	0.2	-29.3	0.1% DMSO
20 µM DHNA	26.8	0.2	-32.7	0.1% DMSO (Derivative)
30 µM DHNA	33.8	0.2	-25.8	0.1% DMSO (Derivative)
50 µM DHNA	30.2	0.6	-29.4	0.1% DMSO (Derivative)
100 µM DHNA	30.1	0.5	-24.4	0.1% DMSO (Derivative)
5 µM DHNA, 2.5 mM TCEP	60.0	0.1	2.2	2.5 mM TCEP, 0.1% DMSO (Derivative)
10 µM DHNA, 2.5 mM TCEP	59.4	0.1	1.6	2.5 mM TCEP, 0.1% DMSO (Derivative)
20 µM DHNA, 2.5 mM TCEP	60.54	0.05	2.7	2.5 mM TCEP, 0.1% DMSO (Derivative)
30 µM DHNA, 2.5 mM TCEP	40.6	2.4	-14.9	2.5 mM TCEP, 0.1% DMSO
50 µM DHNA, 2.5 mM TCEP	60.1	0.1	2.3	2.5 mM TCEP, 0.1% DMSO
100 µM DHNA, 2.5 mM TCEP	60.66	0.06	2.8	2.5 mM TCEP, 0.1% DMSO (Derivative)
5 µM DHNA, 500 µM ThDP	53.8	6.5	-6.0	500 µM ThDP, 0.1% DMSO (2) (Derivative)
10 µM DHNA, 500 µM ThDP	60.6	0.1	0.8	500 µM ThDP, 0.1% DMSO (2) (Derivative)
50 µM DHNA, 500 µM ThDP	49.9	12.0	-10.0	500 µM ThDP, 0.1% DMSO (2) (Derivative)
100 µM DHNA, 500 µM ThDP	83.1	0.3	23.3	500 µM ThDP, 0.1% DMSO (2) (Derivative)
5 µM DHNA, 500 µM ThDP, 2.5 mM TCEP	59.5	0.4	0.2	500 µM ThDP, 0.1% DMSO, 2.5 mM TCEP (2) (Derivative)
10 µM DHNA, 500 µM ThDP, 2.5 mM TCEP	60.9	0.3	1.6	500 µM ThDP, 0.1% DMSO, 2.5 mM TCEP (2) (Derivative)
50 µM DHNA, 500 µM ThDP, 2.5 mM TCEP	60.9	0.2	1.5	500 µM ThDP, 0.1% DMSO, 2.5 mM TCEP (2) (Derivative)
100 µM DHNA, 500 µM ThDP, 2.5 mM TCEP	88.9	0.4	29.6	500 µM ThDP, 0.1% DMSO, 2.5 mM TCEP (2) (Derivative)
5 µM DHNA, 500 µM ThDP, 500 µM 2-oxoglutarate	56.6	8.5	-3.2	500 µM ThDP, 0.1% DMSO (Derivative)
10 µM DHNA, 500 µM ThDP, 500 µM 2-oxoglutarate	57.2	11.6	-0.2	500 µM ThDP 0.1% DMSO
50 µM DHNA, 500 µM ThDP, 500 µM 2-oxoglutarate	44.3	14.5	-15.5	500 µM ThDP, 0.1% DMSO (Derivative)
5 µM DHNA, 500 µM ThDP, 500 µM 2-oxoglutarate, 2.5 mM TCEP	50.2	7.6	-7.1	500 µM ThDP, 500 µM 2-oxoglutarate, 0.1% DMSO, 2.5 mM TCEP

10 µM DHNA, 500 µM ThDP, 500 µM 2-oxoglutarate, 2.5 mM TCEP	60.7	0.3	-3.9	500 µM ThDP, 500 µM 2-oxoglutarate, 0.1% DMSO, 2.5 mM TCEP (Derivative)
50 µM DHNA, 500 µM ThDP, 500 µM 2-oxoglutarate, 2.5 mM TCEP	64.0	3.3	-0.7	500 µM ThDP, 500 µM 2-oxoglutarate, 0.1% DMSO, 2.5 mM TCEP (Derivative)

[1] Compared to no additive conditions from the same experiment tray.

5.4.6 Metals

Due to the large standard errors observed in the $NiCl_2$ results for *Smeg*-MenD, these have been omitted from the discussion on effects by the metals.

Addition of either metal at 5 mM concentration interestingly has the exact same effect upon the T_m of *Smeg*-MenD. Both metals display a T_m increase and therefore a stabilisation effect to *Smeg*-MenD (3.6 °C, Table 46). This same effect between the added metals is not observed in the presence of 500 µM ThDP. While $MnCl_2$ demonstrates no noteworthy T_m change $CaCl_2$ has a T_m increase lower than without ThDP presence (1.6 vs 3.6 °C, Table 46). Further investigation into the optimal metals to be used in the buffer solution could be useful as this could have a more significant effect upon the interactions of *Smeg*-MenD with the other ligands investigated in this work.

Table 46: Melting temperature (T_m) of 5 µM *Smeg*-MenD in different metal conditions. The error is the standard error of the mean. [A dash (-) signifies data unavailable due to an unreadable T_m change. T_m and differences are measured in Celsius].

Additive(s)	T_m	Error	Diff.	Rel. To[1]
5 mM $MnCl_2$	57.5	0.4	3.6	No additive (1)
5 mM $MnCl_2$, 500 µM ThDP	56.8	0.8	-0.1	500 µM ThDP (2)
5 mM $CaCl_2$	57.5	0.2	3.6	No additive (1)
5 mM $CaCl_2$, 500 µM ThDP	58.5	0.2	1.6	500 µM ThDP (2)
5 mM $NiCl_2$	43.9	6.9	10.0	No additive (1)
5 mM $NiCl_2$, 500 µM ThDP	53.4	1.7	-6.4	500 µM ThDP (2) (Derivative)

[1] Compared to no additive conditions from the same experiment tray.

5.4.7 Potential Inhibitors

All potential inhibitors tested demonstrated considerable T_m changes for *Smeg*-MenD, which is an interesting outcome due to the similarity between *Smeg*-MenD and *Mtb*-MenD in structure and origin. The results observed from *Smeg*-MenD may be more indicative of what would be expected to be seen from *Mtb*-MenD and so further optimisation and investigation into particular potential inhibitors have more importance in reference to *Smeg*-MenD. While the majority of the experiments demonstrated T_m increases of approximately 2 °C, there are some inhibitors in which only one result was usable for this work and some in which the standard error is too high to be considered a useful result as well. The inhibitors that should be considered for further investigation are p-phenylene diacetic acid, monobutyl phthalate, and 2-hydroxy-1-napthoic acid. Both monobutyl phthalate and 2-hydroxy-1-napthoic acid provided the only full results with no high standard error and consistent stabilisation effects upon *Smeg*-MenD, suggesting interactions between the protein and ligand. P-Phenylene diacetic acid also appears to have this same T_m increase effect but at a higher change, however at 1 mM p-Phenylene diacetic acid concentration with 500 µM ThDP presence the standard error of the experiment is too high to be usable and so further investigation to confirm the interaction between *Smeg*-MenD and this condition could provide leads on the most likely alternative inhibitor for the protein.

Table 47: Melting temperature (T_m) of 5 µM *Smeg*-MenD in different potential inhibitor conditions. The error is the standard error of the mean. [A dash (-) signifies data unavailable due to an unreadable T_m change. T_m and differences are measured in Celsius].

Additive(s)	T_m	Error	Diff.	Rel. To[1]
100 µM 5-hydroxyinole carboxylic acid	54.7	1.9	-4.7	1% DMSO
100 µM 1-hydroxy-2-napthoic acid	57.5	5.2	-1.9	1% DMSO
1 mM 1-hydroxy-2-napthoic acid	60.6	0.2	1.6	1% DMSO
100 µM 1-hydroxy-2-napthoic acid, 500 µM ThDP	61.2	0.2	2.3	500 µM ThDP, 1% DMSO
1 mM 1-hydroxy-2-napthoic acid, 500 µM ThDP	58.3	3.8	-1.1	500 µM ThDP, 1% DMSO (Derivative)
100 µM p-phenylene diacetic acid	62.7	0.2	3.4	1% DMSO (Derivative)
1 mM p-phenylene diacetic acid	62.3	0.3	3.4	1% DMSO
100 µM p-phenylene diacetic acid, 500 µM ThDP	62.2	0.1	3.3	500 µM ThDP, 1% DMSO
1 mM p-phenylene diacetic acid, 500 µM ThDP	57.8	3.8	-1.6	500 µM ThDP, 1% DMSO
100 µM monobutyl phthalate	61.3	0.3	2.0	1% DMSO
1 mM monobutyl phthalate	62.1	0.2	3.2	1% DMSO
100 µM monobutyl phthalate, 500 µM ThDP	61.6	0.1	2.6	500 µM ThDP, 1% DMSO
1 mM monobutyl phthalate, 500 µM ThDP	61.6	0.1	2.3	500 µM ThDP, 1% DMSO
100 µM 2-napthtoic acid	61.0	0.3	1.6	1% DMSO (Derivative)
1 mM 2-napthtoic acid	61.7	0.1	2.8	1% DMSO (Derivative)
100 µM 2-napthtoic acid, 500 µM ThDP	61.3	0.1	2.4	500 µM ThDP, 1% DMSO
100 µM 2-hydroxy-1-napthoic acid	61.4	0.1	2.1	1% DMSO
1 mM 2-hydroxy-1-napthoic acid	60.8	0.1	1.4	1% DMSO
100 µM 2-hydroxy-1-napthoic acid, 500 µM ThDP	62.1	0.1	3.1	500 µM ThDP, 1% DMSO
1 mM 2-hydroxy-1-napthoic acid, 500 µM ThDP	61.4	0.1	2.4	500 µM ThDP, 1% DMSO (Derivative)
1 mM 6-hydroxy-2-napthoic acid	56.8	4.6	-2.6	1% DMSO (Derivative)
100 µM 6-hydroxy-2-napthoic acid, 500 µM ThDP	62.1	0.8	2.8	500 µM ThDP, 1% DMSO (Derivative)
1 mM 6-hydroxy-2-napthoic acid, 500 µM ThDP	61.6	0.1	2.7	500 µM ThDP, 1% DMSO

[1] Compared to no additive conditions from the same experiment tray.

5.5 Comparisons Between Proteins

5.5.1 ThDP

There is no apparent trend observed to be retained between the three proteins interacting with ThDP at various concentrations. It is difficult to find direct comparisons between the proteins as they exhibit a large variety of effects at each concentration. However, *Ec*-MenD shows the largest T_m changes of the three proteins overall for many of the concentrations in both the situations with only ThDP present. For example, at 1000 µM ThDP concentration a T_m increase approximately three times higher than either *Sau*-MenD or *Smeg*-MenD is observed (9.2 vs 2.7 and 2.3 °C respectively, Table 48).

Table 48: Melting temperature (T_m) comparisons between 5 µM *Sau*-MenD, *Ec*-MenD and *Smeg*-MenD from various ThDP conditions. [A dash (-) signifies data unavailable due to an unreadable T_m change. T_m and differences are measured in Celsius].

Additive(s)	T_m Diff. (*Sau*-MenD)	T_m Diff. (*Ec*-MenD)	T_m Diff. (*Smeg*-MenD)
50 µM ThDP	0.4	-	0.1
100 µM ThDP	0.5	9.2	0.1
250 µM ThDP	0.2	8.55	-
500 µM ThDP (1)	1.4	8.6	-0.7
500 µM ThDP (2)	2.8	0.54	0.2
500 µM ThDP (3)	2.9	0.3	-3.1
500 µM ThDP (4)	2.5	0.6	0.5
1000 µM ThDP	2.7	9.2	2.3
500 µM ThDP, 1 mM TCEP	1.7	-	0.1
500 µM ThDP, 0.1% DMSO	0.2	1.9	-2.0
500 µM ThDP, 1% DMSO (2)	0.1	0.5	3.3
500 µM ThDP, 0.1% DMSO, 2.5 mM TCEP	0.0	-0.4	-0.9

5.5.2 2-Oxoglutarate

Addition of 2-oxoglutarate causes significant differences to be seen between the effects on each protein (Table 49). *Sau*-MenD was observed to have a destabilisation trend from 2-oxoglutarate binding with 500 µM ThDP presence, with all concentrations of 2-oxoglutarate consistently demonstrating this. Conversely, *Ec*-MenD reacted similarly to as it did with increasing ThDP concentration. As 2-oxoglutarate concentration increases as does the T_m for *Ec*-MenD. These T_m increases were considered large increases especially when compared to *Smeg*-MenD which did not appear to display any changes to T_m from 2-oxoglutarate addition. It is more difficult to compare the proteins with 2.5 mM TCEP presence in addition to the previous compounds due to the incomplete results between proteins (Table 49). One interesting note from the 2-oxoglutarate experiments was the finding that without ThDP addition, each protein demonstrated a stabilisation effect at a different magnitude, which was almost comparative to the effects seen with ThDP presence for all three proteins, albeit the inverse effect for *Sau*-MenD (2.5 vs 8.3 vs 0.6 °C for *Sau*-MenD, *Ec*-MenD and *Smeg*-MenD respectively, Table 49).

Table 49: Melting temperature (T_m) comparisons between 5 µM *Sau*-MenD, *Ec*-MenD and *Smeg*-MenD from various 2-oxoglutarate conditions. [A dash (-) signifies data unavailable due to an unreadable T_m change. T_m and differences are measured in Celsius].

Additive(s)	T_m Diff. (*Sau*-MenD)	T_m Diff. (*Ec*-MenD)	T_m Diff. (*Smeg*-MenD)
1000 µM 2-oxoglutarate	2.5	8.3	0.6
500 µM ThDP, 50 µM 2-oxoglutarate	-1.4	0.6	0.3
500 µM ThDP, 100 µM 2-oxoglutarate	-4.8	0.7	0.0
500 µM ThDP, 250 µM 2-oxoglutarate	-2.9	9.4	0.9
500 µM ThDP, 500 µM 2-oxoglutarate	-3.6	1.6	0.4
500 µM ThDP, 1000 µM 2-oxoglutarate	-1.9	8.4	0.2
500 µM ThDP, 500 µM 2-oxoglutarate, 2.5 mM TCEP	-	6.9	0.1
500 µM ThDP, 500 µM 2-oxoglutarate, 0.1% DMSO, 2.5 mM TCEP	-0.1	-	-

5.5.3 CHD

CHD was not a ligand of major focus in this work, but the results provided from the experiments warranted further discussion. In a trend like the results observed from the 2-oxoglutarate experiments the CHD binding experiments demonstrated destabilisation effects in *Sau*-MenD, and stabilisation effects in *Ec*-MenD and *Smeg*-MenD, with a greater stabilisation effect (T_m increase) observed in *Ec*-MenD. This result could be due to the presence of ThDP and 2-oxoglutarate in addition to CHD however as the T_m differences were compared to ThDP binding experiments with similar concentration this can at least eliminate the possibility that all that is observed is ThDP binding effects.

Table 50: Melting temperature (T_m) comparisons between 5 µM *Sau*-MenD, *Ec*-MenD and *Smeg*-MenD from various CHD conditions. [A dash (-) signifies data unavailable due to an unreadable T_m change. T_m and differences are measured in Celsius].

Additive(s)	T_m Diff. (*Sau*-MenD)	T_m Diff. (*Ec*-MenD)	T_m Diff. (*Smeg*-MenD)
500 µM ThDP, 500 µM CHD	-1.4	0.9	0.3
500 µM THDP, 500 µM CHD, 500 µM 2-oxoglutarate	-3.8	0.3	-0.1

5.5.4 DHNA

Due to the lack of data from the *Ec*-MenD experiments it is difficult to fully compare the three proteins and their interactions with DHNA. From what is available without the presence of TCEP or any other ligands, all proteins demonstrate a destabilisation effect from DHNA addition to varying magnitudes of strength.

The presence of TCEP in *Sau*-MenD and *Smeg*-MenD appears to have a significant stabilisation effect, with some exceptions. For *Sau*-MenD, the exception occurs at 50 µM DHNA concentration, suggesting that TCEP has more difficulty at keeping DHNA reduced at higher concentrations, whereas for *Smeg*-MenD this exception occurs at 30 µM DHNA, but is followed by T_m increase at 50 and 100 µM. Disregarding these exceptions, TCEP appears to be a suitable reducing agent for the use with DHNA as it clearly does interact with the allosteric binder to have some effect.

ThDP presence appears to amplify the destabilisation effect observed from DHNA without TCEP presence for *Sau*-MenD, while in *Smeg*-MenD the effect of ThDP is unpredictable, as seen from the varied range of stabilisation and destabilisation effects (Table 51). TCEP presence counteracts this amplified destabilisation effect for *Sau*-MenD, resulting in a lower T_m increase than seen without ThDP presence but still a stabilisation effect. *Smeg*-MenD instead is observed to have only stabilisation effects, with a similar magnitude of T_m increase at 100 µM DHNA as seen without TCEP presence.

Presence of 2-oxoglutarate retains the destabilisation effect previously observed upon *Sau*-MenD, with a newfound T_m increase similarly observed for *Smeg*-MenD. This is still observed with the addition for 2.5 mM TCEP for *Smeg*-MenD, however inconclusive results for *Sau*-MenD do not allow for a conclusion to be made. Overall, DHNA experiments involving the MenD proteins require a large amount of further experimentation, with more consideration involving the buffer contents and the reaction conditions to determine if the experimental technique can provide usable results for future work.

Table 51: Melting temperature (T_m) comparisons between 5 µM *Sau*-MenD, *Ec*-MenD and *Smeg*-MenD from various DHNA conditions. [A dash (-) signifies data unavailable due to an unreadable T_m change. T_m and differences are measured in Celsius].

Additive(s)	T_m Diff. (*Sau*-MenD)	T_m Diff. (*Ec*-MenD)	T_m Diff. (*Smeg*-MenD)
5 µM DHNA	-	-	0.5
10 µM DHNA	-2.8	-0.19	-29.3
20 µM DHNA	-3.2	-1.7	-32.7
30 µM DHNA	-1.9	-2.4	-25.8
50 µM DHNA	-4.9	-3.1	-29.4
100 µM DHNA	-4.0	-1.5	-24.4
5 µM DHNA, 2.5 mM TCEP	1.6	-	2.2
10 µM DHNA, 2.5 mM TCEP	1.0	-	1.6
20 µM DHNA, 2.5 mM TCEP	-0.2	-	2.7
30 µM DHNA, 2.5 mM TCEP	0.8	-	-14.9
50 µM DHNA, 2.5 mM TCEP	-2.8	-	2.3
100 µM DHNA, 2.5 mM TCEP	-	-19.7	2.8
5 µM DHNA, 500 µM ThDP	-3.7	0.2	-6.0
10 µM DHNA, 500 µM ThDP	-5.0	0.36	0.8
50 µM DHNA, 500 µM ThDP	-	0.09	-10.0
100 µM DHNA, 500 µM ThDP	-6.0	0.5	23.3
5 µM DHNA, 500 µM ThDP, 2.5 mM TCEP	-0.1	-	0.2
10 µM DHNA, 500 µM ThDP, 2.5 mM TCEP	0.1	-	1.6
50 µM DHNA, 500 µM ThDP, 2.5 mM TCEP	0.1	-	1.5
100 µM DHNA, 500 µM ThDP, 2.5 mM TCEP	1.8	-	29.6
5 µM DHNA, 500 µM ThDP, 500 µM 2-oxoglutarate	-4.2	-	-3.2
10 µM DHNA, 500 µM ThDP, 500 µM 2-oxoglutarate	-2.9	5.8	-0.2
50 µM DHNA, 500 µM ThDP, 500 µM 2-oxoglutarate	-4.5	0.5	-15.5
5 µM DHNA, 500 µM ThDP, 500 µM 2-oxoglutarate, 2.5 mM TCEP	1.1	-	-7.1
10 µM DHNA, 500 µM ThDP, 500 µM 2-oxoglutarate, 2.5 mM TCEP	-	-	-3.9
50 µM DHNA, 500 µM ThDP, 500 µM 2-oxoglutarate, 2.5 mM TCEP	-	-	-0.7

5.5.5 Metals

$NiCl_2$ experiments failed to provide accurate T_m readings for *Ec*-MenD and *Smeg*-MenD through the use of DSF. This likely reflects the large detrimental effect of certain metal ions, including Ni^{2+} on MenD stability and activity (e.g. Ni^{2+} abolishes *Mtb*-MenD activity).

Sau-MenD displayed almost no T_m shift with the alternative metals $MnCl_2$ and $CaCl_2$ during experimental work. *Ec*-MenD and *Smeg*-MenD however, displayed major changes under the influence of both of these metals, with $CaCl_2$ having a significantly greater effect upon the T_m of *Ec*-MenD than *Smeg*-MenD. The presence of ThDP in both cases reduced this effect upon the T_m substantially, suggesting interactions between the metal ion and ThDP before protein interaction. As magnesium ions were present in the protein buffer at 1 mM this was not a fully controlled metal addition experiment and further experiments could remove all metals prior to doing DSF with different metals.

Table 52: Melting temperature (T_m) comparisons between 5 µM *Sau*-MenD, *Ec*-MenD and *Smeg*-MenD from various Metal conditions. [A dash (-) signifies data unavailable due to an unreadable T_m change. T_m and differences are measured in Celsius].

Additive(s)	T_m Diff. (*Sau*-MenD)	T_m Diff. (*Ec*-MenD)	T_m Diff. (*Smeg*-MenD)
5 mM $MnCl_2$	-0.3	3.0	3.6
5 mM $MnCl_2$, 500 µM ThDP	0.4	-0.9	-0.1
5 mM $CaCl_2$	0.3	8.31	3.6
5 mM $CaCl_2$, 500 µM ThDP	-0.1	0.89	1.6
5 mM $NiCl_2$	-6.9	-	-
5 mM $NiCl_2$, 500 µM ThDP	-5.9	-12.5	-

5.5.6 Potential Inhibitors

The main inhibitors of interest from this work as identified in sections 4.2.7, 4.3.7 and 4.4.7 were found to be 2-napthoic acid, 2-hydroxy-1-napthoic acid, 6-hyroxy-2-napthoic acid, 1-hydroxy-2-napthoic acid, p-phenylene diacetic acid, and monobutyl phthalate. While none of these compounds was found to have commonalities between all three proteins, inhibitors such as *p*-phenylene diacetic acid and 2-hydroxy-1-napthoic acid were found to have effects in 2 or more of the proteins and as such are of greater interest for further testing.

2-Hydroxy-1-napthoic acid is potentially the most interesting of the inhibitors, as it demonstrates significantly different results dependent upon both the protein it is interacting with and the presence of ThDP. *Sau*-MenD demonstrates a destabilisation effect in all cases, with the highest change found with 1 mM concentration and 500 µM ThDP presence. *Smeg*-MenD however, has high stabilisation effects at all concentrations and regardless of ThDP presence, highlighting a major difference in interactions between MenD enzymes. Perhaps the most interesting is *Ec*-MenD, as it demonstrates stabilisation effects in the absence of ThDP and destabilisation effects while in the presence of ThDP. It should also be noted that these destabilisation effects are greater than the stabilisation effects produced, suggesting a potential conformational change in the protein with ThDP presence.

Table 53: Melting temperature (T_m) comparisons between 5 µM *Sau*-MenD, *Ec*-MenD and *Smeg*-MenD from various Potential Inhibitor conditions. [A dash (-) signifies data unavailable due to an unreadable T_m change. T_m and differences are measured in Celsius].

Additive(s)	T_m Diff. (*Sau*-MenD)	T_m Diff. (*Ec*-MenD)	T_m Diff. (*Smeg*-MenD)
100 µM 5-hydroxyinole carboxylic acid	-2.4	0.1	-
1 mM 5-hydroxyinole carboxylic acid	-	-0.4	-
100 µM 5-hydroxyinole carboxylic acid, 500 µM ThDP	-	0.8	-
1 mM 5-hydroxyinole carboxylic acid, 500 µM ThDP	-	0.5	-
100 µM 1-hydroxy-2-napthoic acid	-0.8	0.5	-
1 mM 1-hydroxy-2-napthoic acid	-1.0	-	-1.9
100 µM 1-hydroxy-2-napthoic acid, 500 µM ThDP	-1.0	0.9	1.6
1 mM 1-hydroxy-2-napthoic acid, 500 µM ThDP	-0.8	1.1	2.3
100 µM p-phenylene diacetic acid	-0.9	0.4	-
1 mM p-phenylene diacetic acid	-0.6	-32.7	3.4
100 µM p-phenylene diacetic acid, 500 µM ThDP	-0.8	0.6	3.4
1 mM p-phenylene diacetic acid, 500 µM ThDP	0.1	0.5	3.3
100 µM monobutyl phthalate	-1.1	0.7	-
1 mM monobutyl phthalate	-0.6	0.7	2.0
100 µM monobutyl phthalate, 500 µM ThDP	-0.5	0.6	3.2
1 mM monobutyl phthalate, 500 µM ThDP	-0.3	0.5	2.6
100 µM 2-napthtoic acid	-1.5	0.7	2.3
1 mM 2-napthtoic acid	1.2	0.5	1.6
100 µM 2-napthtoic acid, 500 µM ThDP	-1.2	0.6	2.8
1 mM 2-napthtoic acid, 500 µM ThDP	-	0.3	-
100 µM 2-hydroxy-1-napthoic acid	-0.3	0.7	2.1
1 mM 2-hydroxy-1-napthoic acid	-0.6	0.5	1.4
100 µM 2-hydroxy-1-napthoic acid, 500 µM ThDP	-0.3	-1.3	3.1
1 mM 2-hydroxy-1-napthoic acid, 500 µM ThDP	-1.6	-1.4	2.4
100 µM 6-hydroxy-2-napthoic acid	-	0.4	-
1 mM 6-hydroxy-2-napthoic acid	-0.8	0.4	-2.6
100 µM 6-hydroxy-2-napthoic acid, 500 µM ThDP	-0.3	0.6	2.8
1 mM 6-hydroxy-2-napthoic acid, 500 µM ThDP	-1.3	0.5	2.7

Conclusion

Objectives of this Work

This work's purpose was to further the characterisation and understanding of the interactions of several MenD enzymes from different species. These enzymes (*Smeg*-MenD, *Ec*-MenD and *Sau*-MenD) were selected to discover more information about the pervasiveness of the allosteric site identified in the *Mtb*-MenD enzyme, while also providing useful results pertaining to the inhibition of this essential enzyme in the various species. There were three specific objectives for this work; (1) expressing and purifying *Ec*-MenD and a new TEV cleavable construct of *Smeg*-MenD in quantities large enough for further work, (2) using these two enzymes in addition to *Sau*-MenD in IFQ experiments to analyse known ligand interactions across enzymes, and (3) the use of these three enzymes in DSF experiments to analyse interactions with both known ligands and a set of known potential inhibitor candidates.

Discoveries of this Work

The purification of *Ec*-MenD in a large enough quantity and to a high enough purity was a resounding success in this work, which was completed without any apparent inconveniences throughout. The purification of this new construct of *Smeg*-MenD was also a success, which also provided more information in the techniques required to successfully cleave the His-tag from the protein. This purification requires specific dialysis conditions to be successful and demonstrated a high degree of purity in the final result.

The IFQ experiments while not appearing to show any commonality between all three proteins did provide further insight into the interactions of these proteins with their known ligands. Due to the presence of bimodal and monomodal binding that varied between each MenD enzyme, direct comparisons cannot be made. However it can be noted that in most conditions, the binding of these known ligands to the MenD enzymes were of similar magnitude to one another.

DSF provided clearer comparisons between the three MenD enzymes, however this is an area that requires further work due to the number of inconclusive results. Similar to the IFQ experiments, binding trends of additives did not seem to be the same between the three MenD species, however the differences in interactions from these additives provides a greater understanding than the similarities would. One universal trend observed however was in the interactions with DHNA, with all three proteins demonstrating a destabilisation effect at all concentrations tested. This effect varied between the species, with *Smeg*-MenD experiencing the greatest effect. However, this result does suggest some common interactions between all MenD species. In addition, at least three of the potential inhibitors investigated in this work demonstrated their ability to have an effect on the activity of MenD enzymes, providing an opportunity to refine and explore further.

Future Work

In addition to further investigation into at least two major potential inhibitors of interest (*p*-phenylene diacetic acid and 2-hydroxy-1-napthoic), many of the IFQ and DSF experiments provided inconclusive results which require more work to provide tangible results. The first port of call would be to focus upon these experiments which did not work the way we hoped and to do replicates of the ones that showed interesting results. Following this, optimisation of the MenD enzyme conditions is required. The metal ions used in this work ($MgCl_2$) may not have been the ideal metal for all MenD enzymes, and as such adjusting this could change many of the results observed. Finally, expansion of the MenD species investigated would help us to understand this essential enzyme even better.

Appendices

Appendix 1

Protein sequence alignment experiment highlighting conserved residue between *Mtb*-MenD, *Ec*-MenD, *Smeg*-MenD and *Sau*-MenD. The alignment was conducted using Clustal omega and the highlighting using Clustal X highlighting. This colour scheme highlights hydrophobic residues in blue, positively charged in red, negatively charged in magenta, polar residues in green, cysteines in pink, glycines in orange, prolines in yellow and aromatic residues in cyan. The sequences are ordered *Smeg*-MenD, *Mtb*-MenD, *Ec*-MenD, *Sau*-MenD.

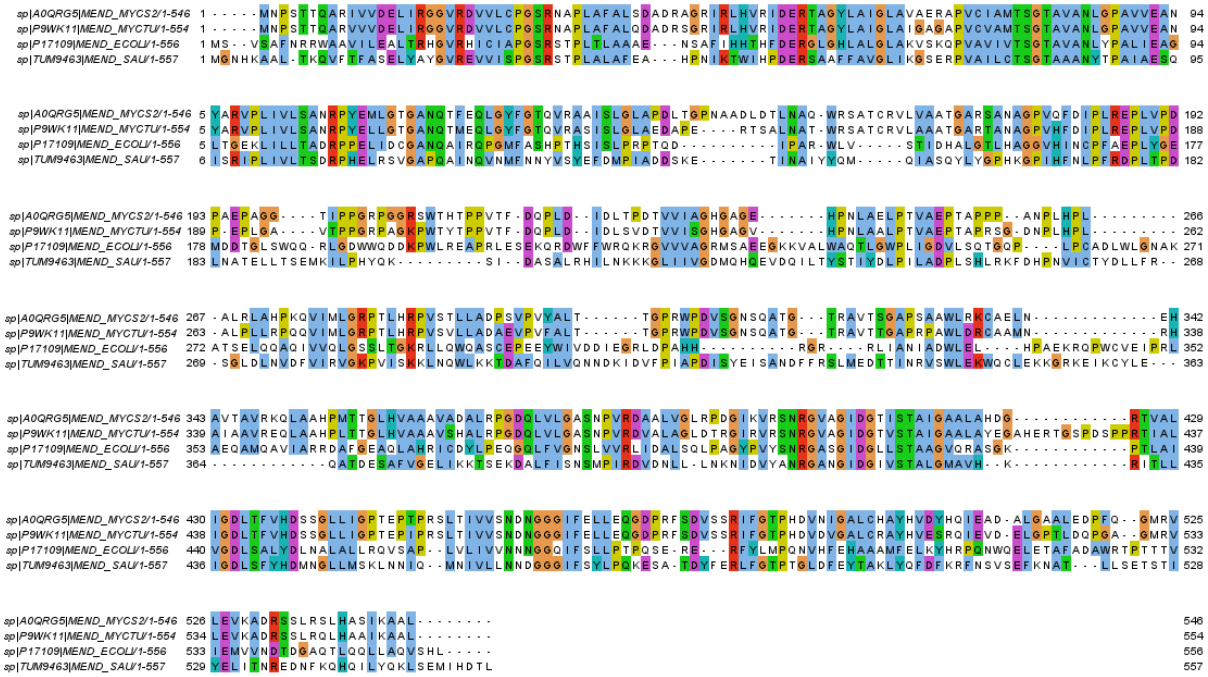

Appendix 2

DSF experiments for *Ec*-MenD involving DHNA with additional additives. These results were too inconclusive to be included in the final results and suggest further experimentation needed upon *Ec*-MenD and its DHNA interactions.

DHNA with 2.5 mM TCEP present:

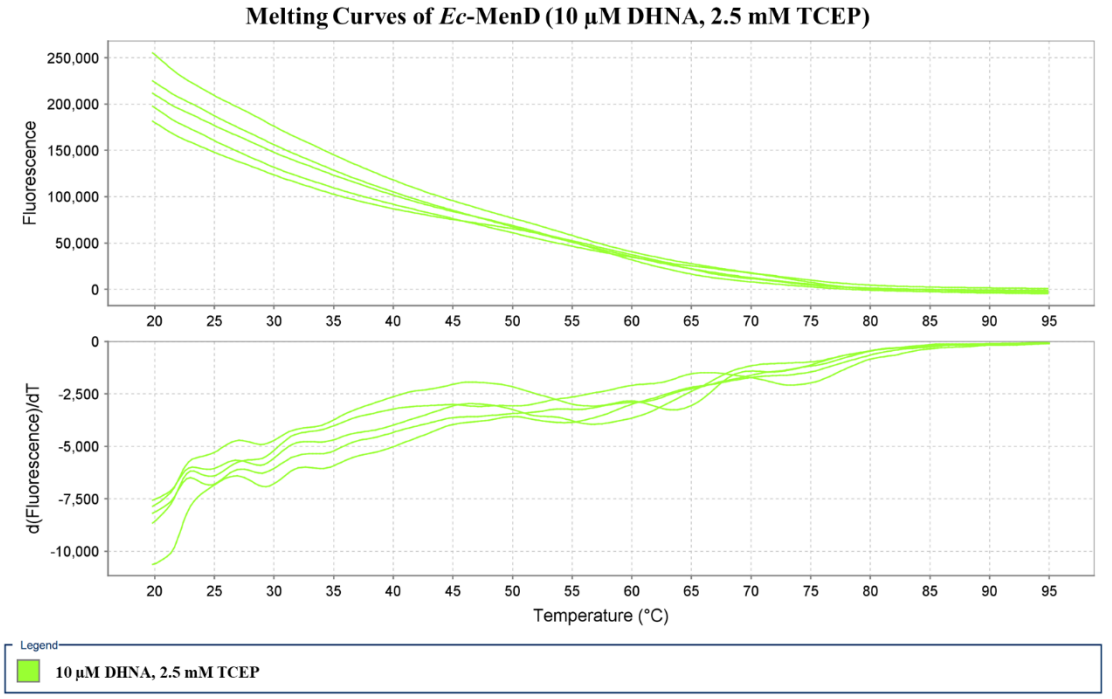

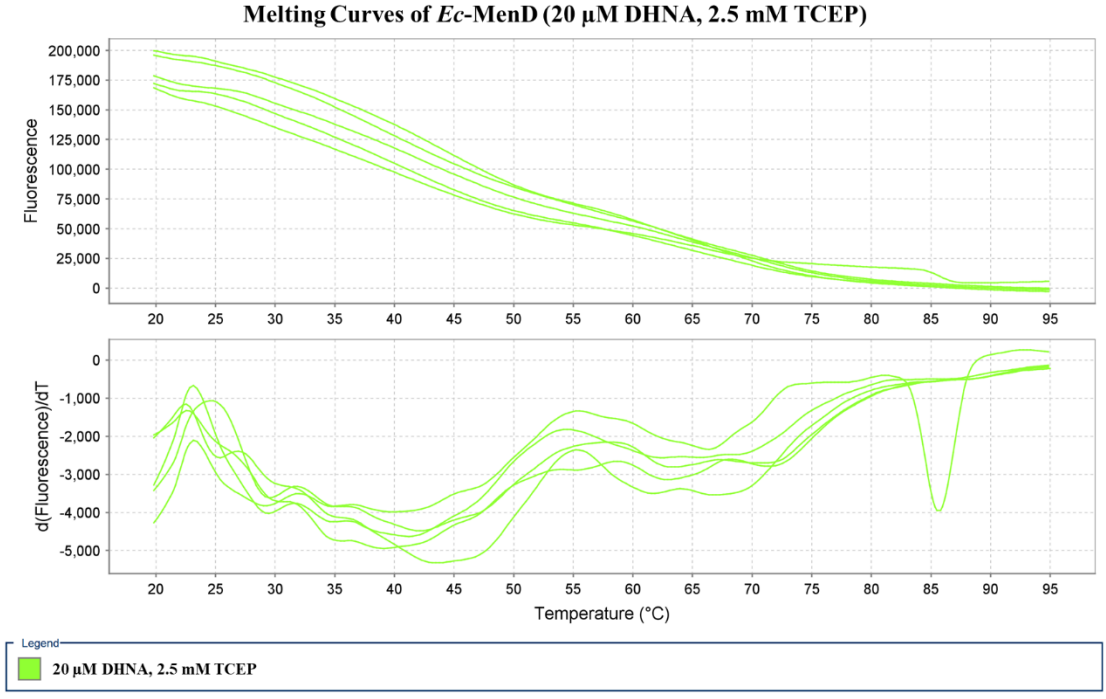

Melting Curves of *Ec*-MenD (30 µM DHNA, 2.5 mM TCEP)

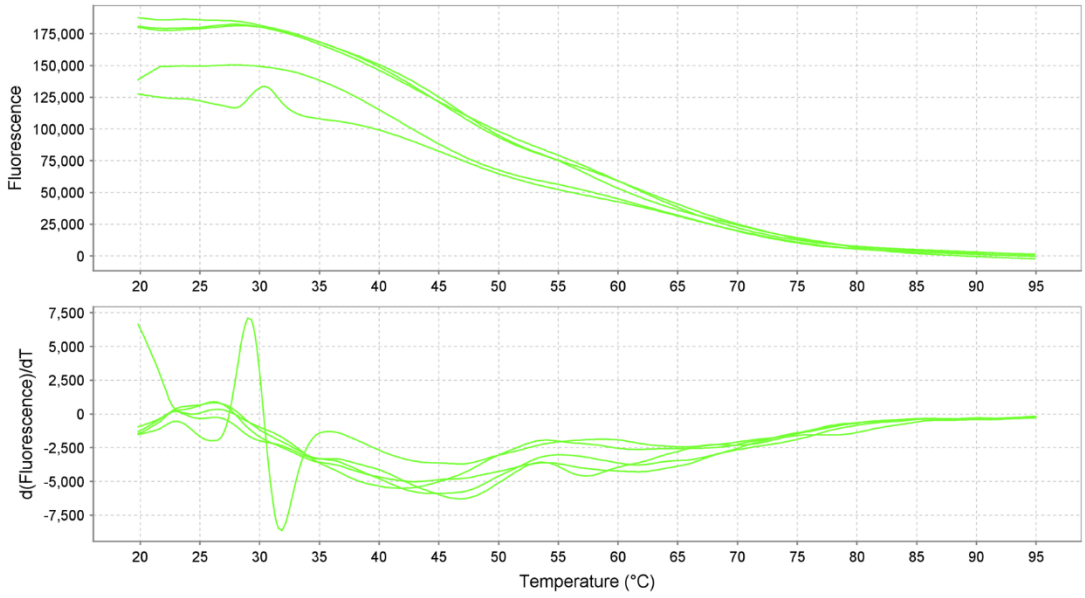

Legend

30 µM DHNA, 2.5 mM TCEP

Melting Curves of *Ec*-MenD (50 µM DHNA, 2.5 mM TCEP)

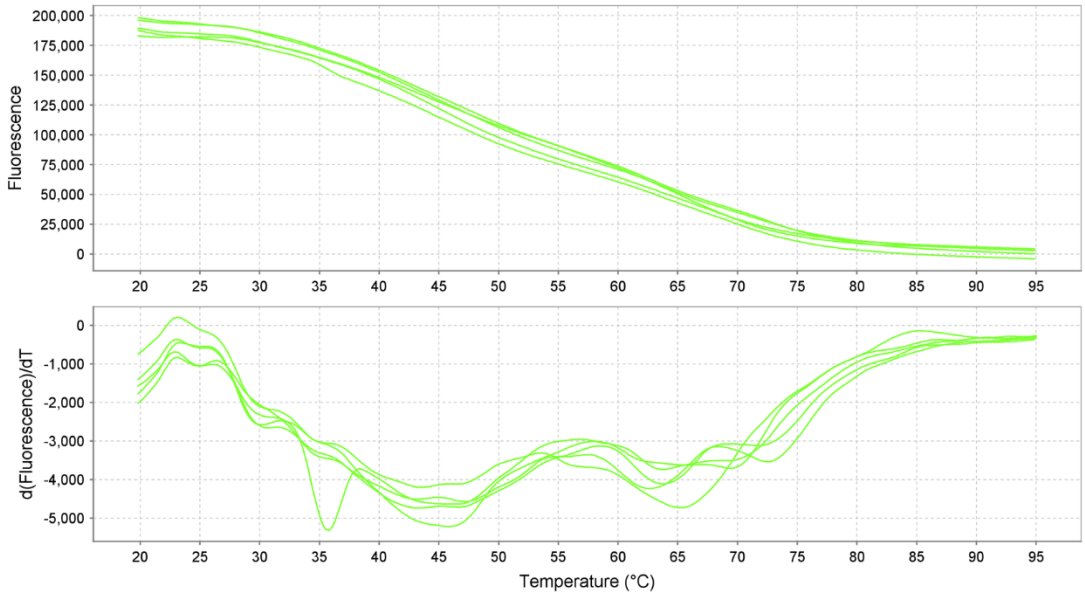

Legend

50 µM DHNA, 2.5 mM TCEP

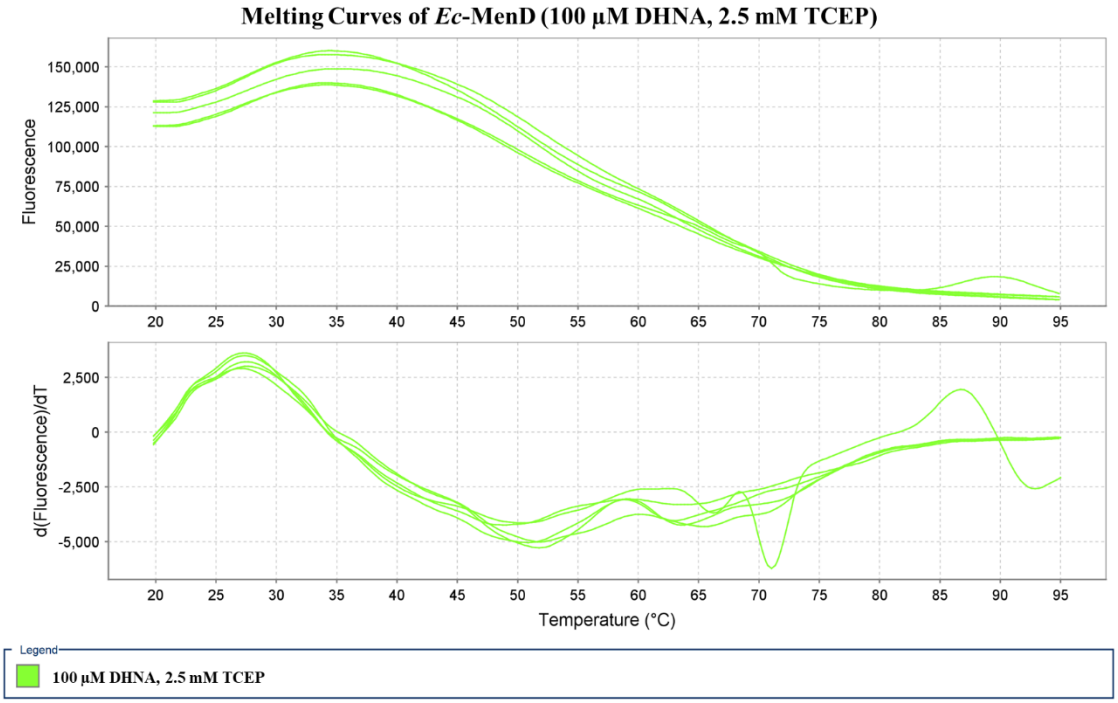
Melting Curves of *Ec*-MenD (100 µM DHNA, 2.5 mM TCEP)
Fluorescence
150,000
125,000
100,000
75,000
50,000
25,000
0
20 25 30 35 40 45 50 55 60 65 70 75 80 85 90 95
d(Fluorescence)/dT
2,500
0
-2,500
-5,000
20 25 30 35 40 45 50 55 60 65 70 75 80 85 90 95
Temperature (°C)
Legend
100 µM DHNA, 2.5 mM TCEP

DHNA with 2.5 mM TCEP and 500 µM ThDP present:

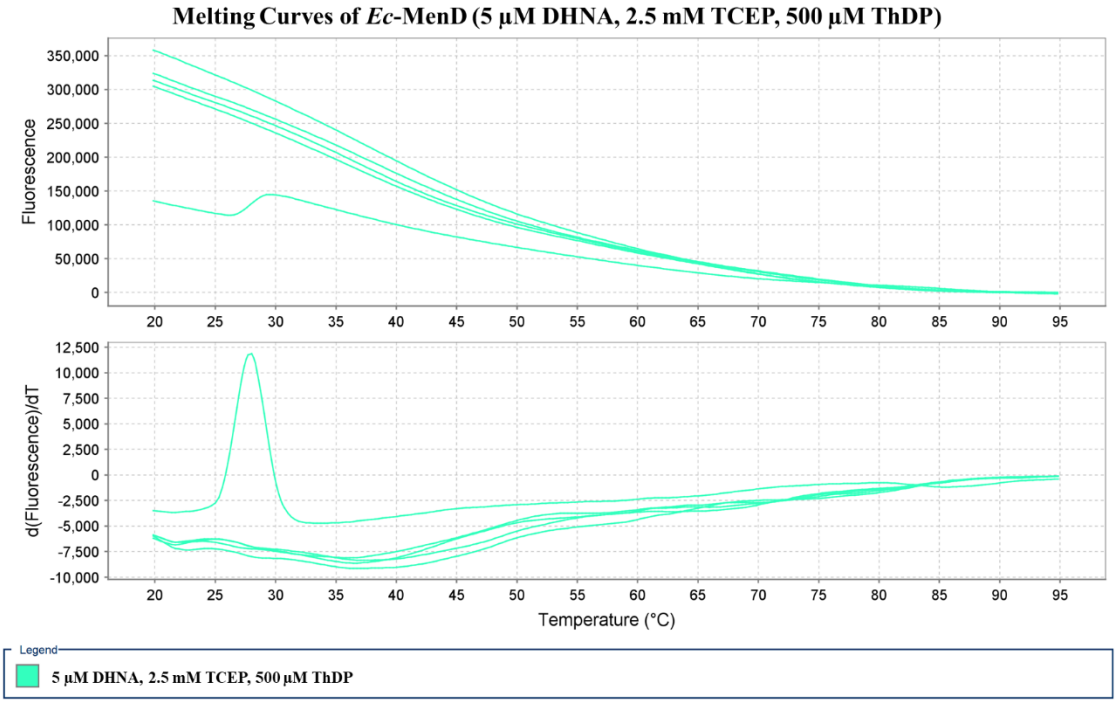

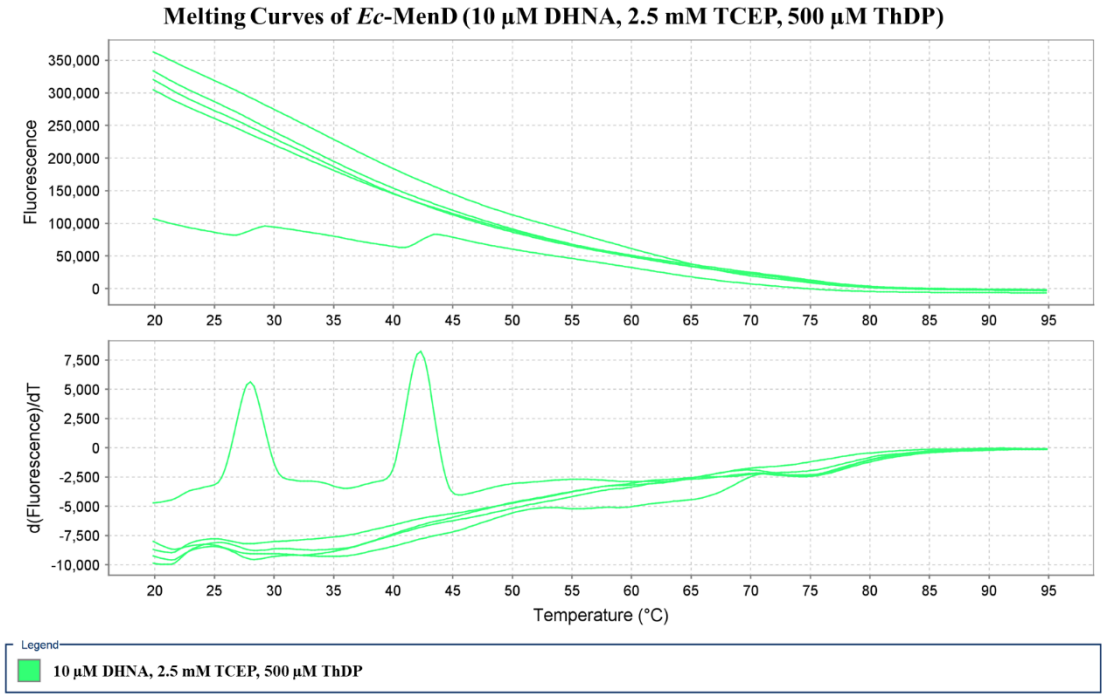

Melting Curves of *Ec*-MenD (50 µM DHNA, 2.5 mM TCEP, 500 µM ThDP)

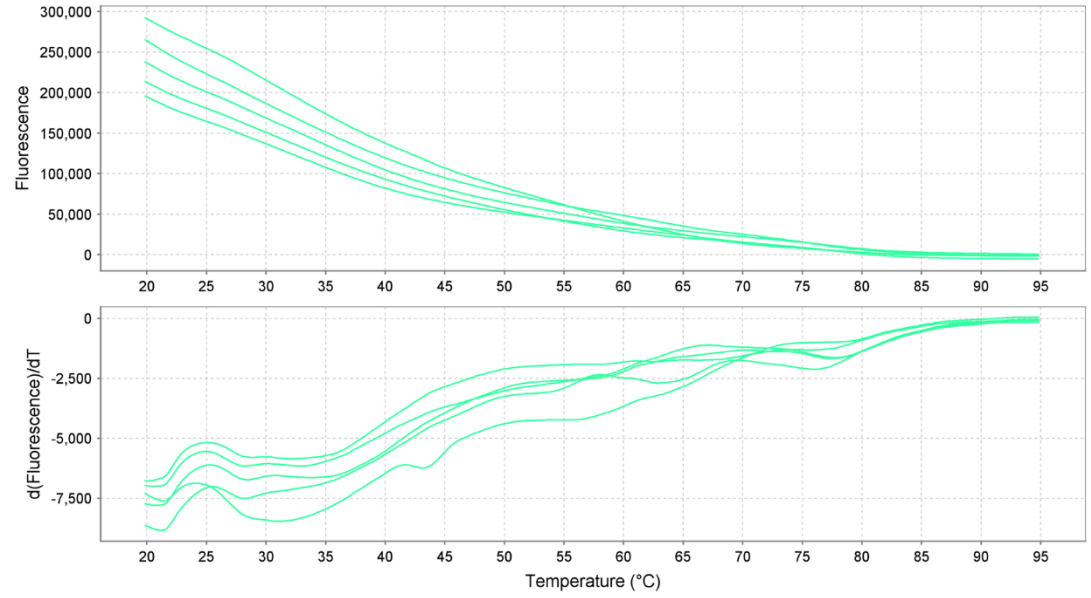

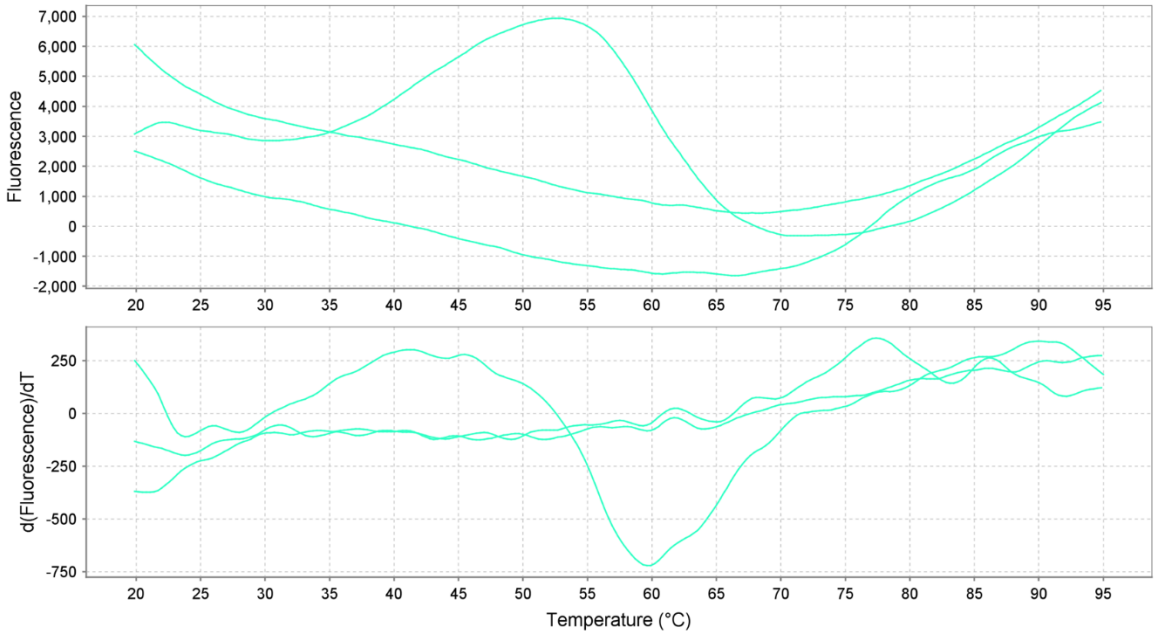

DHNA with 500 µM ThDP and 500 µM 2-Oxoglutarate present:

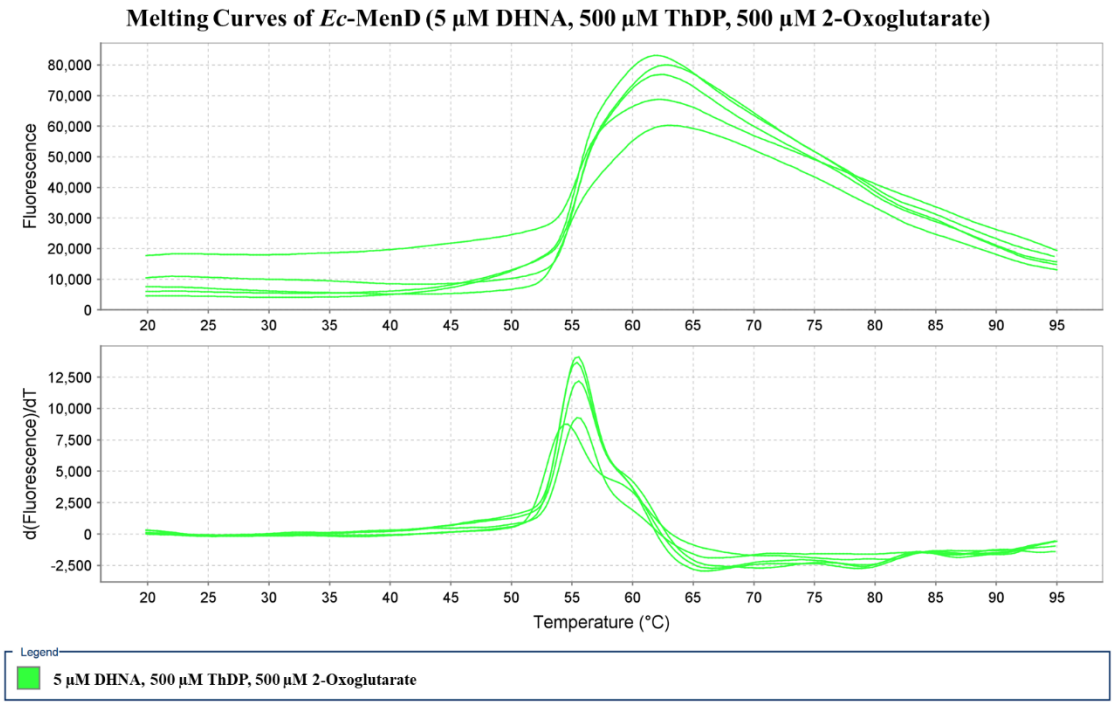

DHNA with 500 µM ThDP, 500 µM 2-Oxoglutarate and 2.5 mM TCEP present:

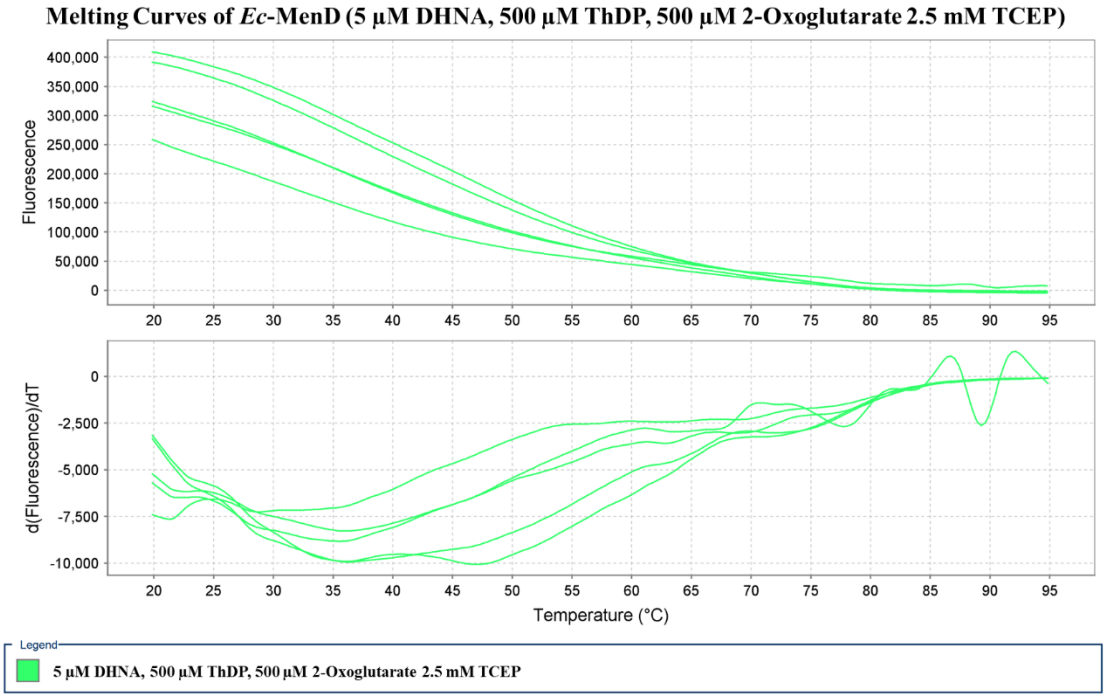

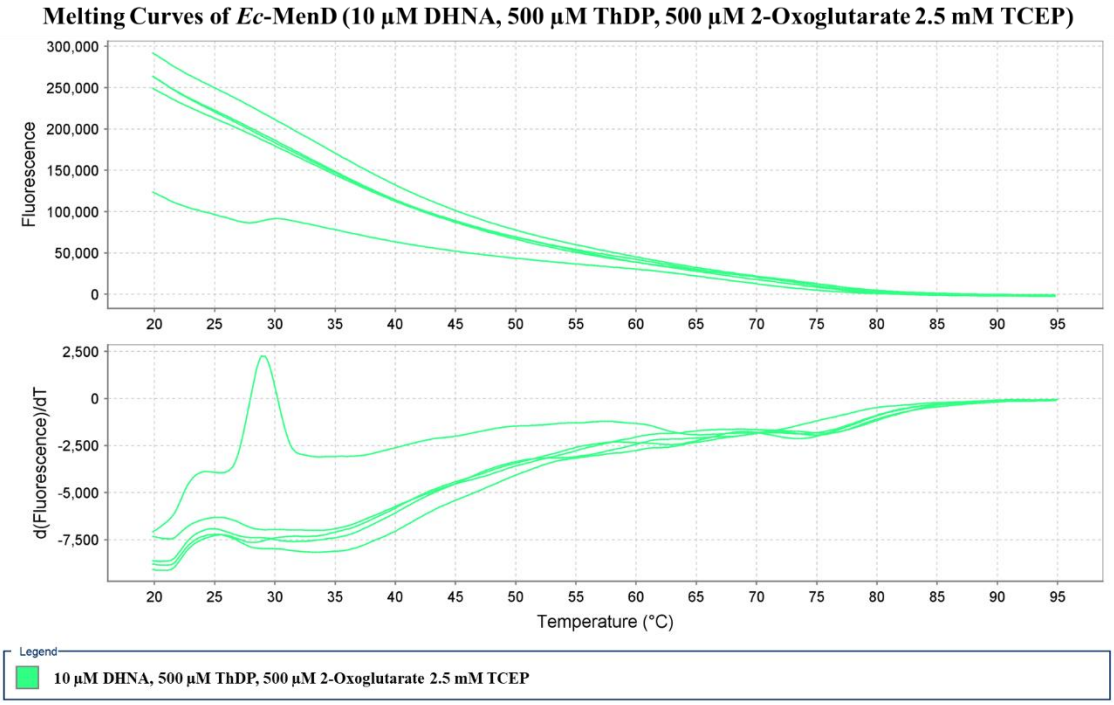

Melting Curves of *Ec*-MenD (50 µM DHNA, 500 µM ThDP, 500 µM 2-Oxoglutarate 2.5 mM TCEP)

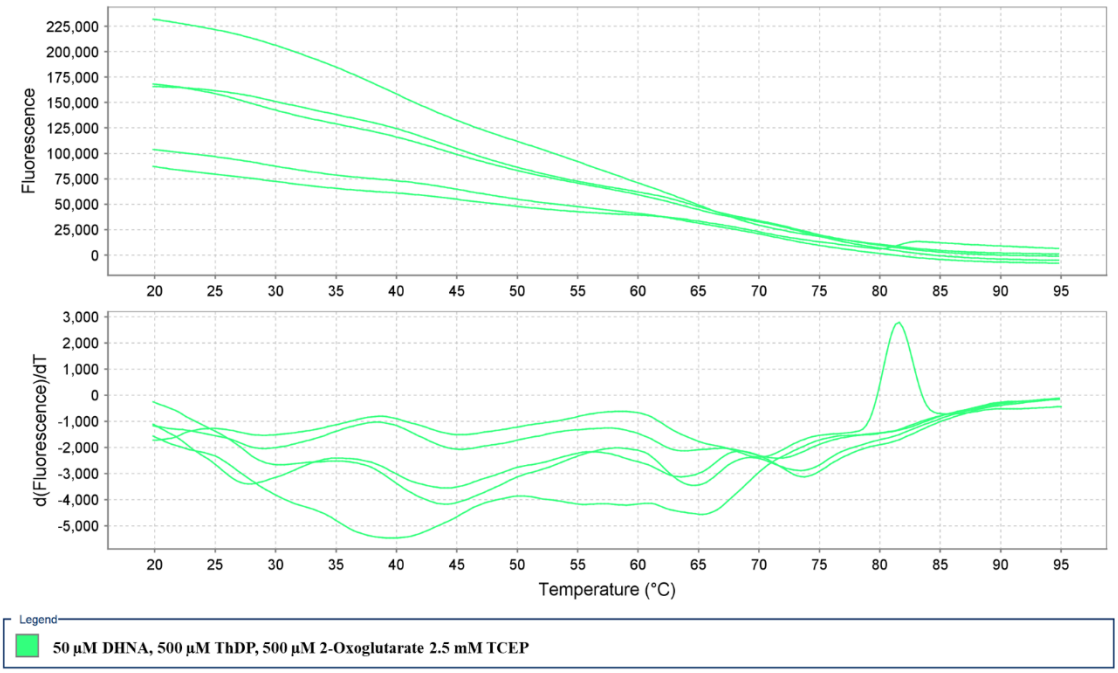

Legend

50 µM DHNA, 500 µM ThDP, 500 µM 2-Oxoglutarate 2.5 mM TCEP

Appendix 3

DSF experiments for *Smeg*-MenD involving DHNA with additional additives. These results were too inconclusive to be included in the final results and suggest further experimentation needed upon *Smeg*-MenD and it's DHNA interactions.

100 µM DHNA with 2.5 mM TCEP and 500 µM ThDP present:

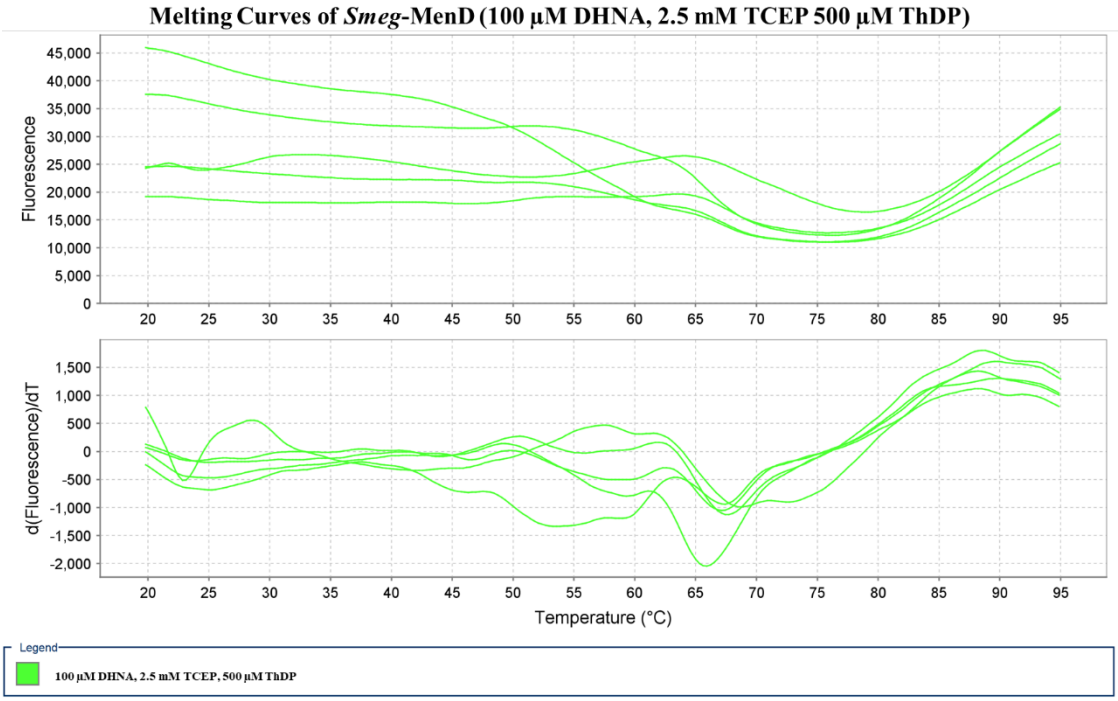

DHNA with 500 µM 2-Oxoglutarate and 500 µM ThDP present:

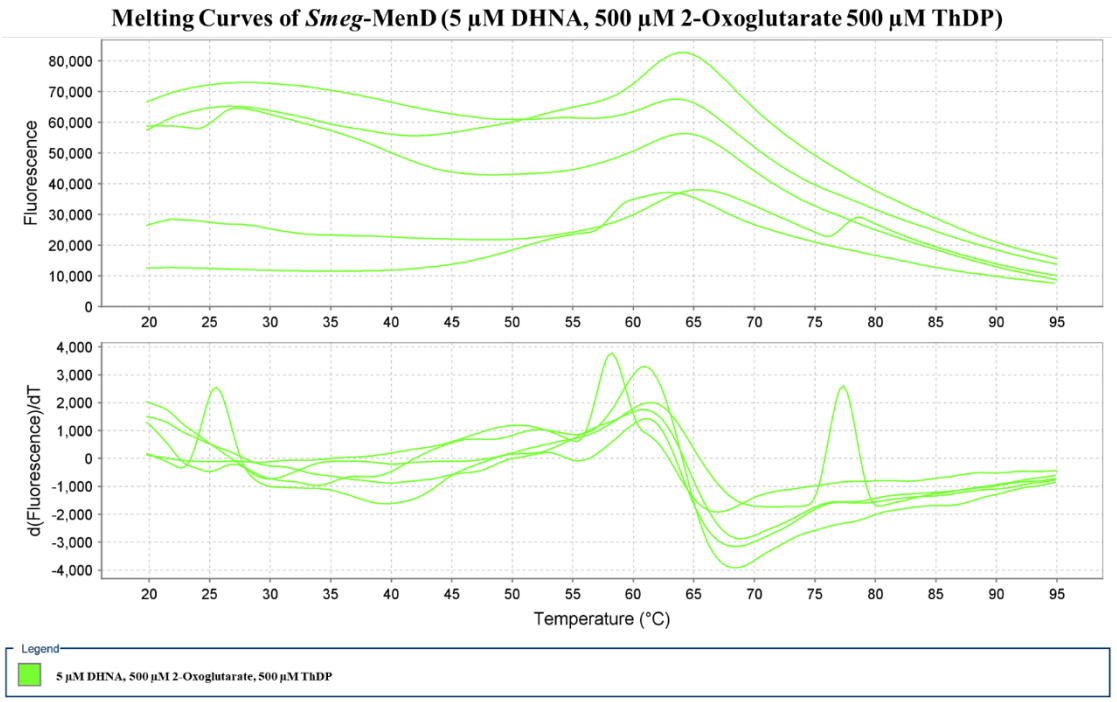

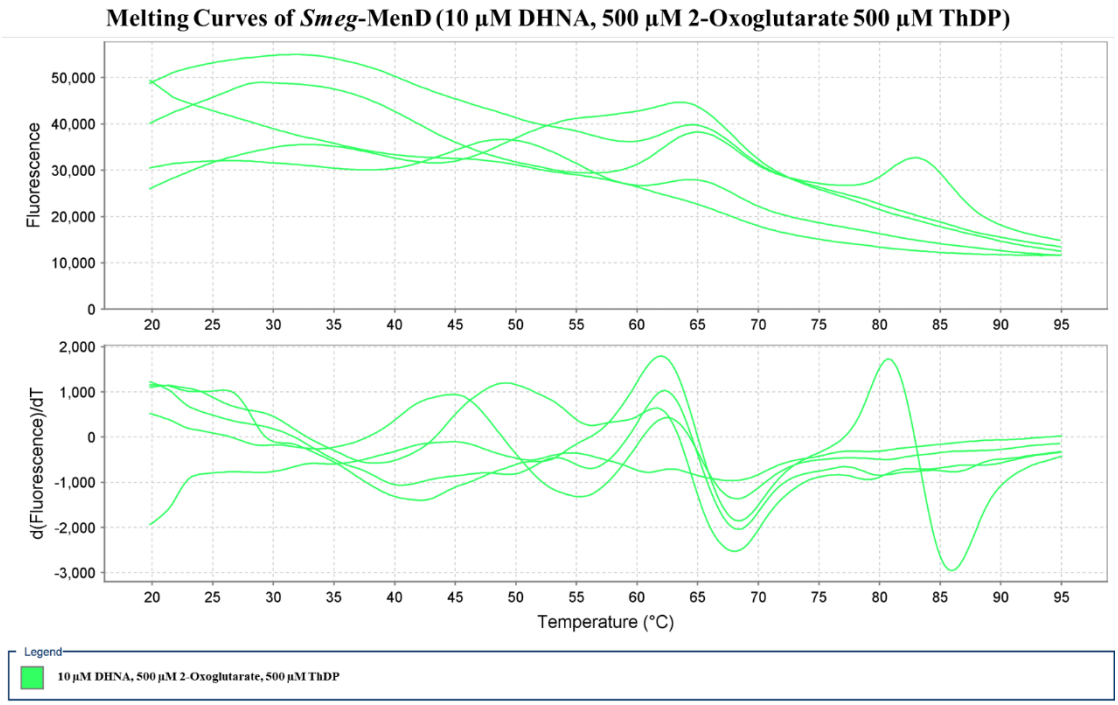

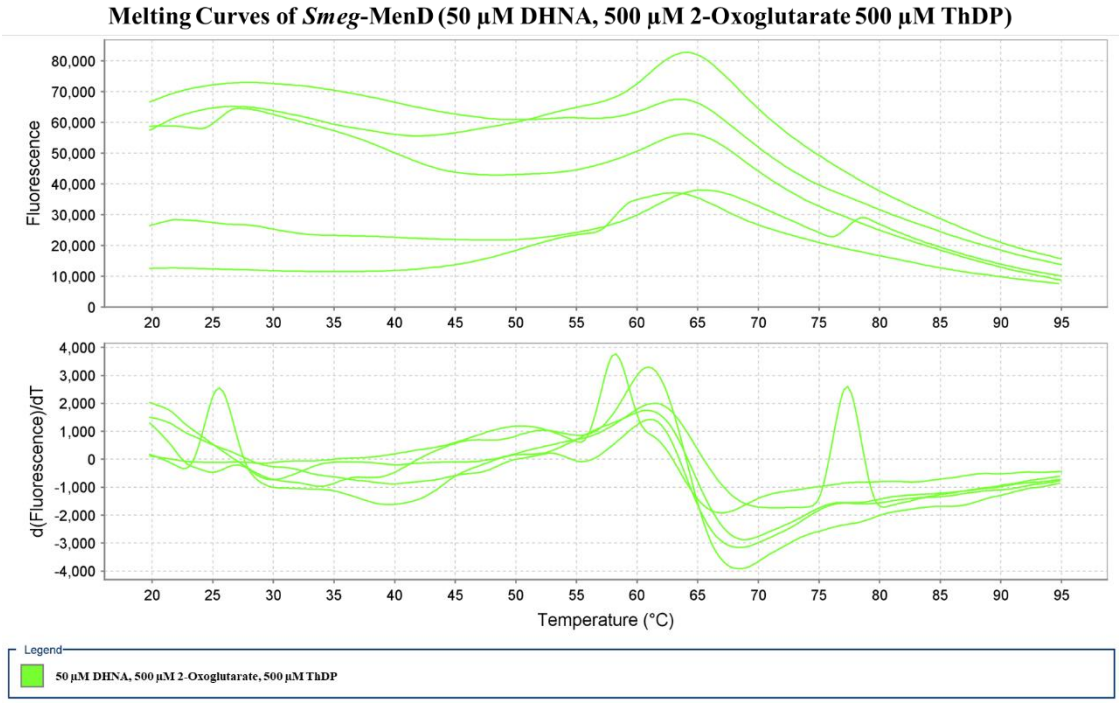

DHNA with 500 µM 2-Oxoglutarate, 500 µM ThDP and 2.5 mM TCEP present:

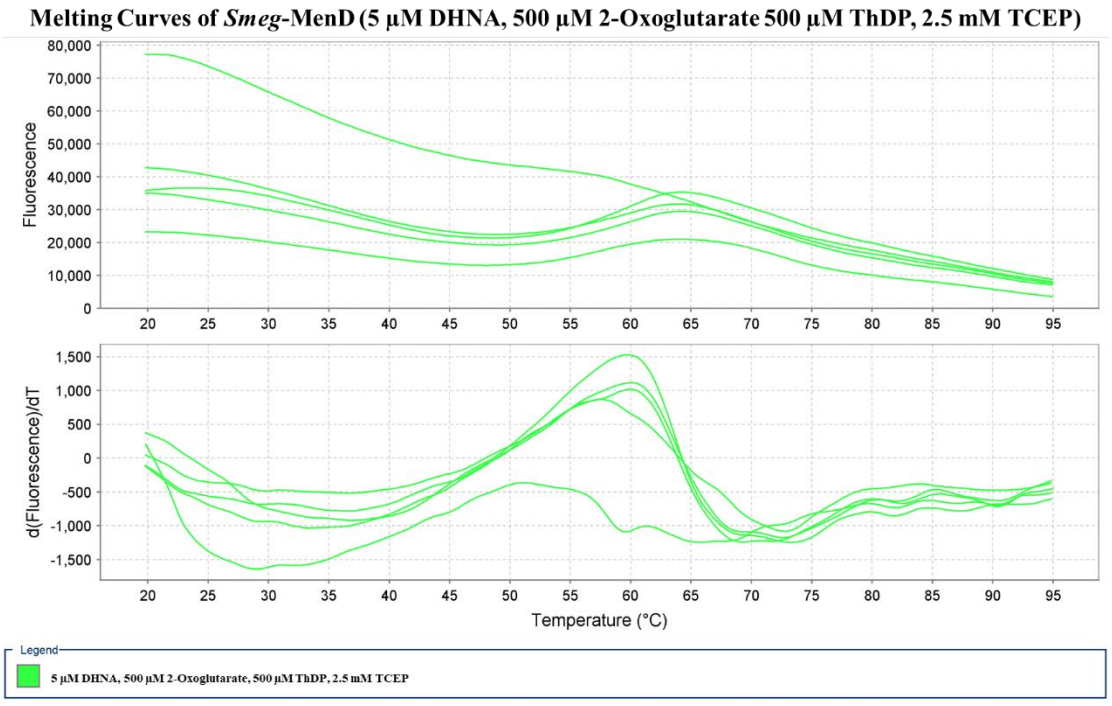

Melting Curves of *Smeg*-MenD (10 µM DHNA, 500 µM 2-Oxoglutarate 500 µM ThDP, 2.5 mM TCEP)

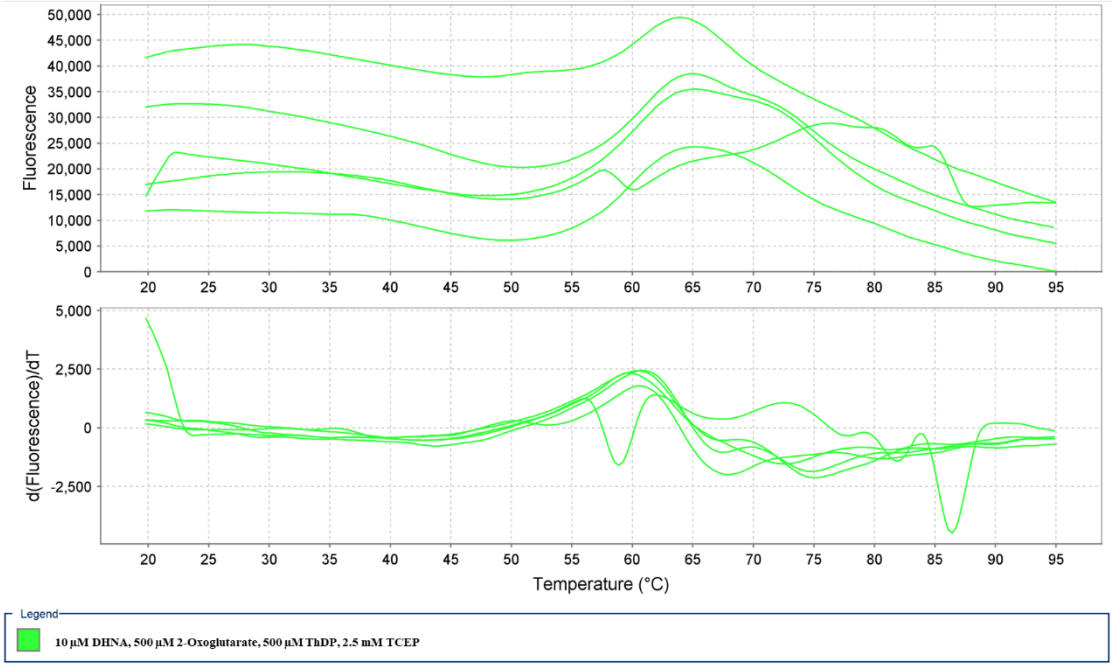

Melting Curves of *Smeg*-MenD (50 µM DHNA, 500 µM 2-Oxoglutarate 500 µM ThDP, 2.5 mM TCEP)

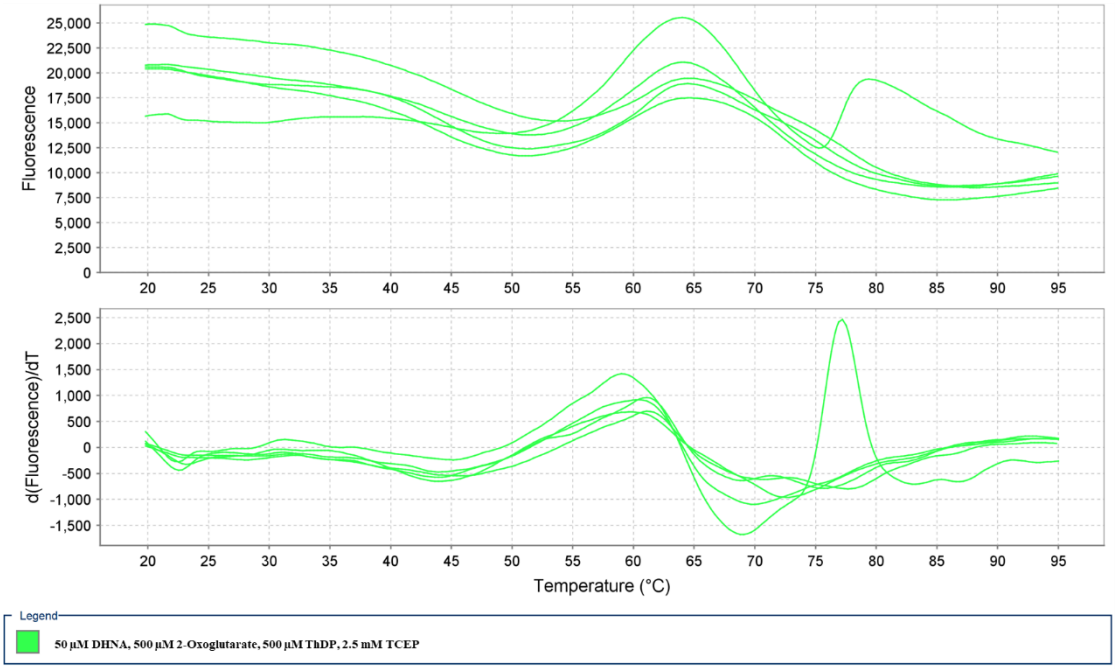

Melting Curves of *Smeg*-MenD (100 µM DHNA, 500 µM 2-Oxoglutarate 500 µM ThDP, 2.5 mM TCEP)

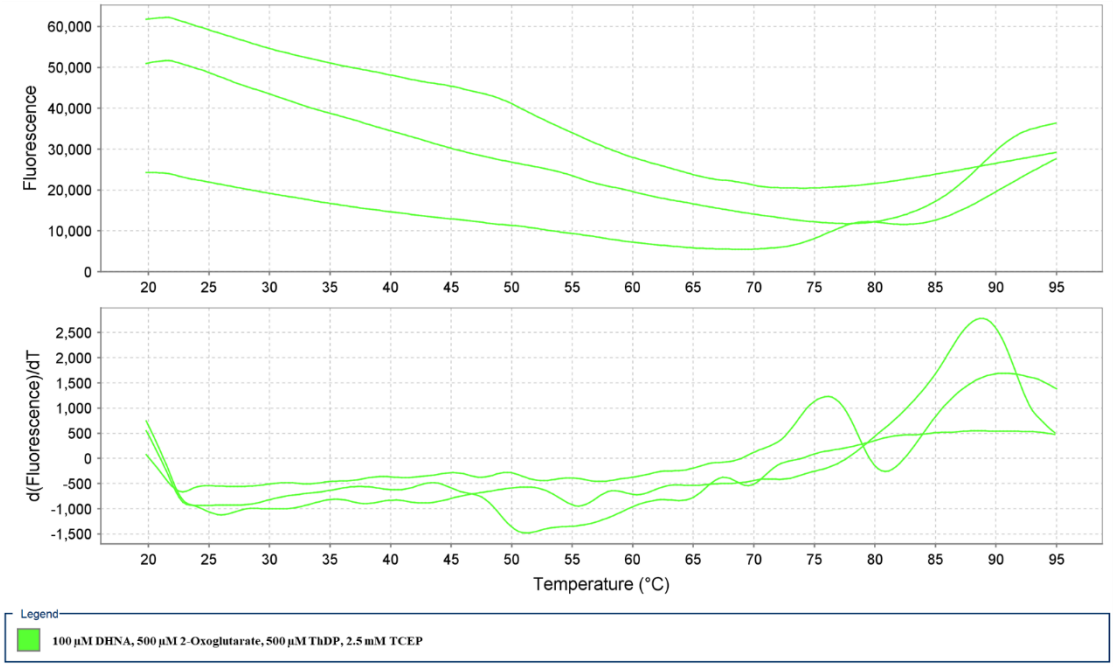

Legend

100 µM DHNA, 500 µM 2-Oxoglutarate, 500 µM ThDP, 2.5 mM TCEP

References

1. Weinstein, E.A.Y., T.; Li, L.; Avarbock, D.; Avarbock, A.; Helm, D.; McColm, A. A.; Duncan, K.; Lonsdale, J. T.; Rubin, H., *Inhibitors of type II NADH:menaquinone oxidoreductase represent a class of antitubercular drugs.* PNAS, 2005. 102(12): p. 4548-4553.
2. Kurosu, M. and E. Begari, *Vitamin K2 in electron transport system: are enzymes involved in vitamin K2 biosynthesis promising drug targets?* Molecules, 2010. 15(3): p. 1531-53.
3. Collins, M.D.J., D., *Distribution of Isoprenoid Quinone Structural Types in Bacteria and Their Taxonomic Implications.* Microbiological Reviews, 1981. 45(2): p. 316-354.
4. Booth, S.L., *Vitamin K: food composition and dietary intakes.* Food Nutr Res, 2012. 56.
5. Debnath, J., et al., *Discovery of selective menaquinone biosynthesis inhibitors against Mycobacterium tuberculosis.* J Med Chem, 2012. 55(8): p. 3739-55.
6. Ravcheev, D.A. and I. Thiele, *Genomic Analysis of the Human Gut Microbiome Suggests Novel Enzymes Involved in Quinone Biosynthesis.* Front Microbiol, 2016. 7: p. 128.
7. Zhi, X.Y., et al., *The futalosine pathway played an important role in menaquinone biosynthesis during early prokaryote evolution.* Genome Biol Evol, 2014. 6(1): p. 149-60.
8. Meganathan, R., *Biosynthesis of menaquinone (vitamin K2) and ubiquinone (coenzyme Q): A perspective on enzymatic mechanisms.* Vitam Horm, 2001. 61.
9. Upadhyay, A., et al., *Partial Saturation of Menaquinone in Mycobacterium tuberculosis: Function and Essentiality of a Novel Reductase, MenJ.* ACS Cent Sci, 2015. 1(6): p. 292-302.
10. Paudel, A., et al., *Menaquinone as a potential target of antibacterial agents.* Drug Discov Ther, 2016. 10(3): p. 123-8.
11. Jiang, M., et al., *Menaquinone biosynthesis in Escherichia coli: identification of 2-succinyl-5-enolpyruvyl-6-hydroxy-3-cyclohexene-1-carboxylate as a novel intermediate and re-evaluation of MenD activity.* Biochemistry, 2007. 46(38): p. 10979-89.
12. Fang, M., et al., *Succinylphosphonate esters are competitive inhibitors of MenD that show active-site discrimination between homologous alpha-ketoglutarate-decarboxylating enzymes.* Biochemistry, 2010. 49(12): p. 2672-9.
13. Bunik, V.I., A. Tylicki, and N.V. Lukashev, *Thiamin diphosphate-dependent enzymes: from enzymology to metabolic regulation, drug design and disease models.* FEBS J, 2013. 280(24): p. 6412-42.
14. Kasparyan, E., et al., *Asymmetric Stetter reactions catalyzed by thiamine diphosphate-dependent enzymes.* Appl Microbiol Biotechnol, 2014. 98(23): p. 9681-90.
15. Jirgis, E.N., et al., *Structural Views along the Mycobacterium tuberculosis MenD Reaction Pathway Illuminate Key Aspects of Thiamin Diphosphate-Dependent Enzyme Mechanisms.* Structure, 2016. 24(7): p. 1167-77.
16. Exchange, G.H.D. *IHME GBD Results Tool*. 2019.
17. Barry, C.E., 3rd, et al., *The spectrum of latent tuberculosis: rethinking the biology and intervention strategies.* Nat Rev Microbiol, 2009. 7(12): p. 845-55.
18. Pieters, J., *Mycobacterium tuberculosis and the macrophage: maintaining a balance.* Cell Host Microbe, 2008. 3(6): p. 399-407.
19. Urdahl, K.B., S. Shafiani, and J.D. Ernst, *Initiation and regulation of T-cell responses in tuberculosis.* Mucosal Immunol, 2011. 4(3): p. 288-93.
20. Wolf, A.J., et al., *Initiation of the adaptive immune response to Mycobacterium tuberculosis depends on antigen production in the local lymph node, not the lungs.* J Exp Med, 2008. 205(1): p. 105-15.
21. W., V.B.M.S.P.J.S.S.B.J.M.T.R.W.R.A.M.B.R.B., *Allelic exchange in Mycobacterium tuberculosis with long linear recombination substrates.* Journal of Bacteriology, 1996. 178(1): p. 273-279.
22. Organisation, W.H., *Guidelines for the programmatic management of drug-resistant tuberculosis Emergency update 2008*. 2008.
23. Delogu, G., M. Sali, and G. Fadda, *The biology of mycobacterium tuberculosis infection.* Mediterr J Hematol Infect Dis, 2013. 5(1): p. e2013070.
24. Gengenbacher, M. and S.H. Kaufmann, *Mycobacterium tuberculosis: success through dormancy.* FEMS Microbiol Rev, 2012. 36(3): p. 514-32.
25. AH., J.T.S., *Active Tuberculosis*. 2019, Treasure Island (FL): StatPearls Publishing.

26. Johnston, J.M., et al., *Structural and functional analysis of Rv0554 from Mycobacterium tuberculosis: testing a putative role in menaquinone biosynthesis.* Acta Crystallogr D Biol Crystallogr, 2010. 66(Pt 8): p. 909-17.
27. Frick, M.J.-L., E., *Report on TB Research Funding Trends 2005-2012*. 2013.
28. Health., M.o., *Guidelines for Tuberculosis Control in New Zealand 2010* M.o. Health, Editor. 2010: Wellington.
29. Health, M.o. *Latent tuberculosis infection*. 2018 [cited 2018; Available from: https://www.health.govt.nz/your-health/conditions-and-treatments/diseases-and-illnesses/latent-tuberculosis-infection.
30. Koul, A., et al., *The challenge of new drug discovery for tuberculosis.* Nature, 2011. 469(7331): p. 483-90.
31. Murray, J.F., D.E. Schraufnagel, and P.C. Hopewell, *Treatment of Tuberculosis. A Historical Perspective.* Ann Am Thorac Soc, 2015. 12(12): p. 1749-59.
32. Hoffbrand, R.J.D.W.R.A.B.C.M.P.C.B.I., *Rifampicin induced light chain proteinuria and renal failure.* Thorax, 1984. 39: p. 952-953.
33. *WHO targets elimination of TB in over 30 countries* Available from: http://www.who.int/mediacentre/news/releases/2014/tb-elimination/en/.
34. Lim, E. and H. Heffernan, *Tuberculosis in New Zealand: Annual Report 2012*. 2013, Institute of Environmental Science and Research Ltd.: Porirua.
35. Littleton, J. and J. Park, *Tuberculosis and syndemics: implications for Pacific health in New Zealand.* Soc Sci Med, 2009. 69(11): p. 1674-80.
36. Colangeli, R., et al., *Whole genome sequencing of Mycobacterium tuberculosis reveals slow growth and low mutation rates during latent infections in humans.* PLoS One, 2014. 9(3): p. e91024.
37. Calder, L., et al., *A school and community outbreak of tuberculosis in Palmerston North, New Zealand.* N Z Med J, 2008. 121(1278): p. 50-61.
38. Marshall, C., *TB testing net widened*, in *NZ Herald*. 2006.
39. Mueller, Y.A.L., Y.; Furey, W.; Schulz, G. E.; Jordan, F.; Schneider, G., *A thiamin diphosphate binding fold revealed by comparison of the crystal structures of transketolase, pyruvate oxidase and pyruvate decarboxylase.* Structure, 1993. 1: p. 95-103.
40. Dawson, A., P.K. Fyfe, and W.N. Hunter, *Specificity and reactivity in menaquinone biosynthesis: the structure of Escherichia coli MenD (2-succinyl-5-enolpyruvyl-6-hydroxy-3-cyclohexadiene-1-carboxylate synthase).* J Mol Biol, 2008. 384(5): p. 1353-68.
41. Bashiri, G., et al., *Allosteric regulation of menaquinone (vitamin K2) biosynthesis in the human pathogen Mycobacterium tuberculosis.* J Biol Chem, 2020. 295(12): p. 3759-3770.
42. Whitman, W.B.C., D. C.; Wiebe, W. J. , *Prokaryotes: The unseen majority.* Proc Natl Acad Sci U S A, 1998. 95: p. 6578-6583.
43. Tenaillon, O., et al., *The population genetics of commensal Escherichia coli.* Nat Rev Microbiol, 2010. 8(3): p. 207-17.
44. Poole, B.S.R.K., *Microbial ubiquinones: multiple roles in respiration, gene regulation and oxidative stress management.* Microbiology, 1999. 145: p. 1827-1830.
45. Guo, M.J.Y.C.Z.G.M.C.X.C.Z., *Menaquinone Biosynthesis in Escherichia coli: Identification of 2-Succinyl-5-enolpyruvyl-6-hydroxy-3-cyclohexene-1-carboxylate as a Novel Intermediate and Re-Evaluation of MenD Activity.* Biochemistry, 2007. 46: p. 10979-10989.
46. Priyadarshi, A., E.E. Kim, and K.Y. Hwang, *Structural and functional analysis of Vitamin K2 synthesis protein MenD.* Biochem Biophys Res Commun, 2009. 388(4): p. 748-51.
47. Priyadarshi, A., et al., *Structural insights of the MenD from Escherichia coli reveal ThDP affinity.* Biochem Biophys Res Commun, 2009. 380(4): p. 797-801.
48. Song, H., et al., *A Thiamine-Dependent Enzyme Utilizes an Active Tetrahedral Intermediate in Vitamin K Biosynthesis.* J Am Chem Soc, 2016. 138(23): p. 7244-7.
49. Qin, M., et al., *Two active site arginines are critical determinants of substrate binding and catalysis in MenD: a thiamine-dependent enzyme in menaquinone biosynthesis.* Biochem J, 2018. 475(22): p. 3651-3667.
50. Duggleby, R.G., *Domain relationships in thiamine diphosphate-dependent enzymes.* Acc. Chem. Res., 2006. 39: p. 550-557.

51. Bhasin, M.B., J. L.; Palmer, D. R. J., *Steady-state kinetics and molecular evolution of Escherichia coli MenD [(1R,6R)-2-succinyl-6-hydroxy-2,4-cyclohexadiene-1-carboxylate synthase], an anomalous thiamin diphosphate-dependent decarboxylase-carboligase.* Biochemistry, 2003. 42: p. 13496-13504.
52. Tyagi, J.S.S., D., *Mycobacterium smegmatis and tuberculosis.* Trends In Microbiology, 2002. 10: p. 68-69.
53. Reyrat, J.M.K., D., *Mycobacterium smegmatis: an absurd model for tuberculosis?* Trends In Microbiology, 2001. 9(10): p. 472-473.
54. Wertheim, H.F.L., et al., *Risk and outcome of nosocomial Staphylococcus aureus bacteraemia in nasal carriers versus non-carriers.* The Lancet, 2004. 364(9435): p. 703-705.
55. Gordon, R.J. and F.D. Lowy, *Pathogenesis of methicillin-resistant Staphylococcus aureus infection.* Clin Infect Dis, 2008. 46 Suppl 5: p. S350-9.
56. DeLeo, F.R., et al., *Community-associated meticillin-resistant Staphylococcus aureus.* The Lancet, 2010. 375(9725): p. 1557-1568.
57. Wakeman, C.A., et al., *Menaquinone biosynthesis potentiates haem toxicity in Staphylococcus aureus.* Mol Microbiol, 2012. 86(6): p. 1376-92.
58. Bentley, R.M., R., *Biosynthesis of Vitamin K (Menaquinone) in Bacteria.* American Society for Microbiology, 1982. 46: p. 241-268.
59. Zamboni, N. and U. Sauer, *Knockout of the high-coupling cytochromeaa3oxidase reduces TCA cycle fluxes inBacillus subtilis.* FEMS Microbiology Letters, 2003. 226(1): p. 121-126.
60. Bashiri, G., et al., *Metabolic engineering of cofactor F420 production in Mycobacterium smegmatis.* PLoS One, 2010. 5(12): p. e15803.
61. Takara. *In-Fusion Cloning HD Plus - Site-directed mutagenesis*. 2020 [cited 2020 1/4/2019]; Available from: https://www.takarabio.com/products/cloning/mutagenesis-kits/site-directed-mutagenesis.
62. Bashiri, G. and E.N. Baker, *Production of recombinant proteins in Mycobacterium smegmatis for structural and functional studies.* Protein Sci, 2015. 24(1): p. 1-10.
63. Studier, F.W., *Protein production by auto-induction in high density shaking cultures.* Protein Expr Purif, 2005. 41(1): p. 207-34.
64. Laboratories, H., *Tartoff - Hobbs Broth (Terrific Broth) (Technical Data)*, H. Laboratories, Editor. 2015, HiMedia Laboratories.
65. Ghisaidoobe, A.B. and S.J. Chung, *Intrinsic tryptophan fluorescence in the detection and analysis of proteins: a focus on Forster resonance energy transfer techniques.* Int J Mol Sci, 2014. 15(12): p. 22518-38.
66. Lakowicz, J.R., *Mechanisms and Dynamic of Fluorescence Quenching* in *Principles of Fluorescence Spectroscopy*. 2006, Springer: Springer. p. 331-351.
67. Doose, S., H. Neuweiler, and M. Sauer, *Fluorescence quenching by photoinduced electron transfer: a reporter for conformational dynamics of macromolecules.* Chemphyschem, 2009. 10(9-10): p. 1389-98.
68. Nemeria, N.S., et al., *Competence of Thiamin Diphosphate-Dependent Enzymes with 2'-Methoxythiamin Diphosphate Derived from Bacimethrin, a Naturally Occurring Thiamin Anti-vitamin.* Biochemistry, 2016. 55(7): p. 1135-48.
69. Leake, M.C., *Biophysics: Tools and Techniques.* 2016: CRC Press.
70. Nemeria, N.C., S.; Bakyal, A.; Korotchkina, L. G.; Patell, M. S.; Jordan, F., *The 1', 4'-iminopyrimidine tautomer of thiamin diphosphate is poised for catalysis in asymmetric active centers on enzymes.* PNAS, 2006. 104: p. 78-82.
71. Niesen, F.H., H. Berglund, and M. Vedadi, *The use of differential scanning fluorimetry to detect ligand interactions that promote protein stability.* Nat Protoc, 2007. 2(9): p. 2212-21.
72. Epps, D.E., et al., *The ligand affinity of proteins measured by isothermal denaturation kinetics.* Anal Biochem, 2001. 292(1): p. 40-50.